α-Catenin

is a dosage-dependent

tumor suppressor gene in MDS

Inaugural-Dissertation
zur
Erlangung des Doktorgrades

Dr. rer. nat.
der Fakultät für
Biologie

an der

Universität Duisburg-Essen

vorgelegt von
Antje Maria Zickler
aus Berlin

April 2016

Die der vorliegenden Arbeit zugrunde liegenden Experimente wurden am Institut für Transfusionsmedizin des Universitätsklinikum Essen durchgeführt.

1. Gutachter: Prof. Dr. Peter A. Horn
2. Gutachter: Prof. Dr. Perihan Nalbant
3. Gutachter: Prof. Dr. Reinhard Henschler

Vorsitzender des Prüfungsausschusses: Prof. Dr. Bernhard Horsthemke

Tag der mündlichen Prüfung: 17. Oktober 2016

Für meine Eltern.

Es kommt nicht darauf an,
mit dem Kopf durch die Wand zu rennen,
sondern mit den Augen die Tür zu finden.

Werner von Siemens

Table of Contents

1 Zusammenfassung 1

2 Abstract 2

3 Introduction 3

3.1 Diagnosis and epidemiology of MDS 3

3.2 Molecular genetics of MDS 4

3.3 Gene dosage insufficiency of tumor suppressor genes 6

3.4 The role of α-Catenin in homeostasis and tumorigenesis 9

3.5 Objective of this thesis 12

4 Results 13

4.1 Eight of 24 shRNA encoding vectors mediated a Ctnna1 expression level of less than 50% of control and were selected for *in vivo* application 13

4.2 Reduced Ctnna1 expression levels in murine HSPCs mediate a myeloid expansion phenotype *in vivo* 14

4.2.1 Reduced Ctnna1 expression levels minimally affect peripheral complete blood counts upon competitive reconstitution 14

4.2.2 Murine HSPCs with reduced Ctnna1 expression expand in the bone marrow 16

4.2.3 Transplanted HSPCs with reduced Ctnna1 expression expand within the myeloid compartment of the bone marrow of mouse M12 18

4.2.4 Clonal dominance of bone marrow cells with reduced Ctnna1 expression leads to decreased erythropoiesis in the bone marrow of transplanted mice 19

4.2.5 After transplantation, murine HSPCs with reduced Ctnna1 expression expand within the HSC compartment of the bone marrow 20

4.2.6 Expansion of HSPCs in the bone marrow of mice M12 and M15 is mediated by the expression of shRNAs 405 and 409 21

4.2.7 Expansion of GFP^+ cells in the bone marrow of mice M12 and M15 was not due to insertional mutagenesis 22

4.3 The clonal dominance phenotype *in vivo* of transplanted HSPCs encoding shRNA 405 is reproducible 23

4.3.1 Single vector-transduced HSPCs encoding shRNA 405 or 409 successfully engraft without causing overt hematologic disease 23

4.3.2 HSPCs expressing shRNA 405 show a clonal dominance in the bone marrow of transplanted mice 25

4.3.3 Cells with reduced Ctnna1 expression expand in the myeloid compartment of the bone marrow 27
4.3.4 Expansion of cells with reduced Ctnna1 expression impairs erythropoiesis in the bone marrow 28
4.3.5 Bone marrow cells with reduced Ctnna1 expression expand within the HSC and progenitor cell compartments 29

4.4 HSPCs expressing shRNA 405 self-renew, expand and lead to clonal dominance in secondary transplanted animals 30
4.4.1 Secondary transplanted HSPCs expressing shRNA 405 engraft sublethally irradiated recipients and give rise to abnormal peripheral blood counts 30
4.4.2 Bone marrow cells with reduced Ctnna1 expression levels mediated by shRNA 405 expression expand in the bone marrow of secondary recipient mice 33
4.4.3 The myeloproliferative phenotype of bone marrow cells expressing shRNA 405 is maintained upon secondary transplantation 34
4.4.4 Expansion of primary bone marrow cells expressing shRNA 405 in secondary recipients diminishes erythropoiesis 35
4.4.5 GFP^+ bone marrow cells from mouse M26 expand within the hematopoietic stem and progenitor cell compartments in secondary recipient mice 36

4.5 Clonal dominance of HSPCs with reduced Ctnna1 expression is reinforced by the co-occurrence of Tp53 inactivation 37
4.5.1 Knockout of Tp53 facilitates the expansion of HSPCs with reduced Ctnna1 expression without causing overt hematological disease 37
4.5.2 The myeloid lineage differentiation bias in the bone marrow of mice transplanted with HSPCs encoding shRNA 405 is not enhanced when Tp53 is inactivated 41
4.5.3 Inactivation of Tp53 does not further reduce the diminished erythropoiesis in the bone marrow of mice transplanted with HSPCs encoding shRNA 405 42
4.5.4 Inactivation of Tp53 reinforced the clonal dominance of GFP^+ cells in the progenitor and stem cell compartments of mice transplanted with HSPCs encoding shRNA 405 43

4.6 Loss of Tp53 reinforces the neoplastic potential of bone marrow cells with reduced Ctnna1 expression upon secondary transplantation 45
4.6.1 Inactivation of Tp53 enhances bone marrow repopulation potential of cells with reduced Ctnna1 expression in secondary recipient mice without impacting peripheral hematological parameters 45

4.6.2 $Tp53^{-/-}$ bone marrow cells with reduced Ctnna1 expression level maintain the differentiation bias towards the myeloid lineage upon secondary transplantation 49
4.6.3 The clonal dominance of bone marrow cells with reduced Ctnna1 expression within the stem and progenitor cell compartments is enhanced by the additional inactivation of Tp53 upon secondary transplantation 50

4.7 Loss of Tp53 and reduced Ctnna1 expression leads to an earlier onset of death, most likely by peripheral blood cell dysplasia and bone marrow failure 52
4.7.1 Genetic inactivation of Tp53 in transplanted HSPCs significantly decreases overall survival of recipient animals 52
4.7.2 Recipient mice of HSPCs expressing shRNA 405 show pronounced peripheral blood cell dysplasia 53

4.8 Expression of shRNA 405 immortalizes primary murine bone marrow cells and confers a myeloproliferative phenotype *in vitro* 55
4.8.1 Primary murine bone marrow cells can be immortalized *in vitro* by the expression of shRNA 405 55
4.8.2 Most immortalized murine bone marrow cells expressing shRNA 405 show a myeloid immunophenotype while a lineage negative subpopulation is maintained 57
4.8.3 Ectopic re-expression of Ctnna1 to different levels gradually reverts the growth phenotype of immortalized bone marrow cells *in vitro* 59

4.9 CTNNA1 expression leads to myeloid differentiation of the human HL60 cell line and thus abrogates their proliferative potential 60
4.9.1 Ectopic Expression of functional CTNNA1 stops proliferation of the human HL60 cell line 60
4.9.2 CTNNA1 expression in HL60 cells leads to a minor decrease in G1-S phase transition of the cell cycle 62
4.9.3 CTNNA1 expression in HL60 cells mediates transcriptional upregulation of CD11b expression and induces myeloid differentiation 63

5 Discussion and Outlook 65

6 Material and Methods 72

6.1 Material 72
6.1.1 Devices 72
6.1.2 Laboratory and cell culture material 73
6.1.3 Chemicals, buffers, solutions and cell culture media 73
6.1.4 Reagent systems (Kits), enzymes and standards 74
6.1.5 PCR Primers, Oligonucleotides and shRNA sequences 75
6.1.6 Software Tools 77
6.1.7 Antibodies 78

6.2 Methods 79
6.2.1 Animal experiments 79
6.2.2 Cell culture 81
6.2.3 Molecular biology methods 83
6.2.4 Molecular Cloning 85
6.2.5 Lentiviral vectors 88
6.2.6 Flow Cytometry 91
6.2.7 Protein biochemistry 93

7 References 95

8 List of Figures 105

9 List of Tables 108

10 List of Abbreviations 108

11 Acknowledgements 112

Lebenslauf 113

Liste der wissenschaftlichen Publikationen 114

Eidesstattliche Erklärung 115

1 Zusammenfassung

Die Myelodysplastischen Syndrome (MDS) sind eine Gruppe heterogener maligner hämatologischer Erkrankungen, die sich durch ineffektive Hämatopoese und einem erhöhten Transformationsrisiko zu Akuter Myeloischer Leukämie (AML) auszeichnen. MDS wird durch Mutationen und chromosomale Aberrationen in hämatopoetischen Stamm- und Vorläuferzellen (HSVZ) ausgelöst, die deren klonale Expansion und Differenzierungsstörungen bewirken. Die häufigste chromosomale Aberration in MDS ist eine heterozygote Deletion des q-Armes auf Chromosom 5. Basierend auf der Hypothese, dass in dieser Region Tumorsuppressorgene lokalisiert sind, konnten über cytogenetische und hochauflösende genomische Analyseverfahren zwei rekurrente Deletionsregionen (CDRs) definiert werden. Bemerkenswerterweise wurde in keiner dieser beiden Abschnitte eine Mutation auf dem intakten Allel identifiziert, sodass die Existenz klassischer Tumorsuppressorgene, für die eine Inaktivierung beider Allele erforderlich ist, in den CDRs ausgeschlossen werden kann. Stattdessen ist eine Gendosisabhängigkeit dieser putativen Tumorsuppressorgene wahrscheinlich. Allerdings sind ihre Identitäten bisher noch weitgehend unbekannt.

In dieser Arbeit analysierte ich die Tumorsuppressorfunktion von α-Catenin, das durch CTNNA1 in der proximalen CDR kodiert wird. In einem kompetitiven Rekonstitutionsansatz untersuchte ich die durch RNAi-vermittelte Gendosisreduktion von α-Catenin in murinen HSVZ. Zudem analysierte ich den Effekt der Re-expression von α-Catenin in einer humanen Leukämiezelllinie mit heterozygoter 5q-Deletion, die den CTNNA1 Lokus einschließt.

Zunächst zeigte ich, dass einer von 8 shRNA-kodierenden Vektoren eine Ctnna1 Gendosisreduktion bewirkte, die transplantierten HSVZ eine klonalen Vorteil vermittelte und zu einem MDS-ähnlichen Phänotyp führte. Die betroffenen hämatopoetischen Zellen zeigten sowohl Selbsterneuerungs- als auch Langzeitrepopulationspotenzial, da sie das Knochenmark der Empfängertiere länger als 6 Monate klonal dominierten und ebenso in sekundären Empfängertieren anwuchsen. Da inaktivierende TP53 Mutationen häufig mit 5q-Deletionen in MDS Patienten assoziiert sind, wurde das Experiment ebenfalls mit HSVZ aus $Tp53^{-/-}$ Mäusen durchgeführt. Die Tp53 Inaktivierung verstärkte die klonale Dominanz der transplantierten HSVZ mit reduzierter Ctnna1 Gendosis und verkürzte die Überlebensrate der transplantierten Mäuse. Meine Arbeit zeigt erstmalig in funktionellen Analysen die gendosisabhängige Tumorsuppressorfunktion von α-Catenin in malignen myeloiden Erkrankungen *in vivo*. Um diese weiter zu untersuchen, kultivierte ich primäre murine HSVZ mit RNAi-vermittelter Gendosisreduktion von α-Catenin. Der *Knockdown* von Ctnna1 führte auch *in vitro* zu erhöhtem Wachstum und zur Immortalisierung der transduzierten Zellen.

Während Gendosisinsuffizienz von α-Catenin murinen hämatopoetischen Zellen einen Wachstums- und Überlebensvorteil vermittelte, zeigte ich in einem reziproken Versuchsansatz in HL60 Zellen, einer humanen Modellzelllinie für 5q-Deletionen, dass die Re-expression von CTNNA1 das Zellwachstum stark beeinträchtigte. Zudem löste α-Catenin Re-expression die Hochregulation von Differenzierungsmarkern in HL60 Zellen aus. Meine Arbeit gibt Aufschluss über die entscheidende Tumorsuppressorgenfunktion von α-Catenin in MDS anhand von funktionalen Daten aus *in vivo* und ergänzenden *in vitro* Studien.

2 Abstract

Myelodysplastic Syndromes (MDS) are a heterogeneous group of malignant hematological disorders characterized by ineffective hematopoiesis and a risk of transformation to acute myeloid leukemia (AML). MDS arises from mutations and chromosomal aberrations in hematopoietic stem and progenitor cells (HSPCs) leading to their clonal expansion and a dysfunction in their maturation. The most frequent chromosomal lesion in MDS is a heterozygous deletion on the long arm of chromosome 5. Following the hypothesis that this region encodes a key tumor suppressor gene, cytogenetic and high-resolution genomic profiling studies of a large patient cohort have defined two commonly deleted regions (CDRs). Remarkably, for both CDRs, no mutation has been reported on the remaining, intact allele excluding the presence of a classical tumor suppressor that requires the inactivation or loss of both copies. Despite extensive efforts, the identity of the predicted, most likely gene dosage insufficient tumor suppressor remains obscure.

In this study, I investigated the tumor suppressor function of the α-Catenin-encoding gene CTNNA1 located in the center of the proximal CDR. I employed a competitive reconstitution approach using RNAi in murine HSPCs to test the gene dosage reduction of α-Catenin *in vivo*. As well, using a reciprocal approach, I assessed the effect of α-Catenin re-expression in a leukemia cell line with a deletion on chromosome 5 encompassing the CTNNA1 locus.

First, I showed that one out of 8 shRNA encoding vectors mediated a reduced Ctnna1 expression that conveyed a clonal advantage to the transplanted HSPCs leading ultimately to a myeloid malignancy *in vivo*. The affected cells showed both self-renewal and long-term repopulation ability, since their clonal dominance was retained in recipient mice for more than six months after transplantation as well as upon secondary transplantation. To implement the frequent co-occurrence of inactivating TP53 mutations with 5q deletions in MDS patients, I performed a competitive reconstitution experiment with HSPCs expressing no Tp53 and reduced Ctnna1 levels. The inactivation of Tp53 conferred an additive effect compared to the clonal dominance of the HSPC with low Ctnna1 expression alone and caused an earlier onset of death of transplanted mice. Thus, my work provides the first functional evidence for α-Catenin as a gene dosage insufficient tumor suppressor in myeloid malignancies *in vivo*. To further analyze the observed phenotype, I cultivated primary bone marrow cells with RNAi-mediated knockdown of Ctnna1. The downregulation of Ctnna1 using one specific RNAi vector led to the survival, proliferation and immortalization of the cells *in vitro*.

While downregulation of Ctnna1 in murine hematopoietic cells invoked a growth and survival advantage, I could show that in HL60 cells, a model cell line for myeloid malignancies with deletion of chromosome 5q, re-expression of CTNNA1 strongly impaired the cell growth. In addition, the cells showed upregulation of differentiation markers. In conclusion, my study revealed key aspects of the tumor suppressive activity of CTNNA1 in hematopoietic cells based on *in vivo* and complementary *in vitro* studies.

3 Introduction

Myelodysplastic Syndromes (MDS) are a heterogeneous group of hematologic disorders caused by malignant transformation of hematopoietic stem and progenitor cells (HSPCs). The impaired and thus ineffective hematopoiesis and the morphologic dysplasia of hematopoietic cells are key properties of this disease. MDS patients suffer from peripheral blood cytopenias causing hemorrhage (thrombocytopenia), infections (neutropenia) and anemia. In 40% of cases, MDS progress to acute myeloid leukemia (AML; Heaney and Golde, 1999; Corey et al., 2007; Li, 2013).

3.1 Diagnosis and epidemiology of MDS

MDS is a common hematological malignancy in adults. Its epidemiology is difficult to assess accurately, because the clinical manifestation of MDS is very heterogeneous and the disease can be difficult to diagnose. The diagnosis can only be made with certainty by complete evaluation of the peripheral blood parameters, full assessment of the patients' case history, cytological analysis of a bone marrow aspirate and the exclusion of non-MDS causes of the clinical findings such as iron deficiency. The current incidence in the United States of America is 30,000-40,000 newly diagnosed MDS cases per year and estimated to be twice as high in Europe (Goldberg et al., 2010; Visser et al., 2012). The mean age at diagnosis is 70 years, thus MDS is prevalent particularly in the elderly population (Goldberg et al., 2010; Cogle et al., 2011; Visser et al., 2012). MDS occurs rarely in children or adolescents, and in those cases it is often associated with inherited bone marrow failure syndromes such as Fanconi anemia, severe congenital neutropenia or Diamond-Blackfan anemia (Corey et al., 2007; Li, 2013).

MDS is closely related to AML. For the correct classification, prognostic stratification, and treatment guidance for MDS it is important to exclude AML. AML is a very aggressive malignant disorder affecting the myeloid lineage of the hematopoietic system. It is characterized by a block in hematopoietic cell differentiation, abnormal proliferation of myeloid progenitor cells and reduced bone marrow cell death leading to an excessive accumulation of immature myeloid cells, so-called "blasts", in the peripheral blood and the bone marrow. In AML the hematopoiesis of erythrocytes, granulocytes and thrombocytes is strongly impaired.

In contrast, MDS is characterized by a low blast count. Typically, blast counts are lower than 10%, high-risk MDS is distinguished from AML by a maximum blast count of less than 20% in the bone marrow. The most characteristic feature of MDS is the cellular dysplasia of differentiated cells in the peripheral blood as well as of myeloid progenitor cells in the bone marrow. Differentiation and self-renewing pathways are dysregulated in bone marrow cells of MDS patients giving rise to dysfunctional and dysplastic peripheral blood cells of the myeloid lineages. The block in differentiation of stem and progenitor cells causes peripheral blood cytopenias that affect the hematopoiesis of erythrocytes, thrombocytes and

granulocytes to various extents. Typically, during the course of the disease, the peripheral blood cytopenias progressively worsen. Paradoxically, the cytopenias coexist with normal or hypercellular bone marrow with active cell turnover (apoptosis) and cell divison (clonal expansion). In contrast to AML, MDS lack massive proliferation of bone marrow cells. Yet, the clonal expansion of malignant cells frequently causes the progression to AML (Klepin et al., 2014).

After diagnosis of MDS, its disease risk stratification is most commonly accomplished according to the Revised International Prognostic Scoring System (IPSS-R; Greenberg et al., 2012). The IPSS-R risk score depends on peripheral blood parameters, number and type of cytopenias in the peripheral blood, blast percentage in the bone marrow, cytogenetics of bone marrow cells and the age of the patient. The score ranges from ≤ 1.5 to > 6 and groups the patient in one out of five prognostic risk categories: very low, low, intermediate, high or very high risk. The median survival times range from 8.8 years (very low-risk group) to 0.8 years (very high-risk group). Besides, the French-American-British (FAB) classification and the World Health Organization (WHO) classification are traditional systems that are still used in parallel. However, in addition to the conventional diagnostic parameters, detailed genetic analysis (see below) is routinely performed in many centers to individualize treatment options.

The primary goals of MDS therapy are the decrease in transfusion needs, the improvement of the bone marrow function and prevention of the progression to AML. Overall, the therapy is supposed to prolong the survival of the patient and to enhance the quality of life (supportive care). The only curative therapeutic option is the allogeneic hematopoietic stem cell transplantation (HSCT). 30-40% of MDS patients undergoing HSCT are long-term disease-free survivors (Gratwohl et al., 2013). However, frequently, the advanced patients' age and its associated co-morbidities render MDS patients ineligible for HSCT (Deeg and de Lima, 2013; Garcia-Manero, 2015). In these cases, patients are left with supportive care, such as lenalidomide treatment, application of hypomethylating agents and chemotherapeutical drugs.

3.2 Molecular genetics of MDS

MDS is caused by the genetic alteration of oncogenes and tumor suppressor genes in bone marrow cells. Recent studies have provided important insights into the genetics of MDS and identified several recurrently mutated genes by employing state-of-the-art sequencing techniques. The most frequently mutated genes in MDS are genes encoding for splice factors (e.g. SF3B1, SRSF2, U2AF1), transcription factors (e.g. RUNX1, TP53, ETV6) and proteins involved in signal transduction (e.g. NRAS, JAK2). Furthermore, genes involved in DNA methylation (e.g. TET2, IDH1, DNMT3A) and histone modification (e.g. ASXL1, EZH2) are often affected by mutations in MDS. Mutations in these genes do not occur in an isolated fashion, the cells rather successively acquire recurrent patterns of driver mutations leading to malignant transformation. Interestingly, some mutations have been found to be mutually

exclusive (Graubert and Walter, 2011; Graubert et al., 2012; Papaemmanuil et al., 2013; Haferlach et al., 2014).

Moreover, the MDS genome is also characterized by the frequent occurrence of karyotypic alterations affecting chromosomal regions. In fact, approx. 50% of all MDS patients display cytogenetic aberrations as identified by conventional karyotyping, array comparative genomic hybridization (array CGH) and single nucleotide polymorphism (SNP) arrays (Haase et al., 2007; Gondek et al., 2008; Heinrichs et al., 2009; Thiel et al., 2011). In contrast to AML recurrent translocations are rare and, notably, most of these aberrations are deletions (Haase et al., 2007). The most frequent recurrent deletion affects chromosome 5: 30% of MDS patients with karyotypic abnormalities display deletions of chromosome 5q. Other frequent recurrent deletions were identified on chromosomes 7 (-7/del(7q), 21%), 18 (-18/del(18q), 7%) or 20 (del(20q), 7%; Haase et al., 2007).

Of note, two distinct commonly deleted regions (CDR) within the del(5q) region have been delineated. The proximal CDR comprises a region on band 31 (Le Beau et al., 1993; Zhao et al., 1997; Horrigan et al., 2000) and the distal CDR is located on band 32-33 (Boultwood et al., 1994; Jaju et al., 1998; Boultwood, 2002). For historic reasons, patients with an isolated deletion of the distal CDR are considered as a separate MDS entity. The so-called "5q– syndrome" is associated with a very good prognosis and an indicated effective therapeutic option, the treatment with Lenalidomide (Ebert, 2009). The delineation of the CDRs on chromosome 5q implied the loss of one or multiple tumor suppressor genes located therein (Horrigan et al., 2000; Lai et al., 2001; Joslin et al., 2007; Ebert et al., 2008). For instance, Ebert et al. identified RPS14, located in the distal CDR, to be one of the tumor suppressor genes involved in the pathogenesis of the 5q– syndrome (Ebert et al., 2008). However, most patients have deletions encompassing both CDRs. Thus, the del(5q) CDRs provide a basis for the search for tumor suppressor genes involved in malignant myeloid transformation (Ebert, 2011).

While the initially identified proximal CDR of 4 Mb (Le Beau et al., 1993; Figure 1) comprised 37 genes, it has been narrowed down to a 700 kb region encompassing nine genes (CDC25C, KDM3B, REEP2, EGR1, ETF1, HSPA9, CTNNA1, SIL1, MATR3; Figure 1). All of them are found to be expressed in $CD34^+$ human HSPCs (Horrigan et al., 2000). Thus, these genes are candidate tumor suppressor genes in MDS. Several studies have proposed a tumor suppressor function in myeloid leukemia for some of these genes, such as CDC25C (Yoshimi et al., 2014), KDM3B (Kim et al., 2012), EGR1 (Joslin et al., 2007), HSPA9 (Xie et al., 2000) and CTNNA1 (Liu et al., 2007; Fu et al., 2010). For EGR1, a tumor suppressor role in hematopoietic cells was shown in Egr1-deficient mice. Mice treated with alkylating agents developed a myeloproliferative disorder when Egr1 was inactivated either on one or both alleles (Joslin et al., 2007). Mice with heterozygous or homozygous inactivation of Egr1 developed the disease to the same extent. This study showed that mono-allelic inactivation of Egr1 was sufficient for disease predisposition. Later, Wagers and colleagues showed that

Egr1 is indispensable for maintenance of the hematopoietic stem cell (HSC) function in mice, promoting HSC quiescence and retention in the niche (Min et al., 2008). However, loss of Egr1 in mice did not reflect the complete disease pathogenesis and the clinical features of MDS in patients. Thus, a functional collaboration of the loss of multiple tumor suppressor genes located in the proximal CDR is proposed to account for the pathogenesis of MDS with del(5q; Jaju et al., 1998; Ebert, 2009; Thiel et al., 2011). Therefore, it is important to unravel the functional role of the remaining candidate tumor suppressors located within the proximal CDR.

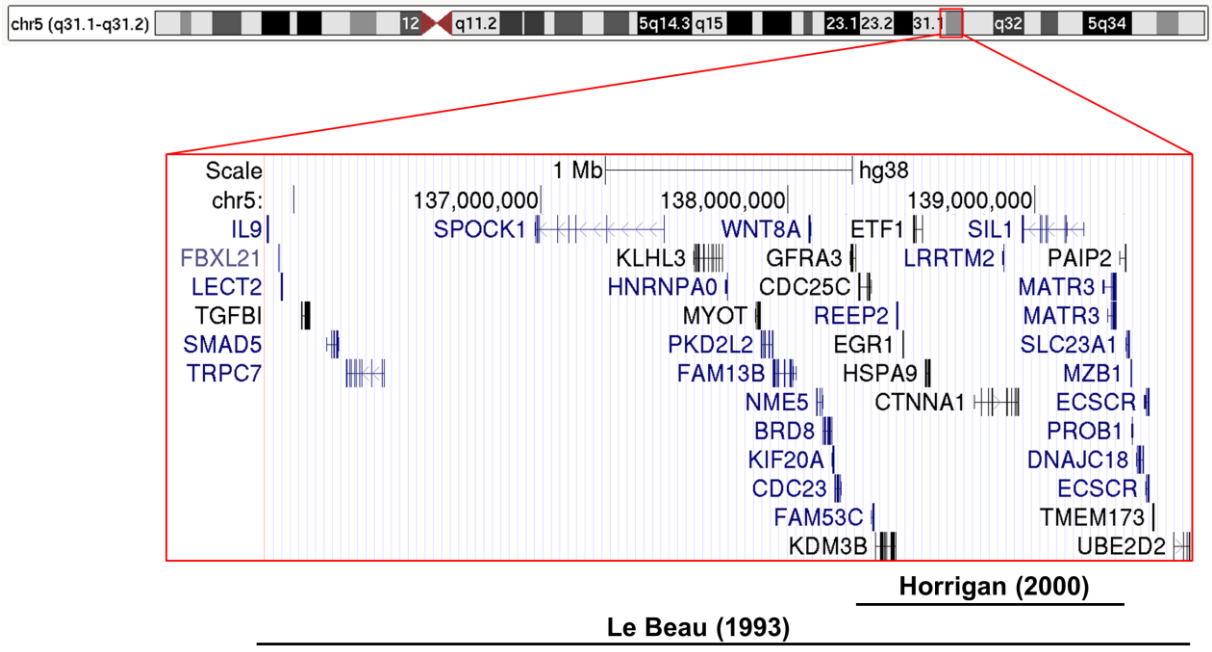

Figure 1: Genes located within the delineated proximal CDR on chromosome 5q31 in MDS.
Schematic chromosomal map of the location of the proximal CDR on 5q31 and annotation of genes therein. Black lines indicate the initially defined 4Mb CDR (Le Beau et al., 1993) and the refined 700 kb CDR (Horrigan et al., 2000). The map was generated from the hg38 assembly of the UCSC genome browser (http://www.genome.ucsc.edu/).

3.3 Gene dosage insufficiency of tumor suppressor genes

MDS is a genetic disease of the hematopoietic system. Frequently, the malignant transformation in MDS is driven by the inactivation of tumor suppressor genes. Both, complete and partial loss of tumor suppressor gene expression in the pathogenesis of cancer has been intensively investigated over the past five decades. Tumor suppressor gene inactivation can occur in a mono-allelic or bi-allelic fashion. If a tumor suppressor gene is inactivated on both alleles, its expression is completely lost. The bi-allelic inactivation of tumor suppressor genes is caused by the successive occurrence of independent genetic events such as point mutations, microdeletions and epigenetic silencing, affecting the same gene (Berger et al., 2011). Furthermore, the conversion of the existing inactivating mutation to the second allele, leading to “copy neutral loss of heterozygosity” (CN-LOH), can result in the bi-allelic inactivation of a tumor suppressor (Berger et al., 2011; Makishima and Maciejewski,

2011). This setting complies with the "two-hit" paradigm of bi-allelic tumor suppressor gene inactivation, which has been shown for tumor suppressor genes such as RB1 (Knudson, 1971; Friend et al., 1986; Foulkes, 2008; Figure 2, left).

However, the remaining allele frequently remains entirely intact in cases of recurrent heterozygous deletions. This suggests that haploinsufficiency (50% gene dosage) of one or more genes located within the deleted region are supporting pathogenesis (Fodde and Smits, 2002; Berger et al., 2011). Haploinsufficiency of gene expression has been an established concept in disease entities other than cancer. They include numerous developmental disorders, such as aniridia (haploinsufficiency of PAX6), Griegs syndrome (GLI3), Hirschprung disease (RET) or Miller-Dieken lissencephaly (LIS1; Fisher and Scambler, 1994). In cancer biology, gene dosage dependency of tumor suppressor function is a rather novel concept (Fodde and Smits, 2002; Berger et al., 2011). According to this model, the mono-allelic inactivation of one or more tumor suppressor genes is sufficient to drive a cell towards malignancy (Berger et al., 2011). One of the most well-known tumor suppressor genes, which has been identified to act as a haploinsufficient tumor suppressor gene, is TP53 (Figure 2, middle). The reduction of p53 gene dosage is found in inherited familial cancer as a result of Li-Fraumeni syndrome. Haploinsufficiency of TP53 reduced the cell's ability to respond to oncogenic stimuli. This led to an attenuated stress response, a disrupted G1 cell cycle arrest and an impaired apoptosis, *in vitro* and *in vivo* (Lynch and Milner, 2006). In the past years, numerous other haploinsufficient tumor suppressor genes have been identified, such as BRCA1 in breast cancer (Bellacosa et al., 2010; Sedic et al., 2015), RPS14 in MDS/5q– syndrome (Ebert et al., 2008), PAX5 in acute lymphoblastic leukemia (ALL; Mullighan et al., 2007), RUNX1 in AML (Song et al., 1999) or APC in intestinal carcinoma (Amos-Landgraf et al., 2012).

Recently, the understanding of discrete steps in tumor suppressor gene inactivation has been extended to a model of a continuum dependency on gene dosage for tumor suppressor genes (Berger et al., 2011) as exemplified by the analysis of the PTEN gene (Chen et al., 2005; Alimonti, 2010; Alimonti et al., 2010; Berger et al., 2011). In myeloid leukemia, the concept of gene dosage insufficiency of tumor suppressor genes concerns mainly haploinsufficiency of tumor suppressor genes located within recurrently deleted genomic regions. Graded downregulation of tumor suppressor gene expression to a sub-haploinsufficient gene dosage level has been shown *in vivo* for only a few tumor suppressor genes. For instance, MYBL2 (Heinrichs et al., 2013), a transcription factor gene located within the recurrently deleted region on chromosome 20q in MDS, and SFPI1 (Rosenbauer et al., 2004), encoding the lineage-specific transcription factor PU.1, have been identified as sub-haploinsufficient tumor suppressor genes in myeloid malignancies. The reduced levels of 30% gene dosage for MYBL2 (Figure 2, right) and 20% for SFPI1 gene dosage could drive a growth and survival advantage to the cells. Complete inactivation of the expression of these

genes, however, was not compatible with cell survival and thus shown to be non-tumorigenic (Rosenbauer et al., 2004; Heinrichs et al., 2013; Figure 2, right).

Of note, deletions of chromosome 5q in MDS are usually heterozygous (Bejar et al., 2011). Though extensive sequencing of the deleted regions has been performed, no mutations have been identified in the genes located on the intact allele. Furthermore, CN-LOH has not been detected for chromosome 5q in patients with MDS (Gondek et al., 2008; Graubert et al., 2009; Heinrichs et al., 2009). These findings suggest that the function of candidate tumor suppressor genes located within the proximal CDR does not depend on the bi-allelic inactivation to promote malignant transformation. Rather haploinsufficiency or reduced gene dosage of one or more of these genes appears to enable pathogenesis of MDS with del(5q).

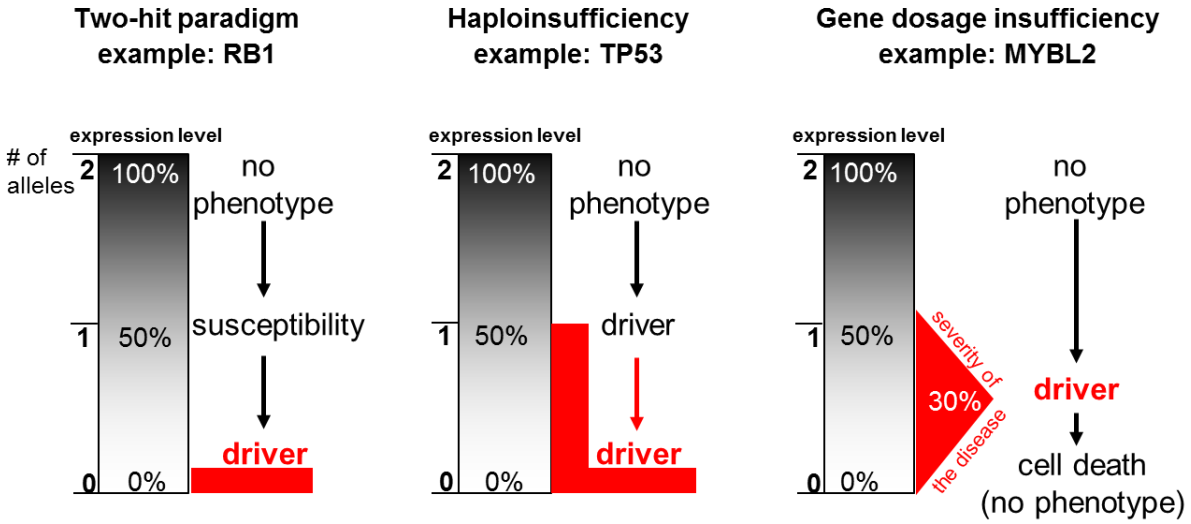

Figure 2: Concepts of tumor suppressor gene inactivation.
Left: According to the two-hit paradigm (Knudson, 1971), tumorigenesis is initiated by the bi-allelic inactivation of "bona fide" tumor suppressor genes, such as RB1. Middle: Haploinsufficiency of tumor suppressor genes (such as TP53) is caused by the mono-allelic gene inactivation. 50% of gene dosage are sufficient for driving a cell towards malignancy. Right: The continuum model of gene dosage insufficiency of tumor suppressors postulates that gene dosage below 50% is driving tumorigenesis. However, complete loss of gene expression is lethal to the cell. Figure adapted from Berger et al., 2011, including results from Heinrichs et al., 2013.

To model gene dosage insufficiency, the graded downregulation of gene expression to levels below haploinsufficiency has to be mimicked in cells. To model changes in tumor suppressor gene dosage as opposed to a complete knockout of gene expression, RNA interference (RNAi) has become the technology of choice (Caplen et al., 2001; Elbashir et al., 2001). RNAi employs the delivery of sequence-specific double-stranded small hairpin RNAs (shRNAs) into a cell. These shRNAs are converted by the endoribonuclease Dicer into small interfering RNAs (siRNAs) that mediate post-transcriptional gene silencing by binding to complementary regions of cellular RNAs, in particular mRNAs. Thereby, they initiate the translational silencing of the targeted mRNAs and their degradation. For example, Rad17 was identified as a haploinsufficient tumor suppressor gene using an RNAi-based screening:

shRNAs partially suppressing its expression in murine HSPCs promoted lymphomagenesis, whereas shRNA sequences mediating a complete repression of Rad17 expression were selected against in the lymphomas (Bric et al., 2009). Similarly, RPS14 was identified in $CD34^+$ human HSPCs to function as a haploinsufficient tumor suppressor in an RNAi screen for tumor suppressor genes in the distal CDR of chromosome 5q in MDS (Ebert et al., 2008). Furthermore, RNAi *in vivo* showed a gene dosage dependency for MYBL2. Look and colleagues showed that reduction of the Mybl2 gene dosage to 30% in murine HSPCs promoted myeloid transformation in mice, whereas lower gene dosages were lethal to the cells (Heinrichs et al., 2013; Figure 2, right).

3.4 The role of α-Catenin in homeostasis and tumorigenesis

The human gene encoding α-Catenin, CTNNA1, localizes to chromosome 5q31 and is one of the candidate tumor suppressor genes in the proximal CDR (Figure 1). It encodes a 102 kDa protein of 906 amino acids consisting of 16 coding exons and one 5' non-coding exon (Oda et al., 1993; Kobielak and Fuchs, 2004). The murine Ctnna1 gene maps to chromosome 18q11.0 and is highly conserved to the human α-Catenin protein (99.3% sequence identity at the amino acid sequence level; Oda et al., 1993; Guenet et al., 1995).

α-Catenin is a member of the catenin family and crucial for the formation of adherens junctions in various types of epithelial tissues (Herrenknecht et al., 1991; Hirano et al., 1992; Torres et al., 1997). Adherens junctions are critical for the maintenance of cell-cell adhesion, cellular polarity and tissue organization (Harris and Tepass, 2010). The cytoplasmic domain of the transmembrane core protein E-Cadherin interacts with β-Catenin, which in turn binds to α-Catenin. α-Catenin integrates the adherens junction protein complex to the actin cytoskeleton and promotes intercellular adhesion and mechanical stability (Kobielak and Fuchs, 2004; Li et al., 2015).

In the past years, a role of α-Catenin as a tumor suppressor in epithelial cancers has been elucidated. The expression of α-Catenin was found to be reduced in solid epithelial tumors of the breast, colon, prostate and skin (Raftopoulos et al., 1998; Aaltomaa et al., 2005; Ding et al., 2010; Hollestelle et al., 2010; Craig et al., 2013). In patient samples, the reduced CTNNA1 expression levels are associated with a higher tumor burden and mediated enhanced metastatic progression (Raftopoulos et al., 1998; Nakopoulou et al., 2002). The downregulation of CTNNA1 expression in primary human tumor cells or cancer cell lines leads to the disruption of epithelial cell integrity and to the loss of cell-cell adhesion, a characteristic trait of invasive tumor cells (Raftopoulos et al., 1998; Aaltomaa et al., 2005; Benjamin and Nelson, 2008; Ding et al., 2010; Hollestelle et al., 2010; Craig et al., 2013). The loss of α-Catenin expression in these epithelial tumor cells originated from different events, such as chromosomal deletion (Horrigan et al., 2000; Ding et al., 2010), DNA methylation (Ye et al., 2009), gene mutation (Hollestelle et al., 2010) or modulation of expression by an ischemic microenvironment (Plumb et al., 2009). These studies have suggested a tumor

suppressor role for α-Catenin in human epithelial tumors. To reveal the tumor suppressor function of α-Catenin in mouse epithelial cells, mouse models for reduced Ctnna1 expression were established. The constitutive knockout of Ctnna1 in mice is lethal, because it impairs the development of the trophoblast epithelium and the resulting mutant blastocysts are incapable to hatch from the zona pellucida and implant into the uterus (Torres et al., 1997). Therefore, several tissue-specific conditional knockout mice (Cre/lox technology) have been established to bypass the requirement for α-Catenin in the early embryonic development. For instance, conditional loss of Ctnna1 expression in skin cells leads to the loss of cell polarity, development of keratinocyte hyperproliferation and squamous skin cell carcinomas (Vasioukhin et al., 2001; Silvis et al., 2011). Furthermore, the Cre-mediated knockout of α-Catenin in neural tissue mediates hyperproliferation of neural progenitor cells, enlargement of the cerebral cortex and defects in radial glial cell polarity (Lien et al., 2006; Schmid et al., 2014). Thus, the tumor suppressor function of α-Catenin in epithelial tissues has been validated in several mouse models of reduced α-Catenin gene expression.

Apart from its role as a structural component of the adherens junctions, other functions of α-Catenin were revealed. It has been shown to act as a negative regulator of three major signaling pathways: NFκB signaling, Wnt signaling and Hippo signaling (Schlegelmilch et al., 2011; Silvis et al., 2011; Lamar et al., 2012; Choi et al., 2013; Piao et al., 2014). These signaling pathways are involved in proliferation, homeostasis and tumorigenesis. The proposed novel functions of α-Catenin in their regulation follow a common theme: in all three pathways, the key effector protein, a transcription factor, is retained in the cytoplasm by direct or indirect interaction with α-Catenin and the transcription of its target genes is prevented (Figure 3). For example, conditional deletion of Ctnna1 in the murine hair follicle stem cell

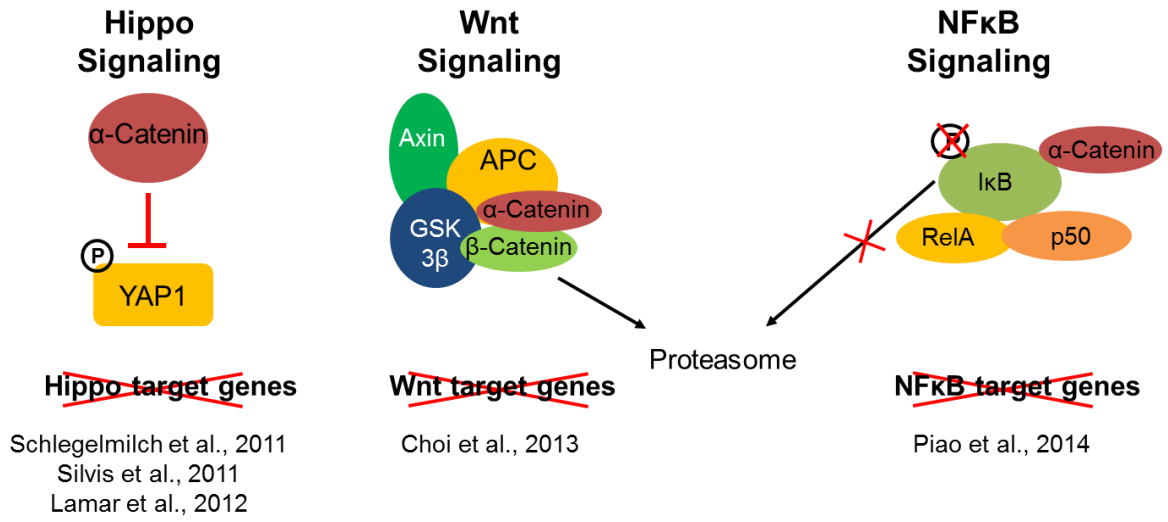

Figure 3: α-Catenin is a negative regulator of Hippo, Wnt and NFκB signaling pathways.
Left: α-Catenin prevents dephosphorylation of the transcription factor YAP1, which is required for its nuclear localization and target gene transcription. Middle: α-Catenin associates with APC and β-Catenin and stabilizes the cytoplasmic β-Catenin "destruction complex" that promotes constant proteasomal degradation of β-Catenin and prevents its nuclear localization. Right: α-Catenin inhibits phosphorylation of IκB and prevents it from proteasomal degradation. IκB retains the NFκB transcription factor complex (here RelA and p50) in the cytoplasm and prevents target gene transcription.

compartment caused keratoacanthomas in mice by the loss of cell-cell contact inhibition (Silvis et al., 2011). α-Catenin acts as an upstream regulator of Yap1, the effector of the Hippo signaling pathway, and determines its subcellular (nuclear or cytoplasmic) localization (Schlegelmilch et al., 2011; Silvis et al., 2011; Lamar et al., 2012; Figure 3, left). Ablation of α-Catenin causes increased Yap1 signaling and leads to uncontrolled proliferation and malignant transformation of follicular and epidermal stem cells of the skin in mice (Schlegelmilch et al., 2011; Silvis et al., 2011). Moreover, Jones and colleagues showed that α-Catenin is able to bind to APC and β-Catenin in HEK-293T cells and the H1 human embryonic stem cell line (Choi et al., 2013; Figure 3, middle). APC is a core protein of the β-Catenin destruction complex in Wnt signaling that regulates the amount of cytosolic β-Catenin and its nuclear localization for Wnt target gene transcription. According to the authors, α-Catenin is required for the retention of β-Catenin in the cytoplasm and the termination of β-Catenin-dependent target gene transcription (Choi et al., 2013). Furthermore, Li Ma and colleagues showed that α-Catenin acts as a tumor suppressor in E-cadherin negative basal-like breast cancer cell lines (Piao et al., 2014). They identified α-Catenin to be required for the stabilization of the IκB protein which in turn inhibits the nuclear localization of the NFκB effector proteins and represses the transcription of NFκB target genes (Piao et al., 2014; Figure 3, right). However, the role of α-Catenin in Wnt and NFκB signaling has not been validated *in vivo*.

Taken together, depending on the cellular context, α-Catenin was shown to act as an essential protein for maintaining tissue homeostasis and cellular integrity and simultaneously act as a negative regulator of mitogenic signaling pathways.

3.5 Objective of this thesis

The most frequent recurrent cytogenetic aberrations in MDS are heterozygous deletions of chromosome 5q (Haase et al., 2007). The investigation of this deletion delineated two distinct commonly deleted regions, a proximal and distal CDR (Le Beau et al., 1993; Boultwood et al., 1994). Though extensive efforts have been undertaken, homozygous inactivation of the genes located within the CDRs were not identified to date. This strongly suggests that MDS with del(5q) is driven by haploinsufficiency or sub-haploinsufficiency (gene dosage of 50% or less) of one or more tumor suppressor genes located within these CDRs (Ebert, 2009). The recent identification of RPS14 as the haploinsufficient tumor suppressor gene in the distal CDR supports this notion. RPS14 was identified as a haploinsufficient tumor suppressor gene by a comprehensive RNAi screening in human $CD34^+$ HSPCs (Ebert et al., 2008). However, the identity of the tumor suppressor genes in the proximal CDR still remains obscure. So far, haploinsufficiency of EGR1, a gene located in the proximal CDR, resulted in the development of a myeloprolerative disorder *in vivo*, however, it did not mimic the natural history of MDS in mice (Joslin et al., 2007). Thus, gene dosage deficiency of other tumor suppressor genes located within the proximal CDR are proposed to be involved in the pathogenesis of MDS with del(5q).

The CTNNA1 gene is located in proximal CDR and has been identified as one of the genes, which are transcribed in human $CD34^+$ HSPCs (Horrigan et al., 2000). Inactivating mutations of the retained allele of CTNNA1 in cells of MDS patients with del(5q) were not identified to date. However, CTNNA1 was strongly downregulated in leukemia-initiating cells (L-ICs, $CD34^+$ $CD38^-$ $CD123^+$ Lin^-) of patients with MDS with del(5q) compared to control cells (Liu et al., 2007). Therefore, in this thesis, I proposed that α-Catenin functions as a gene dosage dependent tumor suppressor gene in MDS with del(5q). So far, the role of α-Catenin as a tumor suppressor candidate gene in myeloid malignancies has been investigated exclusively *in vitro*. Thus, I investigated, whether reduced gene dosage of α-Catenin in murine HSPCs drives the development of a myeloid malignancy *in vivo*. I employed RNAi in a transduction-transplantation setting to model reduced gene dosage of Ctnna1 in murine HSPCs. Furthermore, I combined reduced Ctnna1 expression levels with the genetic inactivation of Tp53. This genetic model enabled me to show that a strongly reduced gene dosage of Ctnna1 drives myeloid malignancy *in vivo*. The pathogenesis of the disease was enhanced when Tp53 was genetically inactivated. Moreover, murine HSPCs were immortalized by RNAi-mediated reduced Ctnna1 expression and the growth advantage could be reverted in a dosage dependent manner by the re-expression of Ctnna1 to different levels. In accordance, the re-expression of CTNNA1 in the human HL60 del(5q) model cell line strongly impaired the growth of the cells and resulted in their monocytic differentiation. Gene expression analysis of these cells will be performed and will provide further insights into the molecular mechanisms of CTNNA1 as a tumor suppressor in myeloid malignancies.

4 Results

4.1 Eight of 24 shRNA encoding vectors mediated a Ctnna1 expression level of less than 50% of control and were selected for *in vivo* application

To identify shRNA sequences suitable for the RNAi-mediated knockdown of Ctnna1, NIH-3T3 cells were transduced with lentiviral vectors encoding one of 24 shRNAs targeting Ctnna1 expression. After transduction and Puromycin selection of the cells, RNA and protein were extracted and the expression level of Ctnna1 was measured by QRT-PCR and Western Blot. Eight vectors (encoding shRNA 405, 408, 409, 410, 412, 413, 418 and 422) showed a knockdown efficiency in NIH-3T3 cells resulting in Ctnna1 expression levels of less than 50% of control (28-49%, Figure 4). These vectors were chosen for competitive reconstitution experiments and their Puromycin expression cassette was exchanged with a Green Fluorescent Protein (GFP) expression cassette.

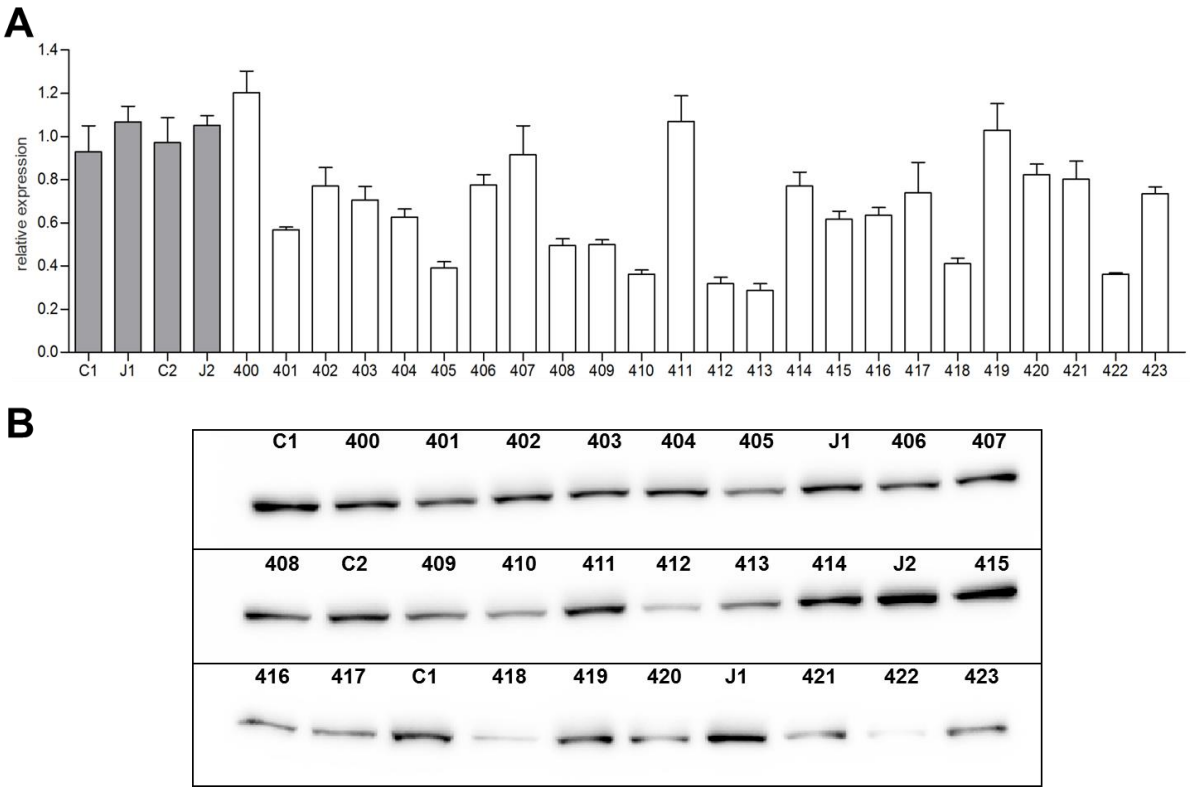

Figure 4: Eight shRNA encoding vectors mediated an expression level of Ctnna1 below 50% gene dosage. Ctnna1 expression levels in NIH-3T3 cells after transduction with lentiviral vectors encoding one out of 24 shRNA sequences targeting Ctnna1 and a Puromycin selection cassette. (A) QRT-PCR of 500 ng RNA: Ctnna1 expression levels of cells transduced with one Ctnna1 shRNA (400-423)-encoding vector were normalized to control transduced cells (shRNA C or J) and the expression of two housekeeping genes. (B) Ctnna1 protein expression in transduced cells detected by Western blot. (30 µg protein/lane, 1°: rb-α-ms-Ctnna1 antibody (Epitomics) 1:10,000, 2°: HRP-gt-α-rb 1:5,000)

4.2 Reduced Ctnna1 expression levels in murine HSPCs mediate a myeloid expansion phenotype *in vivo*

4.2.1 Reduced Ctnna1 expression levels minimally affect peripheral complete blood counts upon competitive reconstitution

To address whether gene dosage insufficiency of Ctnna1 in murine HSPCs provides a competitive advantage *in vivo*, I modeled reduced Ctnna1 expression levels by RNAi. The effect of the encoded shRNAs in transduced HSPCs was tested *in vivo* for the eight previously selected shRNA-expression vectors in a parallel competitive bone marrow reconstitution experiment (Figure 5A). The experiment was designed as a transduction-transplantation setup comparing two groups of mice: the experimental group consisted of eight animals transplanted with pooled HSPCs transduced with shRNA-expression vectors targeting Ctnna1. The control group consisted of three animals transplanted with pooled HSPCs transduced with shRNA-expression vectors encoding scrambled shRNA sequences (shRNAs C and D) unlikely to interfere with any gene expression (Figure 5A). Donor HSPCs were transduced with lentiviral particles encoding one shRNA-expression vector. To avoid multiple vector insertions, the amount of virus was adjusted to yield low transduction frequencies of 5-10% transduced cells. Prior to transplantation, transduced HSPCs were pooled at equal proportions and combined with freshly prepared whole bone marrow cells to support the

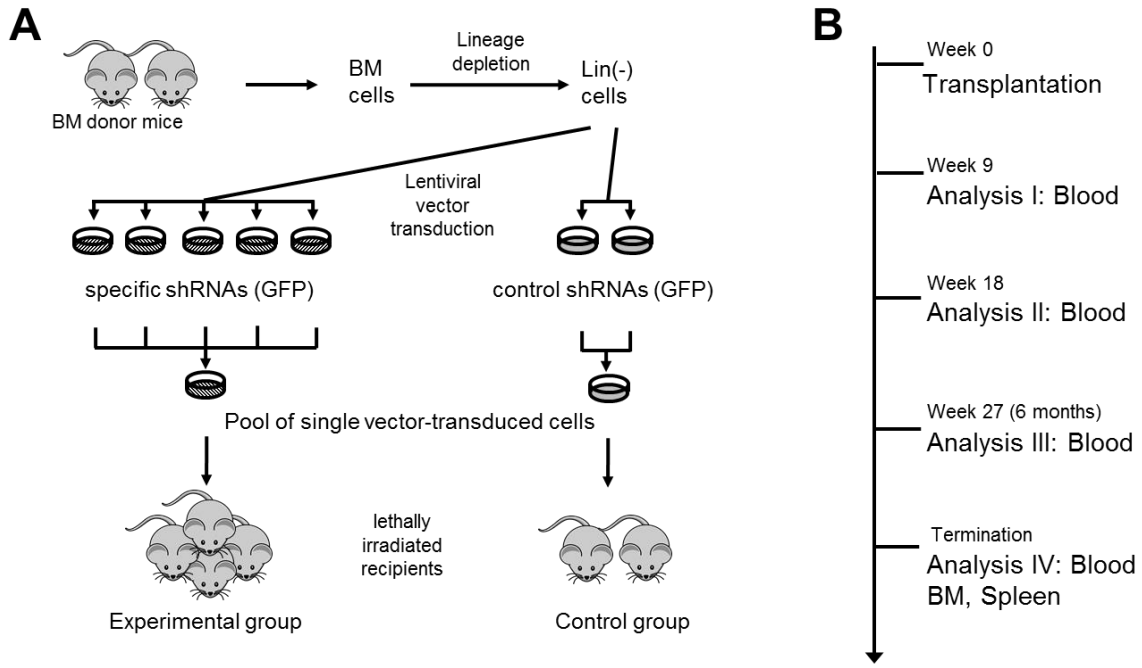

Figure 5: Schematic experimental design of competitive reconstitution experiment *in vivo*.
(A) $0.25x10^6$ lineage depleted murine HSPCs from donor animals were transduced with one out of eight shRNA-expression vectors. 24 hours after transduction single vector-transduced cells were pooled at equal proportions, combined with freshly prepared whole bone marrow cells and transplanted into lethally irradiated recipients ($0.1x10^6$ pooled genetically modified HSPCs and $2x10^6$ whole bone marrow cells per recipient animal). (B) After transplantation, blood was sampled three times over a six months period to monitor complete blood counts (CBCs), GFP^+ cell frequencies and the immunophenotype of the peripheral blood cells by flow cytometry. Upon termination of the experiment, mice were sacrificed and bone marrow cells, splenocytes and peripheral blood cells were prepared and analyzed accordingly.

short-term survival of the recipients. To monitor the expansion of HSPCs with reduced Ctnna1 expression in the bone marrow, blood was sampled four times over a six months period from the transplanted animals (Figure 5B).

Peripheral blood cells were isolated and analyzed by flow cytometry for the frequency of GFP^+ cells as a surrogate for the proportion of blood cells with reduced Ctnna1 expression. Two mice of the experimental group (M12 and M15) showed an increased frequency of GFP^+ cells in the peripheral blood after transplantation compared to the remaining six mice (Figure 6). However, mice of the control group (C11-C13) showed similar frequencies of GFP^+ cells. In healthy animals, this analysis provides a good estimate for the engraftment of GFP^+ HSPCs in the bone marrow. Very low frequencies of GFP^+ cells in the peripheral blood of six mice from the experimental group were indicative for an ineffective engraftment of transduced HSPCs, which were possibly outperformed by the high amount of transplanted non-transduced HSPCs (90-95%). However, malignant expansion of HSPCs with reduced Ctnna1 expression level in the bone marrow could have occurred without transmission of the high frequencies of GFP^+ cells to the peripheral blood.

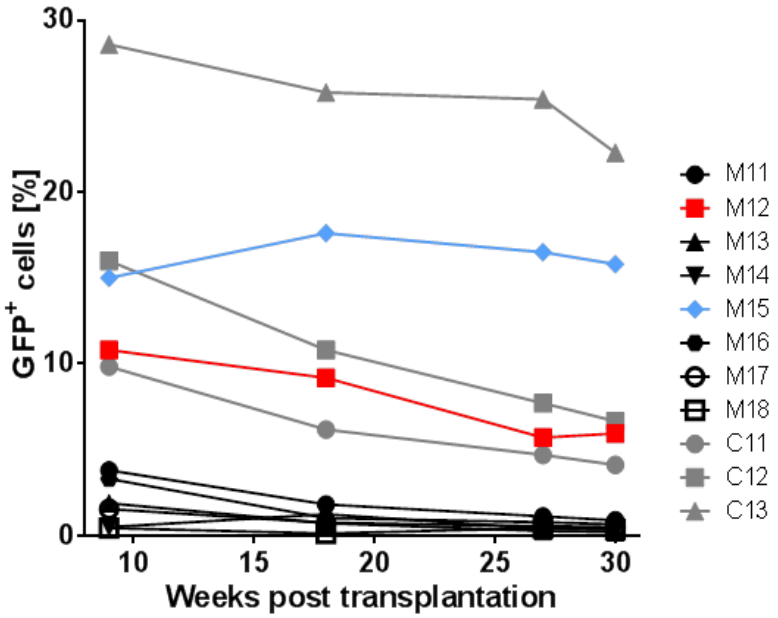

Figure 6: Time course of the frequencies of GFP^+ peripheral blood cells in transplanted mice.
The frequency of GFP^+ cells in the peripheral blood measured by flow cytometry is an estimate for the expansion of HSPCs with reduced Ctnna1 expression in the bone marrow. Mice transplanted with the pool of eight single vector-transduced HSPCs with reduced Ctnna1 expression are termed "M1x" and color-coded by black, red and blue lines and symbols. Mice transplanted with the pool of two single vector-transduced HSPCs containing control shRNA-vectors are termed "C1x" and color-coded by grey lines and symbols.

To find evidence for abnormal hematopoiesis, complete blood counts (CBCs) were measured four times over six months. Elevated counts of WBCs, i.e. leukocytosis, are indicative for acute infections, inflammation, recovery of tissue damage or the existence of a hematopoietic malignancy (Henry et al., 2011). Most transplanted mice of both, the experimental (M11-M18) and the control group (C11-C13), showed a constant rise in the WBC counts, even above the normal range of $14x10^3/\mu l$ at 27 weeks post transplantation

(Figure 7A). This indicated a successful reconstitution of the hematopoietic system, which is characterized by physiological fluctuations during the first six months after transplantation before hematopoiesis reaches an equilibrium (Jordan and Lemischka, 1990; Morrison and Weissman, 1994; Frasca et al., 2000; Serafini et al., 2007). When the experiment was terminated (30 weeks post transplantation), two mice of the experimental group (M12 and M15) showed an elevated WBC count in the peripheral blood compared to all other mice (Figure 7A). Strikingly, these two mice also exhibited increased frequencies of GFP^+ cells in the peripheral blood WBCs (Figure 6). However, the values of all other analyzed parameters (platelets (PLT); red blood cells (RBC), hemoglobin (HGB), hematocrit (HCT) and mean corpuscular volume (MCV)) were within their respective physiological ranges for all transplanted mice (Figure 7B-F).

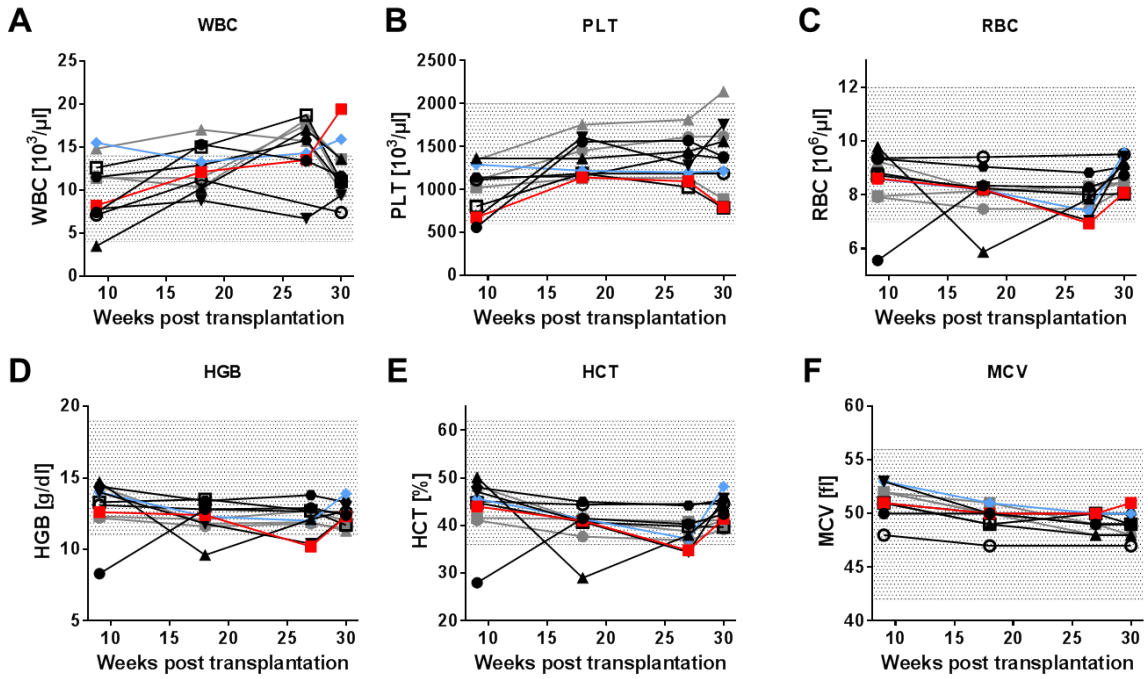

Figure 7: Regular monitoring of successful reconstitution by evaluation of complete blood counts (CBCs) over six months.
(A) White blood cell (WBC) counts, (B) platelet (PLT) counts, (C) red blood cells (RBC) counts, (D) hemoglobin (HGB) concentration, (E) hematocrit (HCT) and (F) mean corpuscular volume (MCV) of whole blood samples from transplanted mice measured four times over six months. Black, blue and red symbols indicate mice of the experimental group, grey symbols indicate mice of the control group (see Figure 6 for full legend). Shaded areas indicate the normal range for each parameter (WBC: 4-14x10^3/µl, PLT: 600-2000x10^3/µl, RBC: 7-12x10^6/µl, HGB: 11-19 g/dl, HCT: 36-62%, MCV: 42-56 fl) for healthy C57BL/6 mice (from: Charles River Laboratories International, Inc., 2012).

4.2.2 Murine HSPCs with reduced Ctnna1 expression expand in the bone marrow

Next, I explored whether the frequencies of GFP^+ cells in the peripheral blood of the transplanted mice reflected those in the bone marrow and the spleen at 30 weeks after transplantation. The animals were sacrificed and hematopoietic cells from these organs were isolated. The frequencies of GFP^+ cells were determined by flow cytometry in each population. Mice of the experimental group, that showed low GFP^+ cell frequencies in the

peripheral blood before, displayed the low frequencies in the bone marrow as well (mice M11, M13, M14, M16-M18; Figure 8). Mouse M15 showed GFP$^+$ cells in all three organs analyzed with the least frequency in the bone marrow (PB: 15.9%, BM: 12.7%, SP: 15.8%; Figure 8). All mice of the control group (C11-C13) displayed the same pattern of GFP$^+$ cell fractions in peripheral blood, bone marrow and spleen as mouse M15. In contrast, mouse M12 showed a high frequency of GFP$^+$ cells in the bone marrow (20%) compared to that found in the peripheral organs (PB: 6% and SP: 1.5%; Figure 8). This finding could indicate a block in maturation of hematopoietic cells with reduced Ctnna1 expression in the bone marrow of mouse M12.

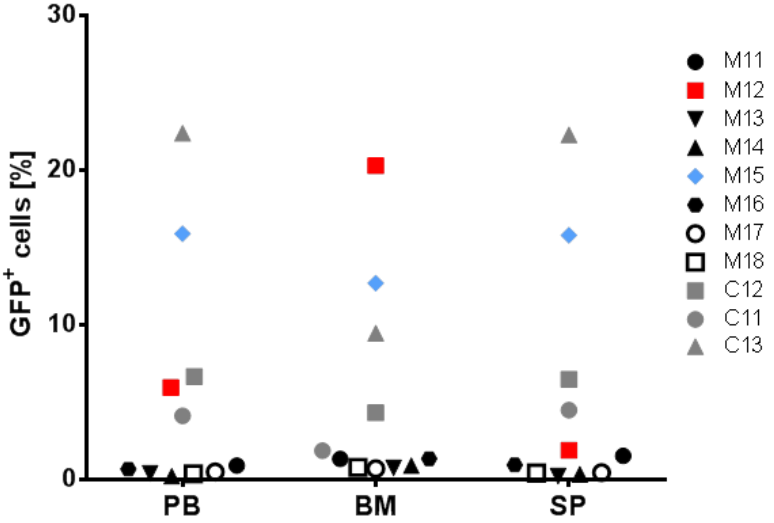

Figure 8: Frequency of GFP$^+$ cells in peripheral blood, bone marrow and spleen of recipient mice.
The frequencies of GFP$^+$ cells as a measure for the proportion of cells with reduced Ctnna1 were analyzed by flow cytometry in primary cells from the peripheral blood (PB), the bone marrow (BM) and the spleen (SP) at 30 weeks post transplantation. Mice transplanted with the pool of 8 single vector-transduced HSPCs with reduced Ctnna1 expression are termed "M1x" and color-coded by black, red and blue symbols. Mice transplanted with the pool of 2 single vector-transduced HSPCs containing control shRNA-vectors are termed "C1x" and color-coded by grey symbols.

To follow up on this finding, I verified the successful knockdown of Ctnna1 expression in GFP$^+$ bone marrow cells. GFP$^+$ cells of mice M12 and M15 were flow-cytometrically sorted, total RNA was extracted and the Ctnna1 expression level was determined by QRT-PCR. As expected, a successful knockdown of Ctnna1 expression to 13% was detected in GFP$^+$ bone marrow cells of mouse M12. GFP$^+$ bone marrow cells of mouse M15, however, did not show a reduced Ctnna1 expression (Figure 9).

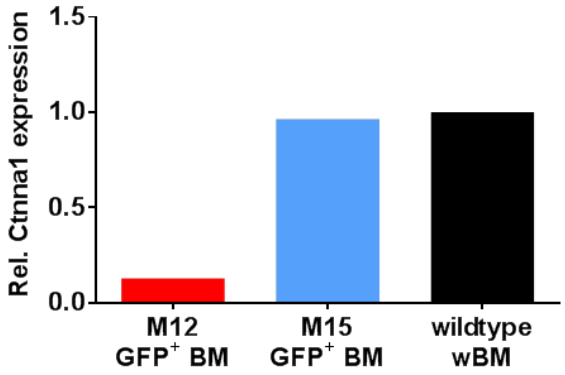

Figure 9: Successful knockdown of Ctnna1 expression by RNAi in GFP$^+$ bone marrow cells of mouse M12. After cDNA synthesis by reverse transcription from 170 ng total RNA, I performed QRT-PCR amplifying transcripts of Ctnna1 and two housekeeping genes (Ubqln1 and Vps39). The expression level of Ctnna1 was normalized on the mean expression level of the two housekeeping genes and compared to the physiological Ctnna1 expression level in whole bone marrow (wBM) cells of a wildtype animal.

4.2.3 Transplanted HSPCs with reduced Ctnna1 expression expand within the myeloid compartment of the bone marrow of mouse M12

To investigate hematological consequences of clonal dominance of bone marrow cells with reduced Ctnna1 expression, e.g. a block in maturation, I immunophenotyped the hematopoietic cells by flow cytometry. I measured the frequencies of myeloid (Ly6G$^+$, CD11b$^+$, Ly6G$^+$ CD11b$^+$) and lymphoid (CD3e$^+$, CD45R$^+$) cells in peripheral blood (PB),

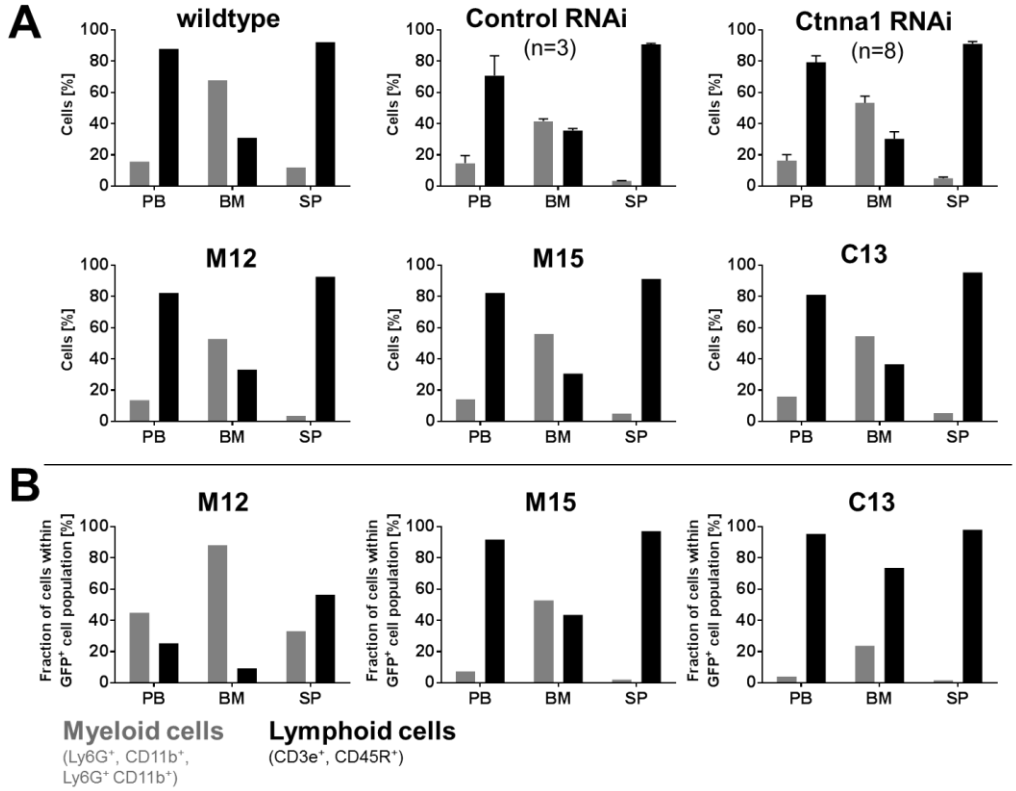

Figure 10: Cells with reduced Ctnna1 expression expanded within the myeloid compartment of the bone marrow of mouse M12.
Mean frequencies of myeloid (grey bars) and lymphoid (black bars) cells measured by flow cytometry of peripheral blood (PB), bone marrow (BM) and spleen (SP). Mice M12, M15 and C13 showed elevated GFP$^+$ cell frequencies in the bone marrow and were additionally analyzed separately. (A) Myeloid and lymphoid cell frequencies of all cells and of (B) GFP$^+$ cells in PB, BM and SP.

bone marrow (BM) and spleen (SP). First, I compared the population frequencies without pre-gating on GFP^+ cells in the transplanted mice to those found in wildtype animals. The proportions of myeloid and lymphoid cells (average values: PB 20% and 80%; BM 55% and 45%; SP 10% and 90%) in the analyzed tissues were not impacted by the expansion of bone marrow cells with reduced Ctnna1 expression (Figure 10A). This indicated a normal hematopoiesis in all transplanted animals.

To address whether the GFP^+ cells expanded within one specific compartment of the hematopoietic organs of mice M12, M15 and C13, I performed the same analysis including a pre-gating on GFP^+ cells. The frequencies of lymphoid cells within the GFP^+ cell population of control mouse C13 were increased in all three tissues analyzed (PB: 95.4%, BM: 73.6%, SP: 98.0%) compared to the respective proportions measured without pre-gating on GFP^+ cells (Figure 10B, compared to A). The cellular composition within the GFP^+ cells of mouse M15 equaled those without pre-gating on GFP^+ cells (Figure 10B, compared to A). In contrast, mouse M12 showed a profound increase of the myeloid cell frequency (88.3%) within the GFP^+ cell population of the bone marrow (Figure 10B, compared to A). This myeloid phenotype was less pronounced in the GFP^+ cells of the peripheral blood (44.9%). Within GFP^+ cells of the spleen, the frequency of myeloid cells (33.2%) was nearly normal. This result indicated a strong differentiation bias towards the myeloid lineage of the cells with reduced Ctnna1 expression in the bone marrow of mouse M12. Moreover, the expansion of myeloid cells within the GFP^+ cells of the peripheral blood was less pronounced, indicating a block in maturation of hematopoietic cells in the bone marrow and a lack of transition to the periphery.

4.2.4 Clonal dominance of bone marrow cells with reduced Ctnna1 expression leads to decreased erythropoiesis in the bone marrow of transplanted mice

To further address the effect of transplanted HSPCs with reduced Ctnna1 expression on hematopoiesis, I analyzed bone marrow cells for their stages of erythroid differentiation. Undifferentiated murine erythroid progenitors are $CD71^-$ $Ter119^-$. With maturation, they start to express CD71 before further differentiation into erythroblasts induces expression of Ter119 on the cell surface, and the cells become $CD71^+$ $Ter119^+$. With enucleation of the erythroblast, CD71 expression is lost and mature reticulocytes/erythrocytes are $CD71^-$ $Ter119^+$ (Dzierzak and Philipsen, 2013). I measured the frequencies of $Ter119^-$ cells (immature erythroblasts) in relation to the frequencies of $Ter119^+$ cells (mature erythroid cells) of an age-matched wildtype animal and mice from the control group to the proportions found in mice from the experimental group.

Mice transplanted with HSPCs with reduced Ctnna1 expression showed increased frequencies of immature erythroblasts (68% $Ter119^-$ cells) compared to mice of the control group (58% $Ter119^-$ cells) and wildtype mice (55% $Ter119^-$ cells; Figure 11). This phenotype was even more pronounced in mice M12 (81% $Ter119^-$ cells) and M15 (74% $Ter119^-$ cells),

in which the GFP$^+$ cell population was expanded in the bone marrow. These results revealed a diminished erythropoiesis upon expansion of cells with reduced Ctnna1 expression in the bone marrow of transplanted mice.

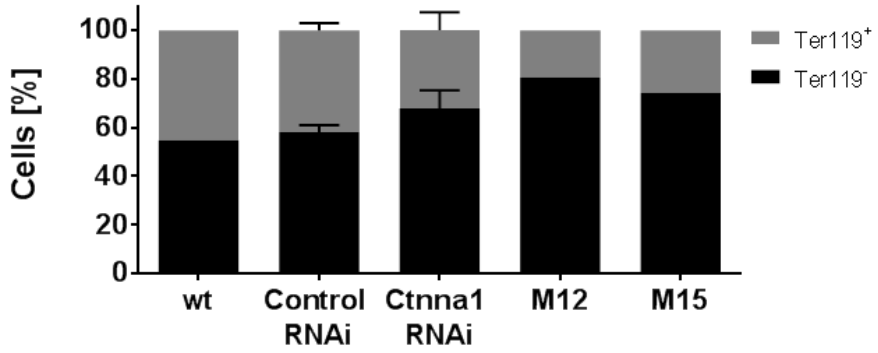

Figure 11: Mice transplanted with HSPCs with reduced Ctnna1 expression showed signs of impaired erythropoiesis in the bone marrow.
Aliquots of freshly prepared bone marrow cells of a wildtype mouse (wt) and transplanted mice of both groups were stained with anti-CD71 and anti-Ter119 antibodies to identify the stages of erythroid maturation. Ter119$^-$ cells (CD71$^-$ Ter119$^-$ and CD71$^+$ Ter119$^-$, black bars) as immature erythroblasts were compared to Ter119$^+$ cells (CD71$^+$ Ter119$^+$ and CD71$^-$ a Ter119$^+$, grey bars) as differentiated erythroid cells.

4.2.5 After transplantation, murine HSPCs with reduced Ctnna1 expression expand within the HSC compartment of the bone marrow

Reduced Ctnna1 expression levels in murine HSPCs affected the hematopoiesis of transplanted mice. To identify the stages of hematopoiesis in the bone marrow affected by the expansion of cells with reduced Ctnna1 expression, I analyzed the frequencies of lineage negative cells (Lin$^-$), LSK cells (Lin$^-$ Sca1$^+$ Kit$^+$ cells), and HSCs (hematopoietic stem cells according to the SLAM-family receptor code, LSK CD48$^-$ CD150$^+$). First, I compared the respective frequencies in the entire bone marrow of mice M12, M15, C13 to an age-matched wildtype mouse. Second, I investigated the fraction of GFP$^+$ cells within these

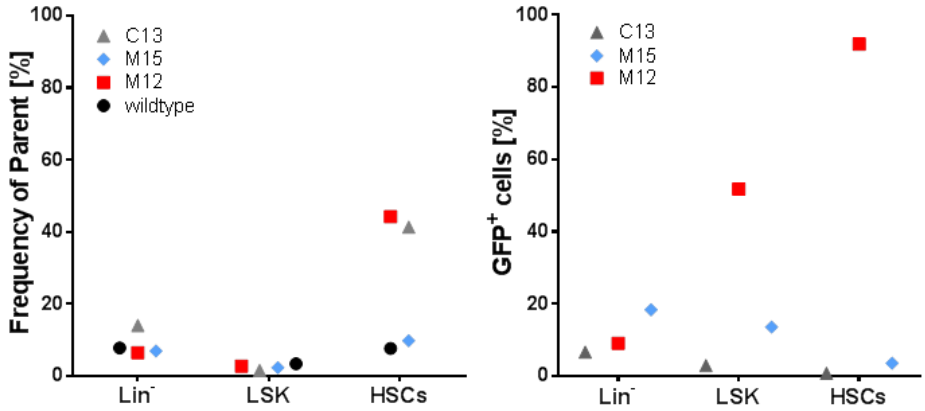

Figure 12: The LSK and HSC populations showed increased frequencies of GFP$^+$ cells in the bone marrow of mouse M12.
Flow cytometric analysis of lineage negative (Lin$^-$) cells, LSK cells and HSCs in the bone marrow of an age-matched wildtype mouse (black circle) and mice M12 (red square), M15 (blue diamond) and C13 (grey triangle). Left: Frequencies of parent population of the indicated hematopoietic subpopulations. Parent of Lin$^-$: P1, parent of LSK: Lin$^-$, parent of HSCs: LSK (as in Figure 57, top). Right: Frequency of the GFP$^+$ cell population within the indicated subpopulation.

subpopulations. The Lin^- and LSK cell frequencies of the transplanted mice were similar to those found in wildtype mice (Figure 12, left). However, mice M12 and C13 showed elevated HSC frequencies (M12: 44.2%, C13: 41.3%) compared to the wildtype mouse (7.6%; Figure 12, left). The frequency of GFP^+ bone marrow cells of mouse M12 was increased within the primitive compartments of hematopoietic cells, comprising 9% of Lin^- cells, 52% of LSK cells and 92% of HSCs (Figure 12, right). This was not observed for the bone marrow cells of mice M15 (Lin^-: 18.4%, LSK: 13.6%, HSC: 3.6%) and C13 (Lin^-: 6.7%, LSK: 3%, HSC: 0.85%), in which the frequencies of GFP^+ cells decreased within the primitive cell compartments (Figure 12, right). The data strongly suggested a competitive advantage of bone marrow cells with reduced Ctnna1 expression within the progenitor cell and HSC compartments of mouse M12.

Taken together, six months after transplantation of HSPCs with reduced Ctnna1 expression, I detected an expansion of GFP^+ cells in the bone marrow of two (M12 and M15) out of eight transplanted mice. The GFP^+ bone marrow cells of mouse M12 showed a strong differentiation bias towards the myeloid lineage and a diminished bone marrow erythropoiesis. Furthermore, the GFP^+ bone marrow cells of mouse M12 expanded within the progenitor cell compartments. However, measurement of CBCs did reveal signs of a hematologic disease in the peripheral blood.

4.2.6 Expansion of HSPCs in the bone marrow of mice M12 and M15 is mediated by the expression of shRNAs 405 and 409

Since mice M12 and M15 both showed a marked increase of the proportion of GFP^+ cells in the bone marrow and those animals had been transplanted with a pool of eight single vector-transduced HSPC preparations, I aimed to determine the fraction of each shRNA sequence within the pool of GFP^+ cells. Genomic DNA (gDNA) of GFP^+ bone marrow cells from both mice, M12 and M15, showed a mixture of shRNA-encoding integrated vector

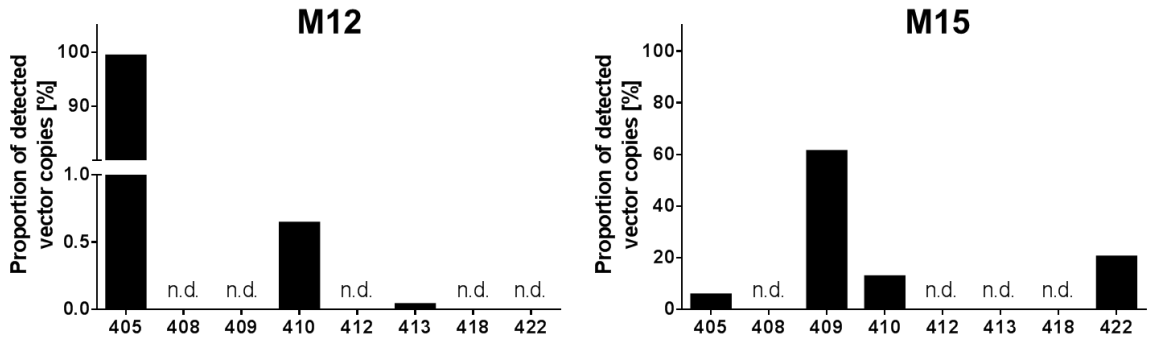

Figure 13: GFP^+ bone marrow cells from mice M12 and M15 were originating from a mixture of transplanted single-vector transduced HSPCs.
QPCR-analysis of the gDNA from whole bone marrow cells of mouse M12 showed the most prominent expansion of cells expressing shRNA 405. They also contributed to the GFP^+ cells in the bone marrow of mouse M15. However, mouse M15 showed the highest signal of integrated vector sequence for shRNA 409. Additionally, shRNAs 410, 413 and 422 were detected in gDNA of both mice. n.d. – not detected

copies. The most prominent signal in the gDNA of mouse M12 was detected from the vector encoding shRNA 405 (99.32%; Figure 13, left). Also, vectors encoding shRNA 410 (0.64%) and 413 (0.04%) were detected at very low copy numbers (Figure 13, left). In the gDNA from bone marrow cells of mouse M15 the strongest amplification signal was detected from the vector encoding shRNA 409 (61.21%; Figure 13, right). The shRNA sequences of 405 (5.72%), 410 (12.74%) and 422 (20.33%) were amplified at lower copy numbers in gDNA of bone marrow cells from mouse M15 as well (Figure 13, right). These results indicated that the GFP^+ cells of mice M12 and M15 originated from different single vector-transduced transplanted HSPCs. Remarkably, in the bone marrow of mouse M12 the HSPC population transduced with the vector encoding shRNA 405 contributed almost entirely to the GFP^+ cell population.

4.2.7 Expansion of GFP^+ cells in the bone marrow of mice M12 and M15 was not due to insertional mutagenesis

To rule out that mutagenic effects of the vector integration drove the expansion of GFP^+ cells in the bone marrow of mice M12 and M15, I performed LAM-PCR to identify the genomic sites of vector integration. I detected one integration site for mouse M12 and three integration sites for mouse M15 (Figure 14). The integration site detected in the gDNA of bone marrow cells from mouse M12 was located on mouse Chr. 14qB (position at

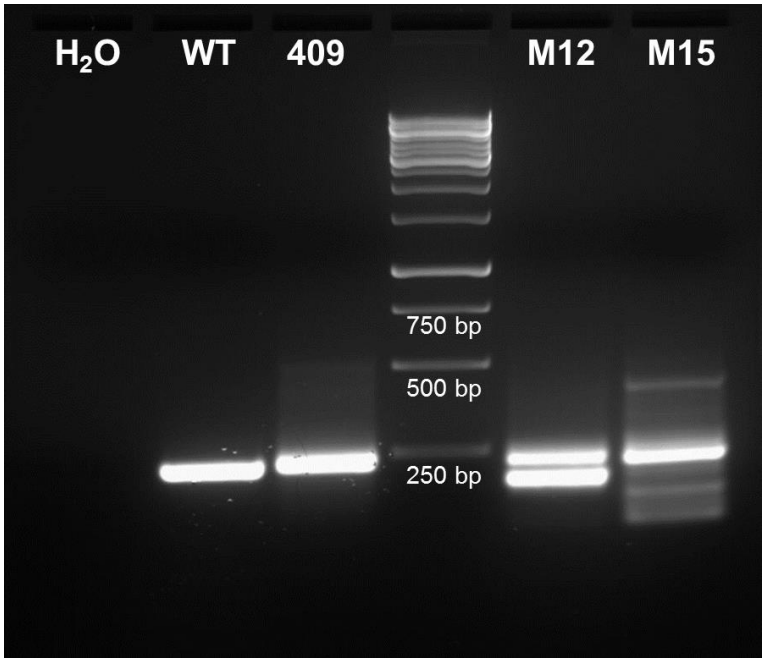

Figure 14: Detection of integration sites in gDNA from bone marrow cells of mice M12 and M15.
LAM-PCR of gDNA from bone marrow cells of mice M12 and M15 showed one integration site for mouse M12 and three integration sites for mouse M15. The DNA from the bands of the 200 bp-product of mouse M12 and the DNA from the 400 bp-, 180 bp- and 150 bp-products were isolated and sequenced. The band amplified at 240 bp in size served as positive control within the vector sequence and was therefore amplified from a dilution of shRNA 409-encoding vector plasmid DNA (lane 409) and from gDNAs of both mice (M12 and M15). The lane containing the PCR-product from wildtype bone marrow gDNA (WT) treated with the same enzyme as the gDNAs from mice M12 and M15 showed an unspecific product that could originate from unspecific linker annealing. 2% Agarose, 400 ms exposure time

37,777,850 bp-37,778,100 bp GRCm38/mm10) in a 1.2 Mb genomic region without any annotated genes, indicating that insertional mutagenesis was unlikely the driver of expansion of GFP^+ cells in the bone marrow of mouse M12.

The 180 bp- and 150 bp-PCR products from gDNA from mouse M15 could not be sequenced successfully. However, the sequencing of the 400 bp-PCR product showed integration in intron 50 of the Dmd gene locus (mouse Chr. XqC1, position at app. 84,458,550 bp-84,458,700 bp, GRCm38/mm10). These results suggested that insertional mutagenesis was unlikely the driver of expansion of GFP^+ cells in the bone marrow of mouse M15, as mutations of the Dmd gene are associated with muscular dystrophy of the skeletal and cardiac muscle and are not involved in malignant hematopoiesis (Jacobs et al., 1981; Murray et al., 1982).

4.3 The clonal dominance phenotype *in vivo* of transplanted HSPCs encoding shRNA 405 is reproducible

4.3.1 Single vector-transduced HSPCs encoding shRNA 405 or 409 successfully engraft without causing overt hematologic disease

I showed that HSPCs transduced with vectors encoding shRNA 405 or shRNA 409 had a competitive reconstitution advantage in the bone marrow of transplanted mice. To

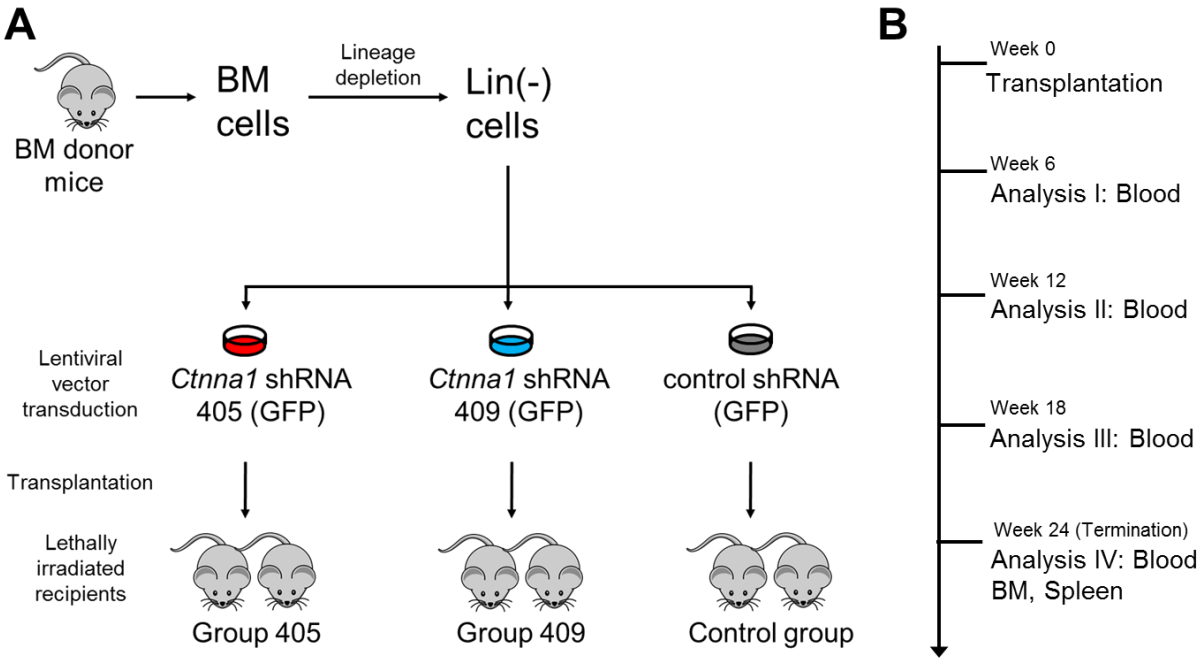

Figure 15: Schematic experimental design of second competitive reconstitution experiment *in vivo*.
(A) $1x10^6$ lineage depleted murine HSPCs from donor animals were transduced with shRNA-expression vectors encoding shRNA 405, 409 or control shRNA. 24 hours after transduction single vector-transduced cells were combined with freshly prepared whole bone marrow cells and transplanted into lethally irradiated recipients ($0.12x10^6$ HSPCs containing single vector-transduced HSPCs at a frequency of 5-10% and $2x10^6$ whole bone marrow cells per recipient animal). (B) After transplantation, blood was sampled three times over a six months period to measure complete blood counts (CBCs), GFP^+ cell frequencies and the immunophenotype of the peripheral blood cells by flow cytometry. Upon termination of the experiment, mice were sacrificed and bone marrow cells, splenocytes and peripheral blood cells were prepared and analyzed accordingly.

confirm this finding, I performed a subsequent reconstitution experiment using only vectors encoding shRNA 405 and 409 in separate mice. Each experimental group comprised six mice (group 405, group 409) and the control group included four mice (Figure 15A).

As indicated in Figure 15B, blood was sampled regularly and GFP^+ cell frequencies were quantified by flow cytometry. All transplanted mice showed GFP^+ cells in the peripheral blood at all measured time points indicating a successful engraftment of transduced HSPCs in the bone marrow (Figure 16). However, in most mice the GFP^+ cell population in the blood decreased over time. At experiment termination, the median GFP^+ cell frequency in the peripheral blood was 8% for mice of the control group, 4% for mice of group 409 and 14% for mice of group 405 (Figure 16, 24 weeks post transplantation).

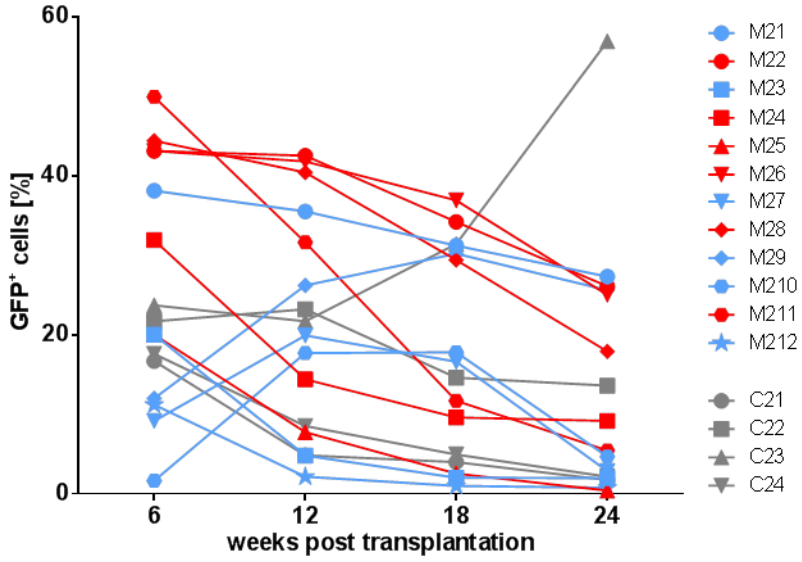

Figure 16: Time course of the frequencies of GFP^+ peripheral blood cells in transplanted mice.
The frequency of GFP^+ cells in the peripheral blood measured by flow cytometry is an estimate for the expansion of HSPCs with reduced Ctnna1 expression in the bone marrow. Mice transplanted with single vector-transduced HSPCs encoding shRNA 405 or shRNA 409 are termed "M2x" and color-coded by red and blue lines and symbols, respectively. Mice transplanted with single vector-transduced HSPCs encoding control shRNA are termed "C2x" and color-coded by grey lines and symbols.

Complete blood counts (CBCs) showed a constant rise of WBC counts in all transplanted mice, even above the normal range of $14x10^3/\mu l$ at 18 weeks post transplantation (Figure 17A), confirming a successful reconstitution of the hematopoietic system. 24 weeks after transplantation two mice of group 405 (M22 and M211) exhibited an elevated WBC count, as did control mouse C23. Mouse M24 presented low PLT and RBC counts at 24 weeks after transplantation. However, the values of all other analyzed parameters were within their normal ranges for these mice (Figure 17B-F). Mouse M28 of group 405 showed a decreased RBC count at experiment termination, indicating the onset of an anemic phenotype. This notion was supported by a low HCT value. CBCs of transplanted mice from group 409 were mostly within the normal ranges at termination. The spleen weights averaged at 65±6 mg for control mice, 73±14 mg for mice of group 405 and 71±5 mg for mice of group

409, all being within the normal range (60-100 mg). Taken together, these results did not reveal any evidence of an overt hematological disease in the transplanted animals.

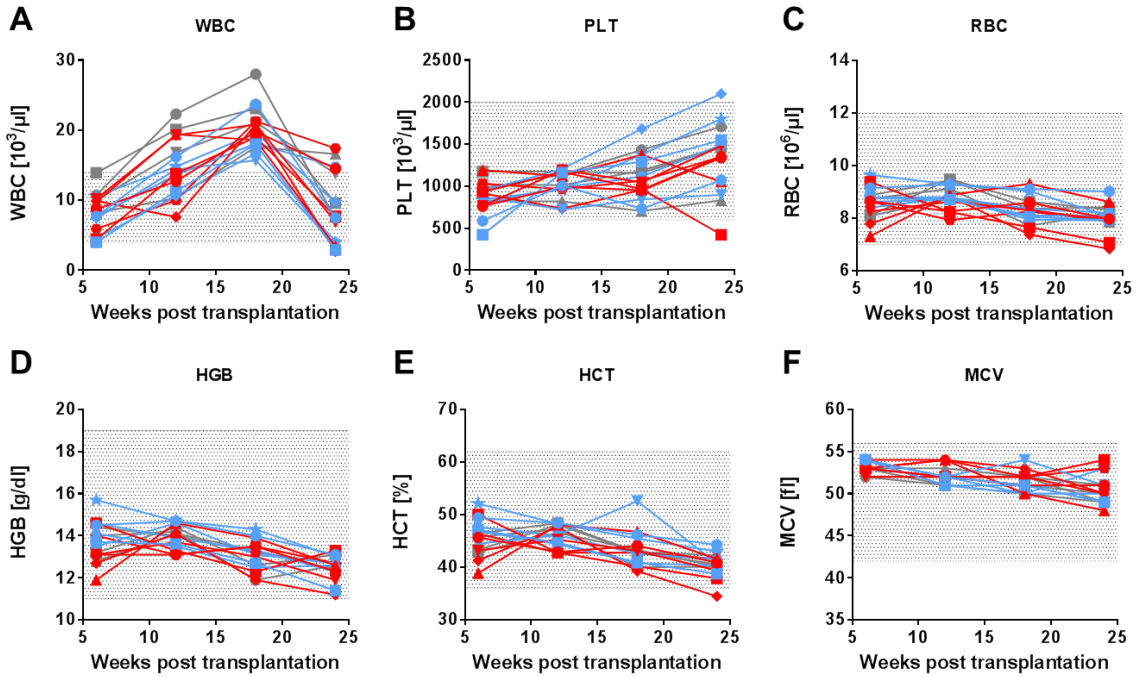

Figure 17: Regular monitoring of successful reconstitution by evaluation of complete blood counts (CBCs) over six months.
(A) White blood cell (WBC) counts, (B) platelet (PLT) counts, (C) red blood cells (RBC) counts, (D) hemoglobin (HGB) concentration, (E) hematocrit (HCT) and (F) mean corpuscular volume (MCV) of whole blood samples from transplanted mice measured four times over six months. Blue and red symbols indicate mice of the experimental groups 405 and 409, grey symbols indicate mice of the control group (see Figure 16 for full legend). Shaded areas indicate the normal range for each parameter (WBC: 4-14x10^3/µl, PLT: 600-2000x10^3/µl, RBC: 7-12x10^6/µl, HGB: 11-19 g/dl, HCT: 36-62%, MCV: 42-56 fl) for healthy C57BL/6 mice (from: Charles River Laboratories International, Inc., 2012).

4.3.2 HSPCs expressing shRNA 405 show a clonal dominance in the bone marrow of transplanted mice

After six months of reconstitution, mice were sacrificed and the frequencies of GFP^+ cell populations were measured in the hematopoietic organs. Four out of six mice of group 405 showed an expansion of GFP^+ cells in the bone marrow (34-44% for mice M22, M24, M26, M28), while the frequencies of GFP^+ cells in peripheral blood (9-26%) and spleen (5-19%) were significantly lower (PB vs. BM: P=0.0136, SP vs. BM: P=0.0142, paired t-test, two-tailed P-value, α=0.05, Figure 18). This observation was in accordance with the GFP^+ cell distribution I previously found in the hematopoietic organs of mouse M12 (Figure 8), in which bone marrow cells expressing shRNA 405 had been expanded. This distribution of GFP^+ cells in tendency applied to mouse C22 of the control group, however, the differences between the GFP^+ cell frequencies in the hematopoietic organs were not as pronounced. In contrast, GFP^+ cell frequencies in the bone marrow of mice of group 409 were equal or less when compared to peripheral blood or spleen in the same mouse (PB vs. BM: 0.6221, SP vs. BM: 0.9832, paired t-test, two-tailed P-value, α=0.05). These findings confirmed that

transplanted HSPCs expressing shRNA 405 showed a clonal dominance in the bone marrow and supported that the phenotype of mouse M12 was not based on an insertional mutagenesis.

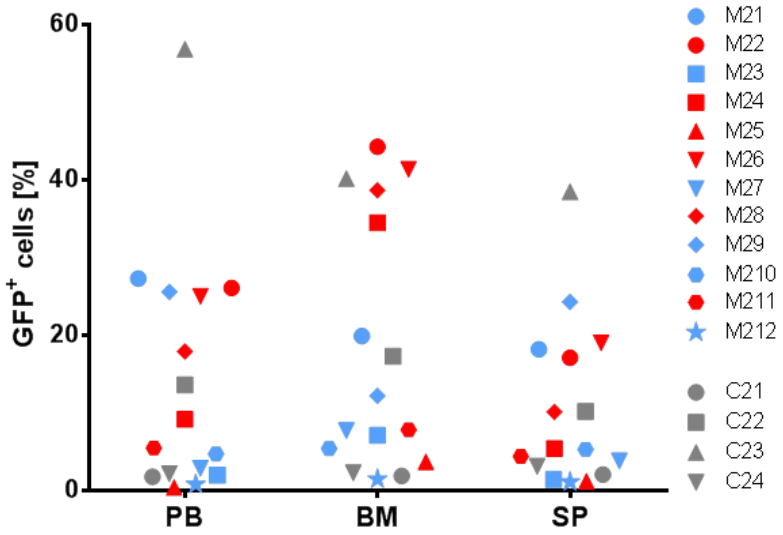

Figure 18: Frequency of GFP$^+$ cells in peripheral blood, bone marrow and spleen of recipient mice.
The frequencies of GFP$^+$ cells as a measure for the proportion of cells with reduced Ctnna1 were analyzed by flow cytometry in cells isolated from the peripheral blood (PB), the bone marrow (BM) and the spleen (SP) at 24 weeks post transplantation. Mice transplanted with single vector-transduced HSPCs encoding shRNAs 405 and 409 are termed "M2x" and color-coded by red and blue symbols, respectively. Mice transplanted with single vector-transduced HSPCs encoding control shRNA-vectors are termed "C2x" and color-coded by grey symbols.

Next, I quantified the Ctnna1 expression level in the GFP$^+$ bone marrow cells and detected normal expression levels for control mice (mean relative expression: 1.17) compared to wildtype bone marrow cells (Figure 19). In GFP$^+$ bone marrow cells of mouse M21 of group 409 the Ctnna1 expression level was reduced to 58% of wildtype level. Mice of group 405 showed a relative Ctnna1 expression level of 39-43% of wildtype level in GFP$^+$ bone marrow cells (Figure 19) revealing that the shRNA expression and the knockdown of Ctnna1 expression is intact.

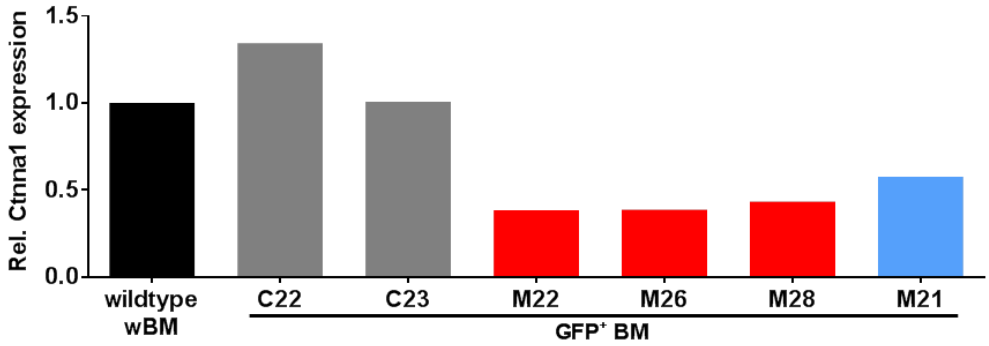

Figure 19: RNAi by expression of shRNAs 405 and 409 in murine bone marrow cells mediated reduced levels of Ctnna1 expression *in vivo*.
Relative Ctnna1 expression levels measured by QRT-PCR in sorted GFP$^+$ bone marrow cells of representative transplanted mice of each group compared to wildtype levels in whole bone marrow (wBM) cells. Black: wildtype mouse; grey: control mice; red and blue: mice of groups 405 and 409, respectively.

4.3.3 Cells with reduced Ctnna1 expression expand in the myeloid compartment of the bone marrow

To pursue the notion of a differentiation bias towards the myeloid lineage as previously observed in mouse M12, I investigated whether the cellular composition of myeloid and lymphoid cells in peripheral blood, bone marrow and spleen was shifted towards one lineage upon GFP^+ cell expansion. The lineage analysis of all mice of the control group, group 405 and 409 showed no shift in the cellular composition of myeloid and lymphoid cells in the three organs analyzed (Figure 20A, top). The separate analysis of the mice of group 405 with GFP^+ cell expansion in the bone marrow (mice M22, M26, M28) showed increased myeloid cell frequencies (51-65%) in the bone marrow (Figure 20A, bottom). Next, I analyzed the myeloid cell frequencies within the GFP^+ cell populations. This analysis showed

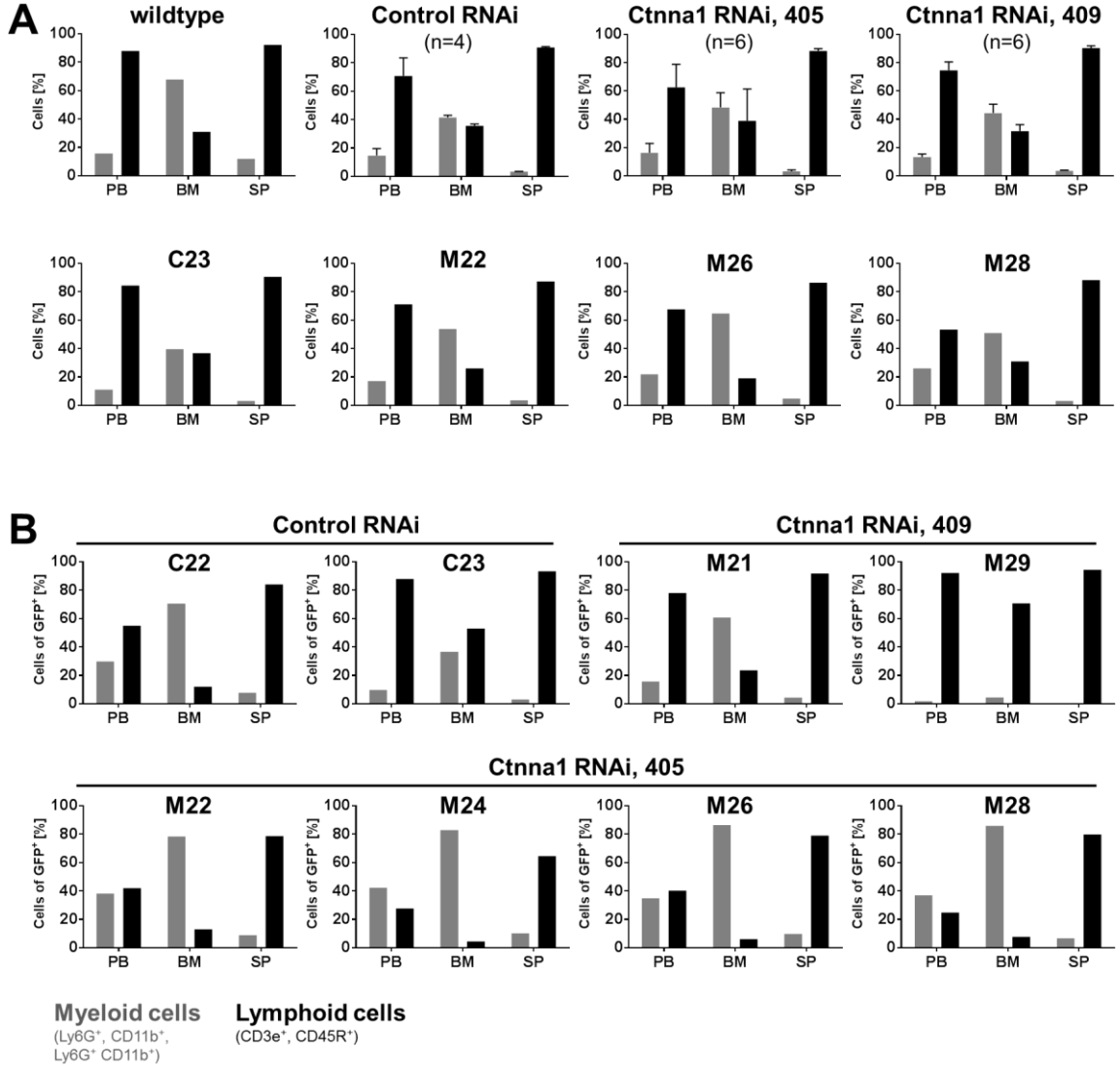

Figure 20: Transplanted mice of group 405 with increased GFP^+ cell population show evidence of a myeloid differentiation bias according to the cellular composition of the bone marrow.
Mean frequencies of myeloid (grey bars) and lymphoid (black bars) cells for peripheral blood (PB), bone marrow (BM) and spleen (SP). (A) Lineage cell frequencies in all cells of mice of the indicated group. Mice C23, M22, M26 and M28 showed the strongest elevation of GFP^+ cell frequencies in the bone marrow and were additionally analyzed separately. (B) Lineage cell frequencies within GFP^+ cells of the indicated organ of indicated mice.

that GFP$^+$ cells of mice C22 and C23 were either lymphoid or myeloid (Figure 20B, top left). The same applied to mice of group 409 (Figure 20B, top right). This finding suggested that control shRNA or shRNA 409 had no impact on cell fate determination. The frequencies within the GFP$^+$ cell population rather reflected the individual contribution to a hematopoietic lineage on a progenitor cell level. In contrast, GFP$^+$ bone marrow cells of mice of group 405 were almost exclusively comprised by myeloid cells (78.3-86.4%; Figure 20B). Furthermore, the proportion of myeloid cells within the GFP$^+$ cells in the peripheral blood was consistently increased (34.7-42.3%) for this group compared to control (9.7-29.8%) or group 409 (1.8-15.6%; Figure 20B). These findings confirmed the results I found in mouse M12, in which the GFP$^+$ cells expressing shRNA 405 were expanded within the myeloid lineage in bone marrow and peripheral blood.

4.3.4 Expansion of cells with reduced Ctnna1 expression impairs erythropoiesis in the bone marrow

Next, I analyzed the frequencies of immature erythroblasts (Ter119$^-$ cells) in the bone marrow of transplanted mice. Wildtype mice and mice of the control group showed a mean frequency of 55±6.2% Ter119$^-$ cells (Figure 21A). Similar frequencies were identified in the bone marrow of mice of group 409 (55±5.4% Ter119$^-$ cells). Mice of group 405, however, showed an increased level of Ter119$^-$cells (65±8.5%) in the bone marrow (Figure 21A). Next, I analyzed the frequencies of the Ter119$^-$ cell population in the bone marrow of single mice

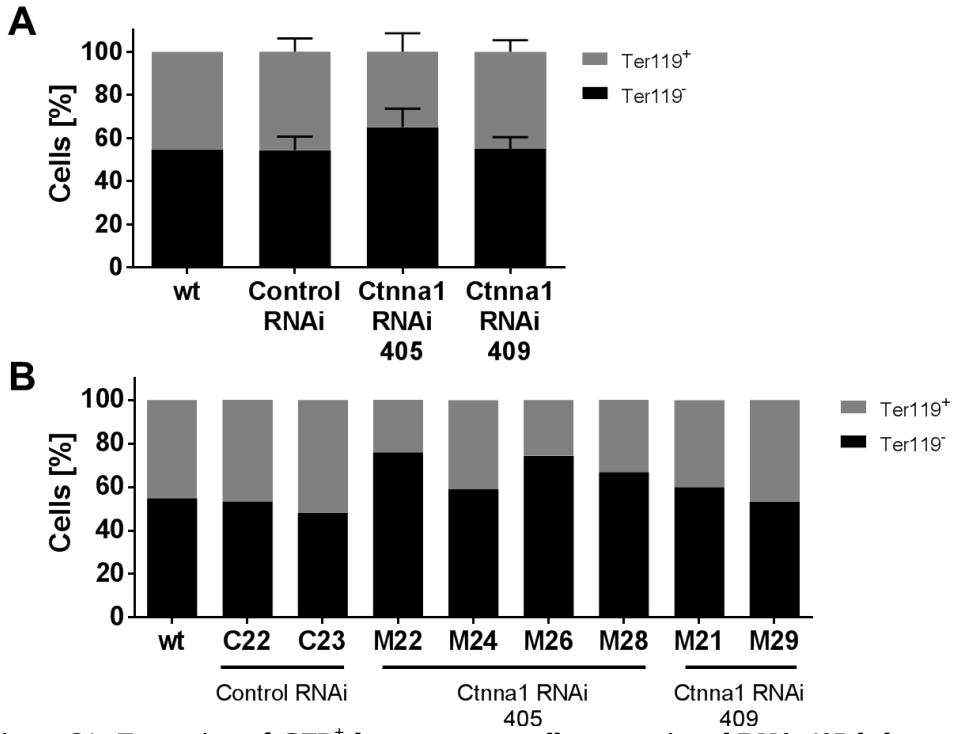

Figure 21: Expansion of GFP$^+$ bone marrow cells expressing shRNA 405 led to reduced bone marrow erythropoiesis.
Mean frequencies of Ter119$^-$ (black bars) and Ter119$^+$ cells (grey bars) in the bone marrow of (A) wildtype mice (wt), control mice (Control RNAi), mice of group 405 (Ctnna1 RNAi, 405) and mice of group 409 (Ctnna1 RNAi, 409) and (B) single mice with expansion of GFP$^+$ cells of the control group, group 405 and group 409.

with expanded GFP$^+$ cell population. Mice C22 and C23 showed 55% Ter119$^-$ as measured in the bone marrow of the wildtype mouse (Figure 21B). The same applied to mouse M29 of group 409. Mouse M21 of group 409, however, displayed a minor increase in Ter119$^-$ cells (60%) when compared to wildtype and control (Figure 21B). All mice of group 405 with expansion of the GFP$^+$ cell population in the bone marrow showed an increase in Ter119$^-$ cells (e.g. mouse M22: 76% Ter119$^-$ cells; Figure 21B). These data strongly suggested a reduced erythropoiesis when HSPCs expressing shRNA 405 were expanded in the bone marrow.

4.3.5 Bone marrow cells with reduced Ctnna1 expression expand within the HSC and progenitor cell compartments

To address to which extent reduced Ctnna1 expression levels in HSPCs in the bone marrow affected their differentiation, I analyzed the frequencies of lineage negative cells, LSK cells, and HSCs and the GFP$^+$ cells therein in the bone marrow of mice with elevated GFP$^+$ cell frequencies.

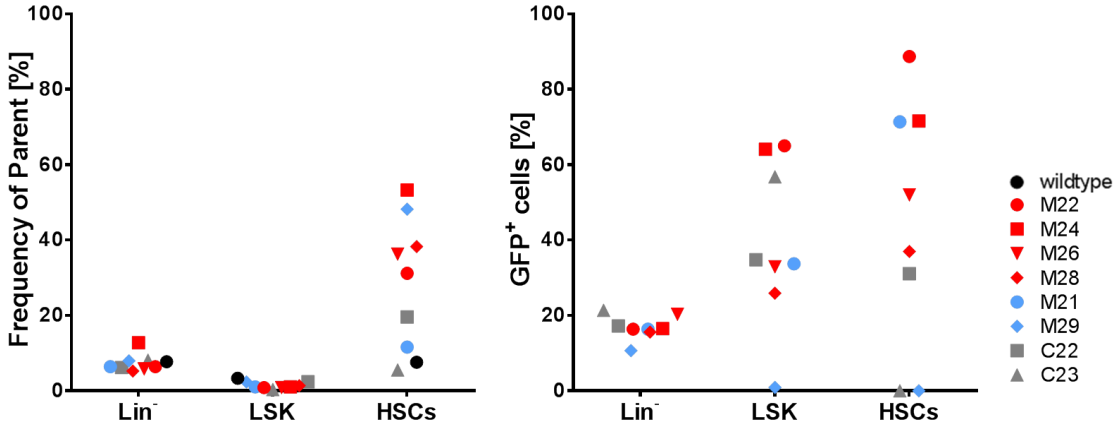

Figure 22: HSPCs with reduced Ctnna1 expression expand within the LSK and HSC compartments of transplanted mice.
Flow cytometric analysis of lineage negative (Lin$^-$) cells, LSK cells and HSCs in the bone marrow of an age-matched wildtype mouse (black circle), mice of group 405 (red symbols), 409 (blue symbols) and control group (grey symbols) with expansion of GFP$^+$ bone marrow cells. Left: Frequencies of parent population of indicated hematopoietic subpopulations. Parent of Lin$^-$: P1, parent of LSK: Lin$^-$, parent of HSCs: LSK (as in Figure 57, top). Right: frequency of the GFP$^+$ cell population within the indicated subpopulation.

The lineage negative cells and the LSK cell compartments in the entire bone marrow of transplanted mice showed no expansion in comparison to wildtype mice (Figure 22, left). However, HSC frequencies were elevated in all mice of group 405 that had an expansion of GFP$^+$ cells in the bone marrow compared to control mice (Figure 22, left). Furthermore, mouse M21 of group 409 showed increased HSC frequencies compared to control mice (Figure 22, left). There was no increase of the GFP$^+$ cell frequencies within the lineage negative cell population of mice of group 405 and 409 compared to control mice (Figure 22, right). However, mice of group 405 showed elevated frequencies of GFP$^+$ cells within the

LSK cell and HSC population, particularly pronounced for mice M22 and M24 (65% within the LSK cells, 89% and 72% within the HSCs; Figure 22, right). Moreover, for mice of group 405 the frequency of GFP^+ cells in the HSC compartment was significantly increased compared to the frequency of GFP^+ cells within the lineage negative or LSK cell compartments (HSC vs. Lin^-: P=0.0293, HSC vs. LSK: P=0.0253, paired t-test, two-tailed P-value, α=0.05). Control mouse C23 showed an almost equally elevated GFP^+ cell frequency in the LSK cells (56%), yet not in the HSCs (0%; Figure 22, right). For mouse M21 of group 409, GFP^+ cell frequencies were increasing within the primitive progenitor cell compartments (16% in Lin^- cells, 34% in LSK cells and 72% in HSCs; Figure 22, right). The data indicated a competitive advantage of bone marrow cells expressing shRNA 405 in the hematopoietic progenitor cell compartments *in vivo*. To a lesser extent (one out of two mice with GFP^+ cells in the bone marrow) this was observed for bone marrow cells expressing shRNA 409.

4.4 HSPCs expressing shRNA 405 self-renew, expand and lead to clonal dominance in secondary transplanted animals

4.4.1 Secondary transplanted HSPCs expressing shRNA 405 engraft sublethally irradiated recipients and give rise to abnormal peripheral blood counts

To determine whether self-renewing neoplastic cells were involved in the clonal

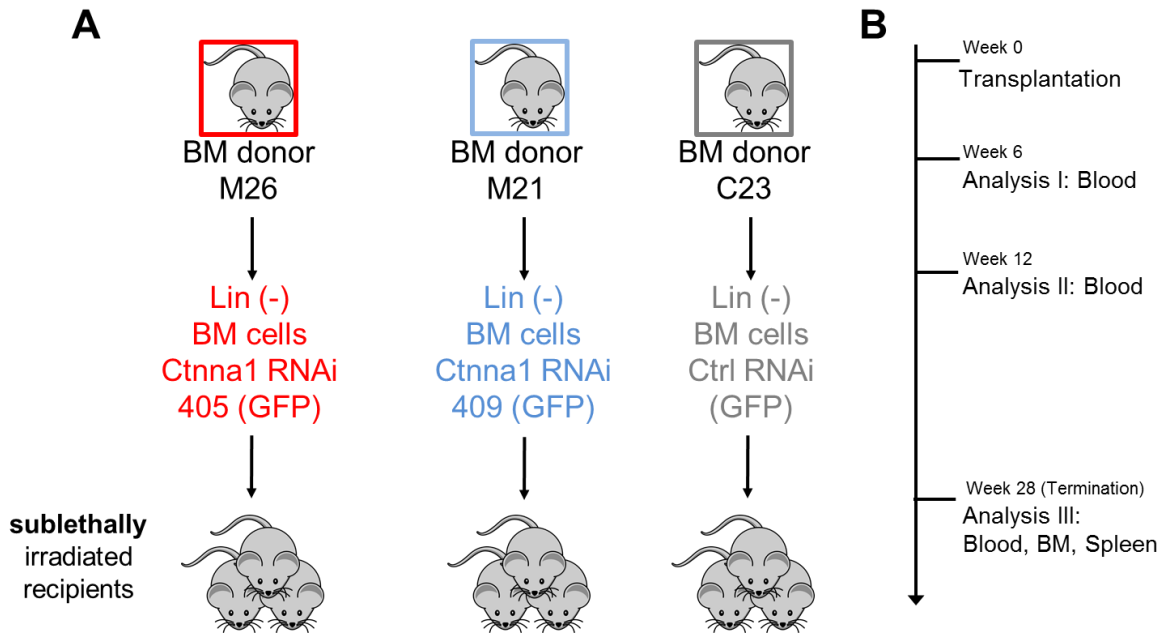

Figure 23: Design of secondary transplantation experiment.
(A) One mouse of each group (M26, M21, C23) was selected as bone marrow donor for secondary transplantations. All three bone marrow donors showed an expansion of GFP^+ cells in the bone marrow. $1x10^5$ lineage depleted donor bone marrow cells were pooled with $2x10^5$ whole bone marrow cells from a wildtype animal and transplanted into twelve sublethally irradiated recipient mice (5xM26, 4xM21, 3xC23). (B) After transplantation, blood was sampled twice to monitor CBCs, GFP^+ cell frequencies and the immunophenotype of the peripheral blood cells by flow cytometry. Upon termination of the experiment, mice were sacrificed and bone marrow cells, splenocytes and peripheral blood cells were prepared and analyzed accordingly.

dominance phenotype observed in mice transplanted with HSPCs encoding shRNAs 405 and 409, I performed secondary transplantations. Lineage depleted bone marrow cells of the primary donor animals were transplanted into sublethally irradiated recipient mice. This transplantation setting provides a highly competitive environment for the transplanted bone marrow cells, since the recipient bone marrow is not completely eradicated by irradiation and the animals do not depend on a life-saving bone marrow transplantation (Cheng et al., 2013). Thus, only neoplastic cells with self-renewing potential are able to engraft, proliferate and survive in the bone marrow of the secondary recipient animals (Daley et al., 1991; Gishizky et al., 1993; Roy et al., 2012).

Bone marrow cells of one donor mouse of each group (shRNA 405: M26, shRNA 409: M21, control shRNA: C23) were transplanted into sublethally irradiated recipients (Figure 23A). Twelve recipient mice were transplanted (group 405: 5 mice, group 409: 4 mice, control group: 3 mice) and the follow-up analysis was performed as before (Figure 23B). To address the question whether transplanted GFP^+ bone marrow cells with reduced Ctnna1 expression were able to engraft in the bone marrow of secondary recipient mice, I first measured the frequencies of GFP^+ cells in the peripheral blood of the recipients during reconstitution of the bone marrow. Exclusively mice transplanted with bone marrow cells from donor mouse M26 showed GFP^+ cells in the peripheral blood. GFP^+ bone marrow cells from mice M21 (group 409) or C23 (control group) did not engraft in secondary recipients, as they did not show GFP^+ cells in the peripheral blood (Figure 24). This finding strongly indicated a competitive advantage exclusively of bone marrow cells expressing shRNA 405. Moreover, after an initial peak at 12 weeks post transplantation, GFP^+ cell frequencies in the peripheral blood decreased over time for mice of this group (Figure 24). This finding hinted at

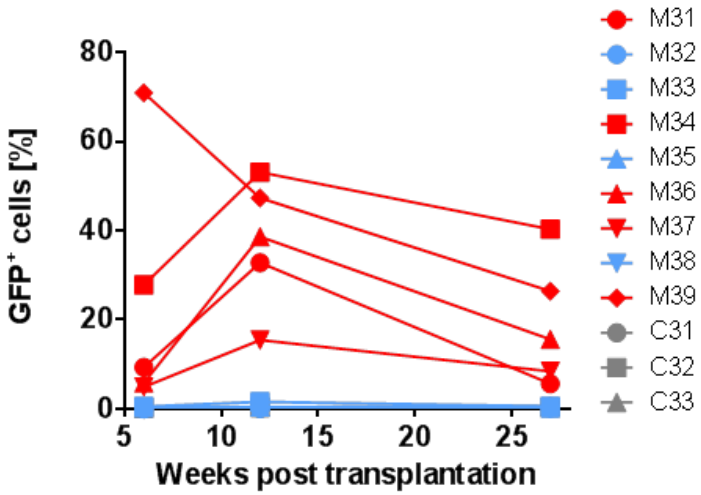

Figure 24: Exclusively bone marrow cells expressing shRNA 405 from the primary donor mouse M26 were able to give rise to GFP^+ cells in the peripheral blood of secondary transplanted mice.
GFP^+ cell frequencies were assessed by flow cytometry in peripheral blood cells from the secondary recipients during reconstitution of the bone marrow. Exclusively mice transplanted with bone marrow cells from donor mouse M26 showed GFP^+ cells in the peripheral blood. Red symbols and lines: mice transplanted with bone marrow cells from mouse M26 (shRNA 405), blue symbols and lines: mice transplanted with bone marrow cells from mouse M21 (shRNA 409), grey symbols and lines: mice transplanted with bone marrow cells from mouse C23 (control shRNA).

a loss of differentiation potential in GFP^+ bone marrow cells expressing shRNA 405 over time.

CBCs of the peripheral blood of the secondary recipient mice showed a significant reduction in erythroid parameter values (RBC, HGB level and HCT) for recipients of group 405 compared to all others (Figure 25C, D, E). Furthermore, the MCV was increased for these mice (Figure 25F). These results indicated an impairment of the erythropoiesis in mice of group 405. However, their spleen weights were within the normal ranges (78±17 mg) ruling out extramedullary erythropoiesis in the spleen. Additionally, mice of group 405 showed signs of leukopenia at termination, as their WBC counts were reduced compared to all other transplanted mice (Figure 25A). These results indicated that downregulation of Ctnna1 expression by shRNA 405 in secondary transplanted bone marrow cells impacted the differentiation of erythroid progenitor cells and the maturation of leukocytes. In contrast, CBCs as well as spleen weights (409: 78±24 mg, control: 74±3 mg) of all mice of group 409 and the control group were within the normal ranges.

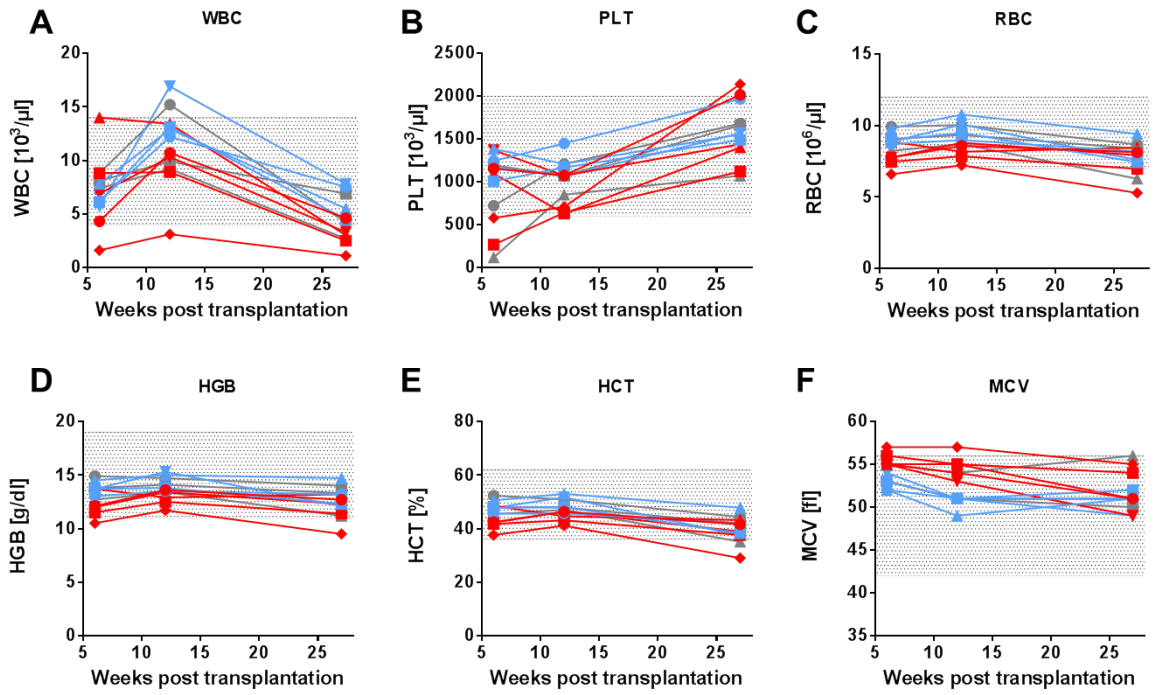

Figure 25: Mice transplanted with bone marrow cells from the primary donor mouse M26 (group 405) showed signs of leukopenia and anemia.
(A) White blood cell (WBC) counts, (B) platelet (PLT) counts, (C) red blood cells (RBC) counts, (D) hemoglobin (HGB) concentration, (E) hematocrit (HCT) and (F) mean corpuscular volume (MCV) of whole blood samples from secondary transplanted mice measured three times over six months. Blue and red symbols indicate mice transplanted with bone marrow of mice M21 and M26, respectively, grey symbols indicate mice transplanted with bone marrow of control mouse C23 (see Figure 24 for full legend). Shaded areas indicate the normal range for each parameter (WBC: 4-14x10^3/µl, PLT: 600-2000x10^3/µl, RBC: 7-12x10^6/µl, HGB: 11-19 g/dl, HCT: 36-62%, MCV: 42-56 fl) for healthy C57BL/6 mice (from: Charles River Laboratories International, Inc., 2012).

4.4.2 Bone marrow cells with reduced Ctnna1 expression levels mediated by shRNA 405 expression expand in the bone marrow of secondary recipient mice

To analyze the engraftment of GFP^+ bone marrow cells in secondary recipients, I measured the frequencies of GFP^+ cells in their bone marrow, spleen and peripheral blood. As expected from the GFP^+ cell frequencies measured in the peripheral blood during reconstitution, exclusively GFP^+ bone marrow cells of donor mouse M26 (shRNA 405) engrafted in sublethally irradiated secondary recipient mice (Figure 26, middle). In two out of five mice of this group the frequencies of GFP^+ cells in the bone marrow were higher (62% and 67%, recipients M34 and M39) than in the primary transplant donor mouse (41%, donor M26, Figure 26, middle). Most notably, these two mice also displayed the most pronounced dysregulation in the erythroid parameters of the CBCs (Figure 25 C-F). In contrast, cells transplanted from mouse M21 (shRNA 409) and mouse C23 (control) did not engraft upon secondary transplantation (Figure 26, left and right).

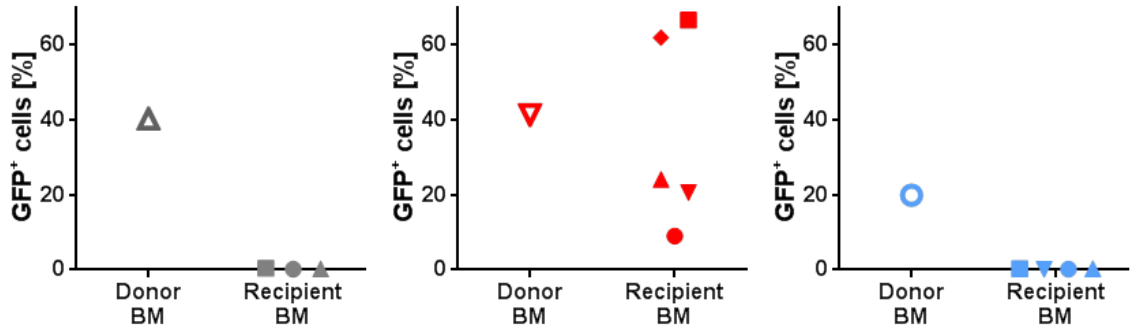

Figure 26: Primary GFP^+ bone marrow cells of mouse M26 (shRNA 405) expanded upon secondary transplantation.
Frequencies of GFP^+ bone marrow cells of the donor mice compared to the frequencies of GFP^+ cells found in the bone marrow of secondary recipient mice. Grey: C23 as primary donor (control shRNA), red: M26 as primary donor (shRNA 405), blue: M21 as primary donor (shRNA 409). See Figure 24 for full legend of the recipient mice.

Mice transplanted with bone marrow cells from mouse M26 showed GFP^+ cells in the spleen and peripheral blood, while these organs were devoid of GFP^+ cells in secondary recipient mice transplanted with bone marrow cells from mice M21 (shRNA 409) and C23 (control shRNA, Figure 27). In the previous competitive reconstitution experiments the frequency of GFP^+ cells expressing shRNA 405 was consistently higher in the bone marrow of transplanted mice than in the peripheral blood and spleen (mouse M12 from the first experiment, mice of group 405 from the second experiment). According to these results, secondary recipients of bone marrow cells from mouse M26 showed the same distribution of GFP^+ cells in bone marrow, peripheral blood and spleen (Figure 27). This observation was independent from the respective extent of GFP^+ cell expansion in the bone marrow and indicated a clonal dominance phenotype associated with a lack in maturation of GFP^+ bone marrow cells expressing shRNA 405. Taken together, these data suggested enhanced self-renewing and expansion potential of the secondary transplanted GFP^+ cells expressing shRNA

405, but not shRNA 409. Moreover, the engraftment of GFP$^+$ cells from mouse M26 in secondary recipients mediated an impairment of hematopoietic cell differentiation and most likely impacted erythropoiesis as revealed by the peripheral blood parameters (Figure 25).

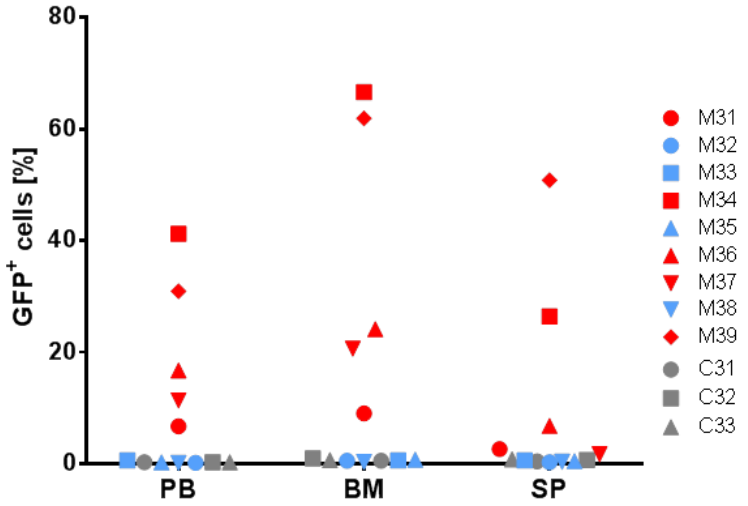

Figure 27: GFP$^+$ bone marrow cells of mouse M26 showed a clonal dominance phenotype upon secondary transplantation
The frequencies of GFP$^+$ cells as a measure for the proportion of cells with reduced Ctnna1 expression were analyzed by flow cytometry in mononuclear cells isolated from the peripheral blood (PB), the bone marrow (BM) and the spleen (SP) at 28 weeks after secondary transplantation. Red and blue symbols indicate mice transplanted with bone marrow of mice M26 (shRNA 405) and M21 (shRNA 409), respectively, grey symbols indicate mice transplanted with bone marrow of control mouse C23.

4.4.3 The myeloproliferative phenotype of bone marrow cells expressing shRNA 405 is maintained upon secondary transplantation

To analyze the lineage phenotype of bone marrow, spleen and peripheral blood cells in the secondary recipients, I measured the frequencies of myeloid and lymphoid cells in these organs. The analysis showed an elevated frequency of myeloid cells (56±9%) in the bone marrow of mice transplanted with bone marrow cells from mouse M26 (Ctnna1 RNAi, 405) when compared to wildtype or control mice (Control RNAi, 48±17%; Figure 28A, top). This phenotype was most pronounced in mice M34 (69%), M36 (62%) and M39 (56%; Figure 28A, bottom). Mouse M39 also displayed a strong myeloid differentiation bias in peripheral blood and spleen; however, the pronounced cytopenia detected in the peripheral blood (low WBC, Figure 25A) could apply for all three organs and therefore have led to this observation. As expected, mice transplanted with bone marrow from mouse M21 (Ctnna1 RNAi, 409) did not show a difference in their myeloid and lymphoid cell frequencies in peripheral blood, bone marrow and spleen when compared to control or wildtype mice (Figure 28A, top), since secondary transplanted GFP$^+$ cells did not engraft in their bone marrow.

Next, I analyzed the myeloid and lymphoid cell fractions within the GFP$^+$ cells of mice of group 405 and found that GFP$^+$ cells in the bone marrow were almost exclusively

differentiated within the myeloid lineage (76-91%) and the proportion of lymphoid cells was decreased accordingly (0.7-4.5%, Figure 28B). This phenotype, however less pronounced, was also detected in GFP^+ peripheral blood cells of all mice and in GFP^+ splenocytes of mice M34, M37, M39.

These data showed that bone marrow cells with reduced Ctnna1 expression mediated by shRNA 405 retained the myeloproliferative phenotype upon secondary transplantation.

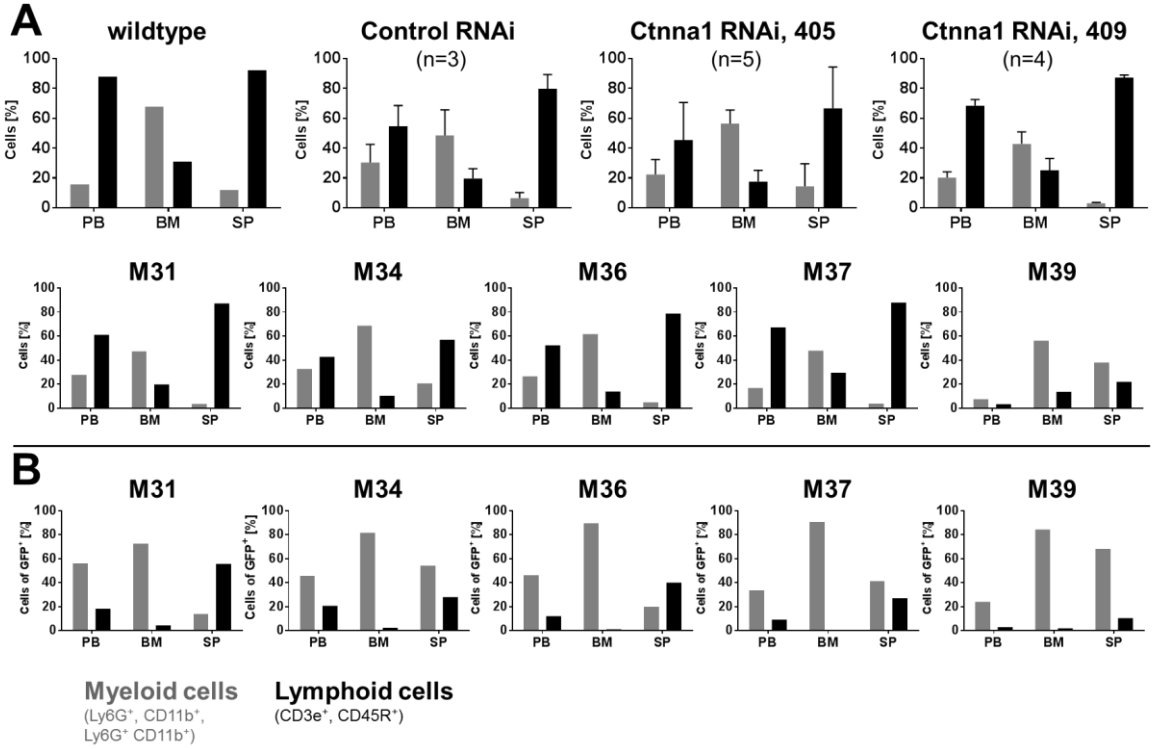

Figure 28: Mice transplanted with bone marrow cells from mouse M26 showed a differentiation bias towards the myeloid lineage in the GFP^+ cells of peripheral blood, bone marrow and spleen.
Mean frequencies of myeloid (grey bars) and lymphoid cells (black bars) are shown for peripheral blood (PB), bone marrow (BM) and spleen (SP). (A) Frequencies of all cells. Top: Analysis of experimental groups and wildtype, bottom: separate analysis of mice M31, M34, M36, M37 and M39 (shRNA405). (B) Frequencies within the GFP^+ cell population of mice M31, M34, M36, M37 and M39 (shRNA405).

4.4.4 Expansion of primary bone marrow cells expressing shRNA 405 in secondary recipients diminishes erythropoiesis

The primary transplant donor mice M26 of group 405 showed reduced bone marrow erythropoiesis (Figure 21) without an overt manifestation in the peripheral blood parameters (Figure 17 C-F). However, in the CBCs of the secondary recipient mice, I detected unambiguous signs of impaired erythropoiesis (Figure 25 C-F) compared to mice of group 409 or control mice. Thus, I addressed the question whether erythropoiesis was impacted by the expansion of GFP^+ cells in the bone marrow of these mice compared to control mice and mice of group 409 by measuring the frequencies of $Ter119^-$ cells in their bone marrow. Mice of group 405 showed increased frequencies of $Ter119^-$ cells (57±14%) compared to control

mice (45±12%) and mice of group 409 (50±8%; Figure 29). However, data of the separate analysis of mice of group 405 revealed that only two mice (M34, M37) showed an increase in the frequencies of Ter119$^-$ cells, mostly pronounced for mouse M34 (80%). Strikingly, M34 also showed the highest frequency of GFP$^+$ cells in the bone marrow (Figures 26 and 27). These data indicated that the expansion of secondary transplanted GFP$^+$ cells expressing shRNA 405 is accompanied by a reduced erythroid differentiation in the bone marrow.

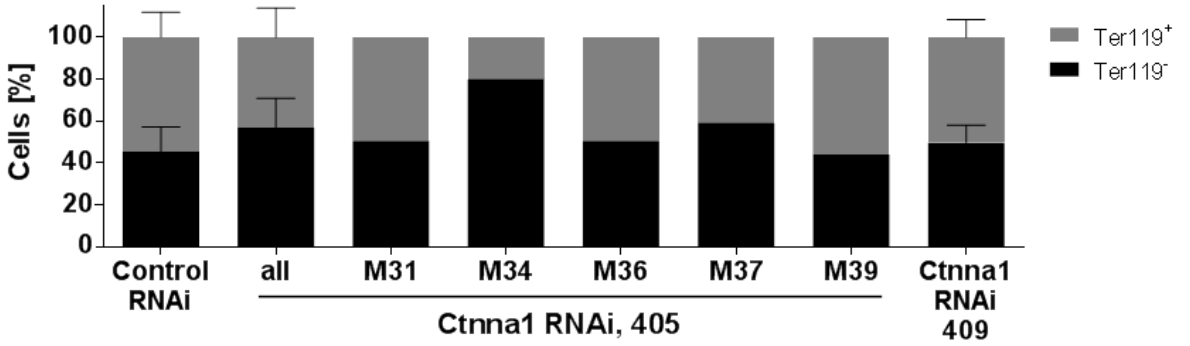

Figure 29: Secondary recipient mice transplanted with bone marrow from mouse M26 showed reduced bone marrow erythropoiesis.
Frequencies of immature erythroblasts (Ter119$^-$, black bars) and mature erythropoietic cells (Ter119$^+$, grey bars) in the bone marrow of secondary recipients transplanted with bone marrow from mouse C23 (Control RNAi), M26 (Ctnna1 RNAi, 405) or M21 (Ctnna1 RNAi, 409).

4.4.5 GFP$^+$ bone marrow cells from mouse M26 expand within the hematopoietic stem and progenitor cell compartments in secondary recipient mice

To determine the expansion of GFP$^+$ cells in the stem and progenitor cell compartments of mice of group 405, I measured the frequencies of lineage negative cells, LSK cells and HSCs in their bone marrow and the frequencies of the GFP$^+$ cell populations therein. Mice of group 409 were excluded from the analysis, as GFP$^+$ cells did not engraft in their bone marrow. Two out of five mice of group 405 showed an increased frequency of HSCs, while the frequencies of lineage negative and LSK cells were normal in all mice compared to control mice and wildtype mice (Figure 30, left). Strikingly, all mice of group 405 showed increased GFP$^+$ cell frequencies within the progenitor cell compartments (Figure 30, right). Moreover, the GFP$^+$ cell frequency was significantly elevated within the HSC compartment (P=0.0105, paired t-test, two-tailed P-value, α=0.05). This expansion was most pronounced for mice M34 and M39. In the bone marrow of mouse M39 the LSK cell and HSC compartments were almost exclusively comprised of GFP$^+$ cells (96% in LSK cells and 94.2% in HSCs; Figure 30, right). Thus, the transplanted GFP$^+$ bone marrow cells from mouse M26 dominated the stem and progenitor cell compartments of the secondary recipient mice. This finding suggested that GFP$^+$ cells expressing shRNA 405 retain their competitive advantage within the stem and progenitor cell compartment of the bone marrow upon secondary transplantation.

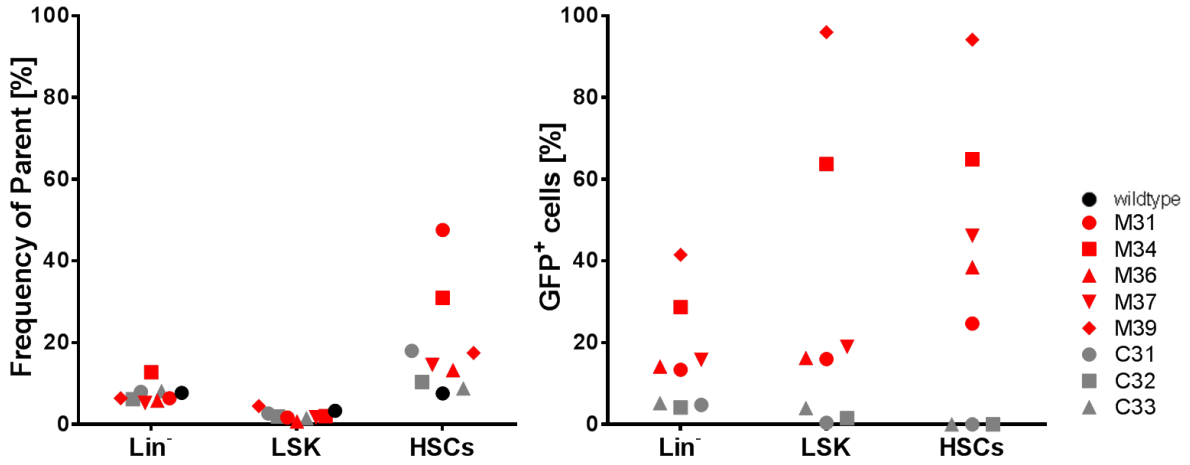

Figure 30: GFP$^+$ cells expressing shRNA 405 expanded within the LSK cell and HSC compartments of secondary recipient mice.
Flow cytometric analysis of lineage negative (Lin$^-$) cells, LSK cells and HSCs in the bone marrow of an age-matched wildtype mouse (black circle), mice of group 405 (red symbols) and the control group (grey symbols). Left: Frequencies of parent population of indicated hematopoietic subpopulations. Parent of Lin$^-$: P1, parent of LSK: Lin$^-$, parent of HSCs: LSK (as in Figure 57, top). Right: frequency of the GFP$^+$ cell population within the indicated subpopulation. Mice of group 409 were excluded from the analysis as GFP$^+$ cells did not engraft in their bone marrow.

4.5 Clonal dominance of HSPCs with reduced Ctnna1 expression is reinforced by the co-occurrence of Tp53 inactivation

4.5.1 Knockout of Tp53 facilitates the expansion of HSPCs with reduced Ctnna1 expression without causing overt hematological disease

Recent studies dissecting the genetics of MDS showed a frequent co-occurrence of inactivating TP53 mutations with deletions of chromosome 5q in MDS patients (Jadersten et al., 2011; Kulasekararaj et al., 2013; Papaemmanuil et al., 2013; Haferlach et al., 2014; Volkert et al., 2014). Furthermore, inactivation of Tp53 in murine HSPCs in cooperation with other genetic lesions had been shown to accelerate leukemic onset and enhance the severity of the disease in mice (Xu et al., 2012; Stoddart et al., 2014a; Stoddart et al., 2014b). To test whether loss of Tp53 collaborates with gene dosage insufficiency of Ctnna1 I used donor HSPCs of Tp53$^{-/-}$ mice in a competitive bone marrow reconstitution experiment.

The experiment comprised six groups of bone marrow recipients. Mice in three groups received transduced bone marrow cells from Tp53$^{-/-}$ donors, while mice of three control groups were transplanted with transduced bone marrow cells from wildtype donors (Figure 31). The recipient mice were sacrificed two months after transplantation without regular blood monitoring.

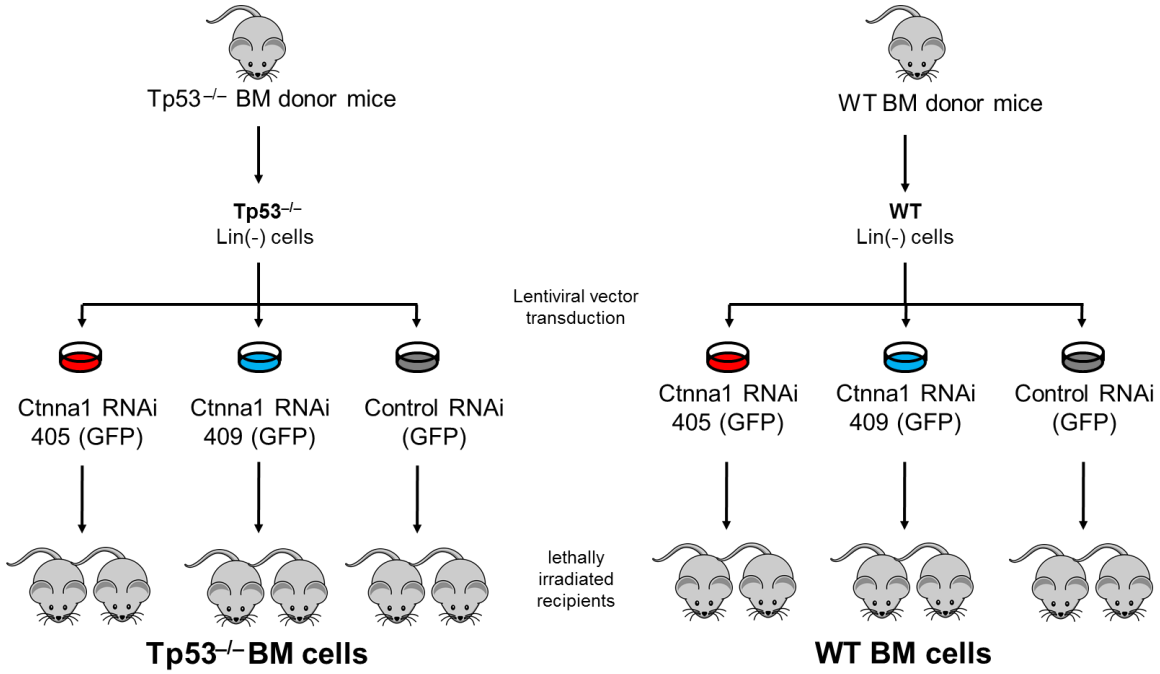

Figure 31: Schematic experimental design of the competitive reconstitution experiment *in vivo* implementing a functional inactivation of Tp53.
$0.7x10^6$ lineage depleted murine HSPCs from $Tp53^{-/-}$ and wildtype (WT) donor animals were transduced with shRNA-expression vectors encoding shRNA 405, 409 or control. 24 hrs after transduction single vector-transduced cells were combined with freshly prepared whole bone marrow cells and transplanted into lethally irradiated recipients ($0.1x10^6$ HSPCs containing single vector-transduced HSPCs at a frequency of 5-10% and $2x10^6$ whole bone marrow cells per recipient animal). Two months after transplantation the recipient mice were sacrificed and bone marrow cells, splenocytes and peripheral blood cells were prepared and analyzed.

Upon termination of the experiment, the peripheral blood, bone marrow and spleen of the recipients were analyzed for the frequencies of GFP^+ cells. Exclusively mice transplanted with HSPCs encoding shRNA 405 showed an expansion of GFP^+ cells in both genetic backgrounds ($Tp53^{-/-}$: 29-55% in PB, 43-68% in BM, 22-38% in SP; WT: 21-32% in PB, 35-55% in BM, 13-20% in SP) compared to mice transplanted with HSPCs encoding control shRNAs ($Tp53^{-/-}$: 11-15% in PB, 8.5-24% in BM, 7-12% in SP; WT: 1-19% in PB, 0.5-22% in BM, 1,5-12% in SP; Figure 32). GFP^+ HSPCs encoding shRNA 409, however, did not expand in the hematopoietic organs of transplanted mice compared to control mice irrespective of the genetic background ($Tp53^{-/-}$: 11-19% in PB, 13-27% in BM, 8-16% in SP; WT: 1-2% in PB, BM and SP; Figure 32). Overall, the genetic inactivation of Tp53 in transplanted HSPCs had an additive effect on the repopulation capability of GFP^+ cells in all transplanted mice compared to the respective group of mice transplanted with wildtype HSPCs.

GFP^+ cell frequencies in the bone marrow of mice transplanted with $Tp53^{-/-}$ HSPCs encoding shRNA 405 were significantly higher than in the peripheral blood (BM vs. PB: P=0.0016, paired t-test, two-tailed P-value, α=0.05). Moreover, this was also observed in mice transplanted with WT HSPCs encoding shRNA 405. In contrast, for mice transplanted with $Tp53^{-/-}$ HSPCs encoding shRNA 409 or control shRNA the GFP^+ bone marrow cell

frequencies were not significantly different than those in the peripheral blood (409: BM vs. PB: P=0.0816, Control: BM vs. PB: P=0.2143, paired t-test, two-tailed P-value, α=0.05; Figure 32). This indicated a block in differentiation of GFP$^+$ cells in the bone marrow of mice transplanted with Tp53$^{-/-}$ or WT HSPCs encoding shRNA 405 as observed before. However, the extent of GFP$^+$ cell expansion was enhanced when Tp53 was inactivated, indicating a reinforcing effect of Tp53 inactivation on the clonal dominance of HSPCs encoding shRNA 405.

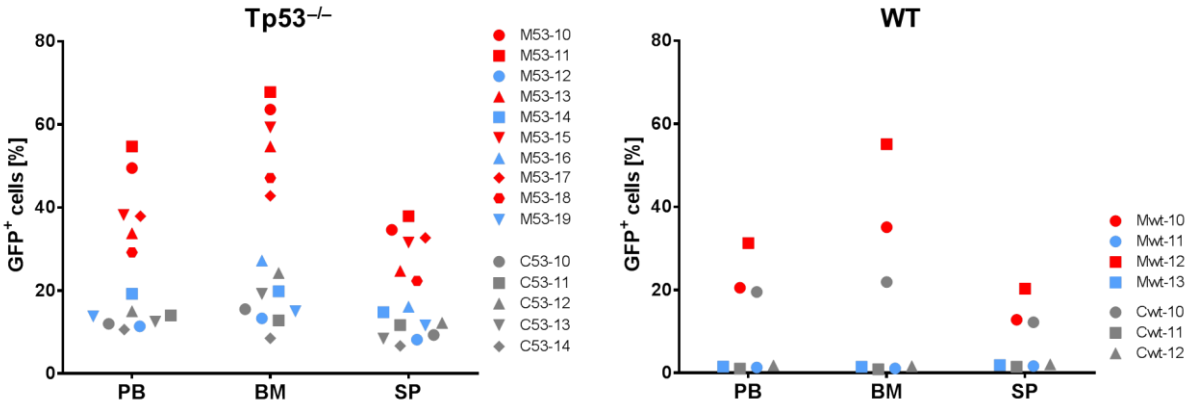

Figure 32: Frequency of Tp53$^{-/-}$ and WT GFP$^+$ cells in peripheral blood, bone marrow and spleen of recipient mice.
The frequencies of GFP$^+$ cells as a measure for the proportion of cells with reduced Ctnna1 expression were analyzed by flow cytometry in mononuclear cells isolated from the peripheral blood (PB), the bone marrow (BM) and the spleen (SP) at 8 weeks after transplantation. Red and blue symbols indicate mice transplanted with HSPCs encoding shRNA 405 and 409, respectively. Grey symbols indicate mice transplanted with HSPCs encoding control shRNA. The left panel shows the GFP$^+$ cell frequencies in PB, BM and SP of all mice transplanted with cells with Tp53$^{-/-}$ background, the right panel shows GFP$^+$ cell frequencies in PB, BM and SP of all mice transplanted with HSPCs with wildtype (WT) background.

Next, Ctnna1 expression levels in GFP$^+$ bone marrow cells were measured by QRT-PCR. As expected, the Ctnna1 expression levels were reduced to 27-30% of control cells in the GFP$^+$ bone marrow cells of mice transplanted with Tp53$^{-/-}$ or wildtype HSPCs encoding shRNA 405 (Figure 33), verifying the results obtained from the previous experiments. Mice transplanted with Tp53$^{-/-}$ HSPCs encoding shRNA 409 showed a reduction of Ctnna1 expression to 59% of control in the GFP$^+$ bone marrow cells as observed before (Figure 33).

Taken together, these results indicate an additive effect of Tp53 inactivation on the clonal dominance bone marrow cells encoding shRNA 405. Moreover, Tp53$^{-/-}$ HSPCs encoding shRNA 409 were able to engraft in the bone marrow as opposed to wildtype HSPCs encoding shRNA 409 (Figure 26). However, though Tp53 was genetically inactivated, the Ctnna1 expression level of 59% mediated by expression of shRNA 409 was most likely not sufficient to enforce a clonal dominance of GFP$^+$ cells in the bone marrow of transplanted mice.

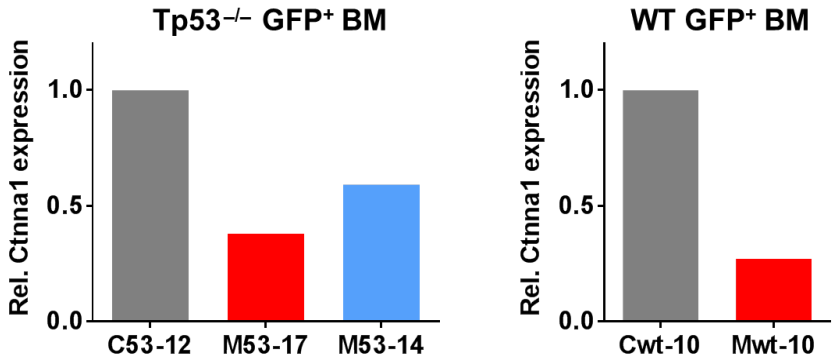

Figure 33: RNAi by expression of shRNAs 405 and 409 in murine bone marrow cells mediated reduced levels of Ctnna1 expression *in vivo*.
Relative Ctnna1 expression levels measured by QRT-PCR in GFP$^+$ bone marrow cells of representative transplanted mice compared to control expression levels in whole bone marrow. Grey – control; red and blue – mice of groups 405 and 409, respectively.

To evaluate the effect of the expansion of GFP$^+$ cells in the bone marrow of transplanted mice on hematopoiesis, I measured the CBCs in the peripheral blood of the recipients at the termination of the experiment.

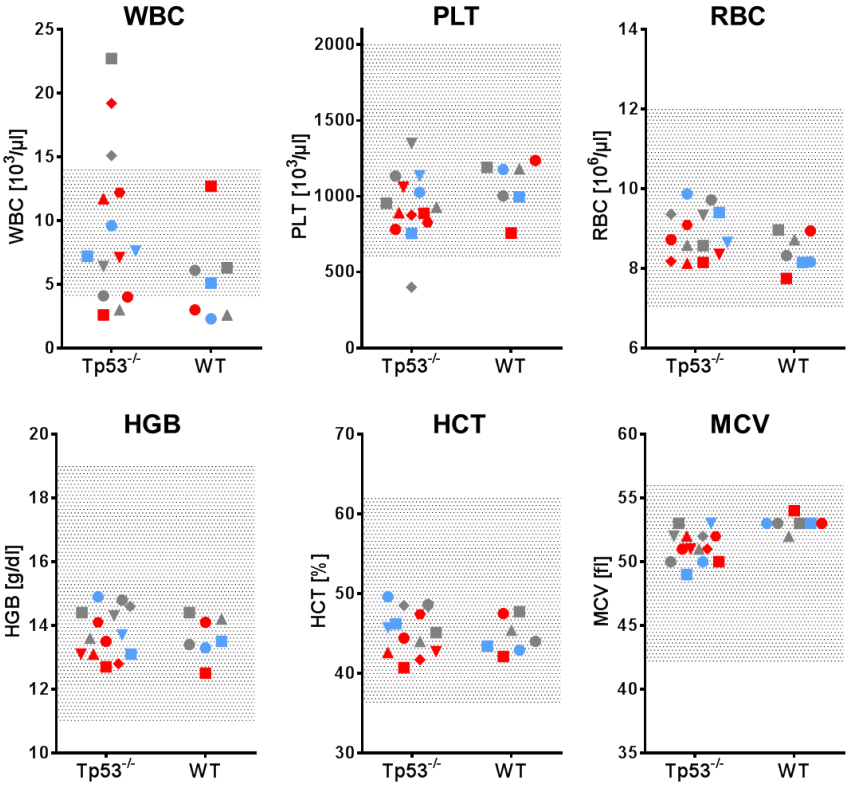

Figure 34: Mice transplanted with HSPCs encoding shRNA 405, 409 or control shRNAs did not show signs of hematological disease irrespective of the genetic background of the transplanted HSPCs.
White blood cell (WBC) counts, platelet (PLT) counts, red blood cells (RBC) counts, hemoglobin (HGB) concentration, hematocrit (HCT) and mean corpuscular volume (MCV) of whole blood samples from transplanted mice measured at 8 weeks after transplantation. Blue and red symbols indicate mice transplanted with HSPCs encoding shRNA 405 and shRNA 409, respectively, grey symbols indicate mice transplanted with HSPCs encoding control shRNA (see Figure 32 for full legend). Shaded areas indicate the normal range for each each parameter (WBC: 4-14x10^3/µl, PLT: 600-2000x10^3/µl, RBC: 7-12x10^6/µl, HGB: 11-19 g/dl, HCT: 36-62%, MCV: 42-56 fl) for healthy C57BL/6 mice (from: Charles River Laboratories International, Inc., 2012).

The CBCs of the recipient mice that received Tp53$^{-/-}$ bone marrow showed a pronounced variation in the WBC counts (Figure 34). To a lesser extent this was also observed in mice that received wildtype bone marrow cells. This finding is likely due to the relatively short time of bone marrow reconstitution of 8 weeks after lethal irradiation. All other CBC parameters were within the normal ranges for all recipient mice (Figure 34). Thus, none of the recipient mice showed signs of overt hematological disease, irrespective of the genetic background of the transplanted HSPCs.

4.5.2 The myeloid lineage differentiation bias in the bone marrow of mice transplanted with HSPCs encoding shRNA 405 is not enhanced when Tp53 is inactivated

Next, I evaluated whether a differentiation bias towards the myeloid lineage in the bone marrow could be observed as in the previous experiments. Mice transplanted with HSPCs of both genetic backgrounds (Tp53$^{-/-}$ and WT) encoding shRNA 405 showed an

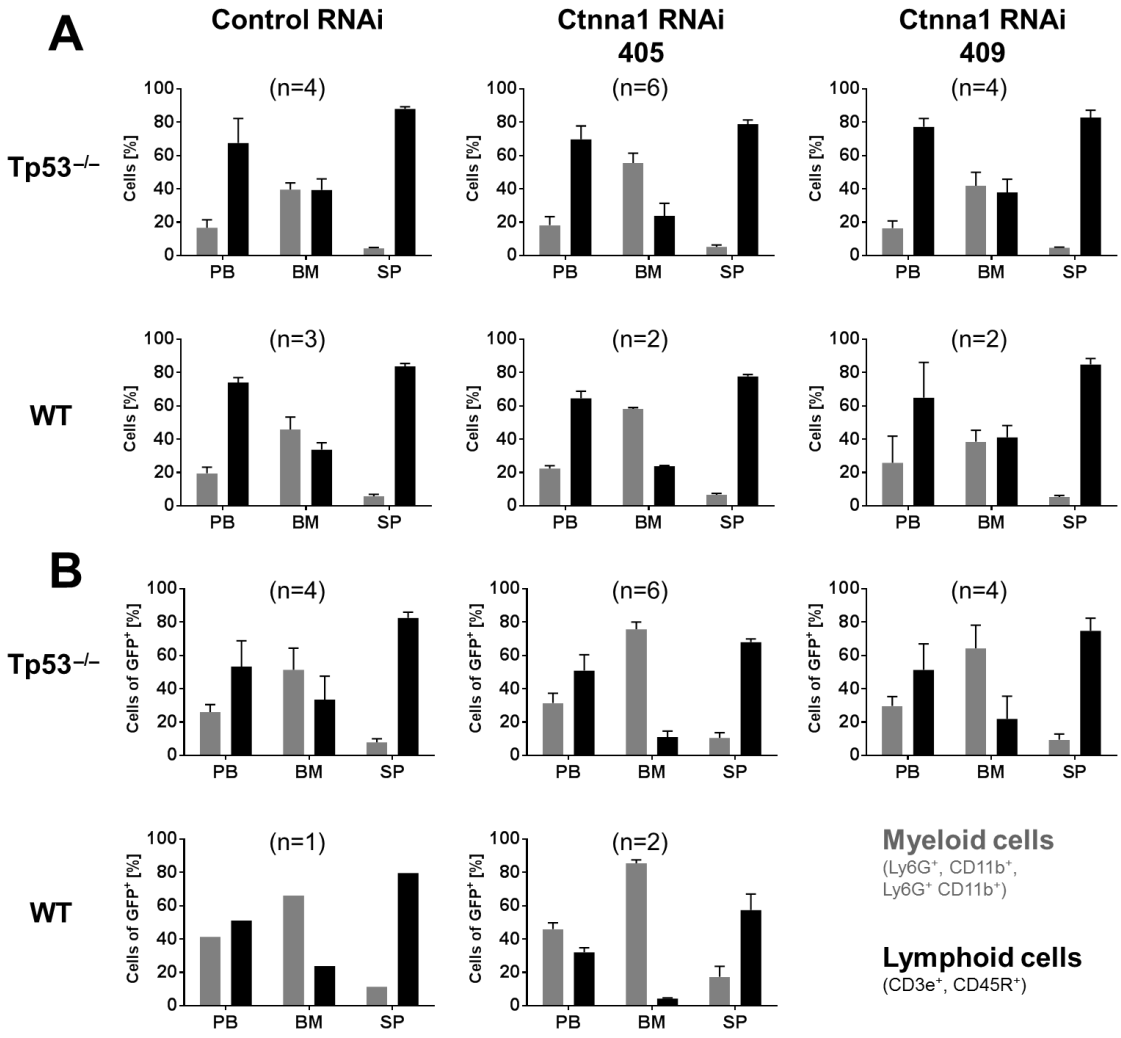

Figure 35: Transplanted bone marrow cells with reduced Ctnna1 expression were mostly differentiated within the myeloid lineage.
Flow cytometric analysis of myeloid (grey bars) and lymphoid cells (black bars) in peripheral blood (PB), bone marrow (BM) and spleen (SP) of mice transplanted HSPCs encoding control shRNA (left), shRNA 405 (middle) or shRNA 409 (right) in Tp53$^{-/-}$ background (top panel) and WT background (bottom panel). (A) Frequencies of all cells in indicated organs, (B) frequencies of the GFP^{+} cell population.

increase of the frequencies of myeloid cells (60%) and a decrease of lymphoid cells (25%) in the bone marrow compared to control mice (45% myeloid cells, 40% lymphoid cells; Figure 35A). However, this differentiation bias towards the myeloid lineage was not observed in the peripheral blood or spleen of these mice, as their frequencies were similar to those found in control mice (PB: 20% myeloid cells, 70% lymphoid cells; SP: 10% myeloid cells, 85% lymphoid cells; Figure 35A). This indicated a bias in differentiation of hematopoietic cells towards the myeloid lineage in the bone marrow of mice transplanted with HSPCs expressing shRNA 405 irrespective of the genetic background of transplanted HSPCs. This phenotype was accompanied by a partial block in differentiation as the frequencies of myeloid cells were higher in the bone marrow than in the peripheral organs. In contrast, this observation did not apply to mice transplanted with $Tp53^{-/-}$ or WT HSPCs expressing shRNA 409, since they showed similar frequencies of myeloid and lymphoid cells in bone marrow, spleen and peripheral blood as control mice (Figure 35A).

The myeloid phenotype of bone marrow cells of mice that received HSPCs encoding shRNA 405 was even more pronounced within the GFP^+ bone marrow cell fraction. It was comprised almost exclusively of myeloid cells (75% of $Tp53^{-/-}$ bone marrow cells, 86% of wildtype bone marrow cells; Figure 35B). However, the combination of reduced Ctnna1 expression level with inactivation of Tp53 did not reinforce this phenotype. Since GFP^+ cells did not engraft in the bone marrow of recipient mice transplanted with WT HSPCs encoding shRNA 409, I could only analyze the lineage differentiation in the GFP^+ cells of the respective group of mice transplanted with $Tp53^{-/-}$ bone marrow cells. They showed an increase in myeloid cell frequencies (65%) and a decrease in lymphoid cell frequencies (22%) compared to control mice (Figure 35B), however, it was not as pronounced as in the GFP^+ cells of mice transplanted with shRNA 405. Taken together, these results indicated a pronounced differentiation bias towards the myeloid lineage of bone marrow cells expressing shRNA 405, which was not reinforced when Tp53 was additionally inactivated.

4.5.3 Inactivation of Tp53 does not further reduce the diminished erythropoiesis in the bone marrow of mice transplanted with HSPCs encoding shRNA 405

To evaluate the effect of combined Tp53 inactivation with reduced Ctnna1 expression on erythropoiesis, I determined the frequencies of $Ter119^-$ cells in the bone marrow of mice of the different groups.

In the bone marrow of the recipients transplanted with WT or $Tp53^{-/-}$ HSPCs encoding shRNA 405 the frequency of $Ter119^-$ cells was increased (65%) in comparison to respective control mice (55% $Ter119^-$ cells). This was independent from the genetic background of the transplanted HSPCs. Mice transplanted with HSPCs encoding shRNA 409 did not show reduced bone marrow hematopoiesis (55% $Ter119^-$ cells) compared to control mice irrespective of the genetic background of the transplanted HSPCs. Thus, the combination of Tp53 inactivation with reduced Ctnna1 expression levels did not further

reduce the diminished bone marrow erythropoiesis caused by the expansion of cells expressing shRNA 405 compared to wildtype bone marrow.

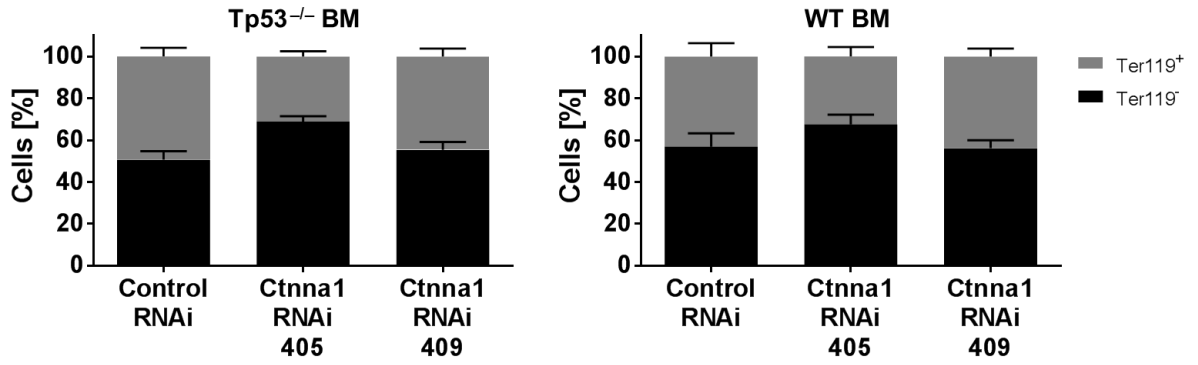

Figure 36: Reduced bone marrow erythropoiesis caused by expansion of cells encoding shRNA 405 in transplanted mice was not further diminished by additional inactivation of Tp53.
Mean frequencies of Ter119$^-$ (black bars) and Ter119$^+$ cells (grey bars) in the bone marrow of control mice (Control RNAi) and mice transplanted with HSPCs encoding shRNA 405 (Ctnna1 RNAi, 405) and shRNA 409 (Ctnna1 RNAi, 409) in Tp53$^{-/-}$ (left panel) and wildtype (WT, right panel) background. Increase of Ter119$^-$ cells in the bone marrow of mice transplanted with HSPCs encoding shRNA 405 (Ctnna1 RNAi, 405) indicated diminished bone marrow erythropoiesis, which was not further reduced when Tp53 was additionally inactivated.

4.5.4 Inactivation of Tp53 reinforced the clonal dominance of GFP$^+$ cells in the progenitor and stem cell compartments of mice transplanted with HSPCs encoding shRNA 405

Previously, the recipients of HSPCs encoding shRNA 405 showed an expansion of GFP$^+$ cells in the hematopoietic stem and progenitor cell compartments of the bone marrow. To evaluate whether the additional inactivation of Tp53 enhances this phenotype, I determined the frequencies of lineage negative cells, LSK cells and HSCs in the bone marrow of the recipient mice. The frequencies of the cell populations (lineage negative, LSK and HSCs) within the entire bone marrow were similar in all transplanted mice (Figure 37, top and bottom left). However, in recipients transplanted with Tp53$^{-/-}$ HSPCs encoding shRNA 405, the fraction of GFP$^+$ cells was strongly increased in all three populations analyzed (up to 58% in lineage negative cells, up to 74% in LSK cells and up to 73% in HSCs, Figure 37, top right). For this group of mice, the frequency of GFP$^+$ cells was significantly increased within the LSK subpopulation compared to the GFP$^+$ cell frequency within the lineage negative cell population ($P<0.0001$, paired t-test, two-tailed P-value, $\alpha=0.05$). Mice of the respective wildtype group showed an increase of GFP$^+$ cells in the LSK and HSC compartment in one out of two mice compared to mice of the control group (Figure 37, bottom right). However, the expansion of GFP$^+$ cells was not as pronounced (up to 59% in LSK cells and 42% in HSCs, Figure 37, bottom right) as in the respective group of mice transplanted with Tp53$^{-/-}$ HSPCs (Figure 37, top right). The expansion of GFP$^+$ cells within the progenitor cell compartments was also less pronounced in mice transplanted with Tp53$^{-/-}$ HSPCs encoding shRNA 409. Compared to control, only one out of four mice showed an expansion of GFP$^+$ cells within the LSK compartment (M53-16, 57%; Figure 37, top right). Three out of four

mice of group 409 displayed an increased GFP$^+$ cell frequency in the HSC compartment (up to 52%). The frequency of GFP$^+$ cells in the HSC compartment in the bone marrow of mice of group 409 was significantly increased compared to the lineage negative subpopulation (P=0.0433, paired t-test, two-tailed P-value, α=0.05). An expansion of wildtype GFP$^+$ cells encoding shRNA 409 was not observed (Figure 37, bottom right).

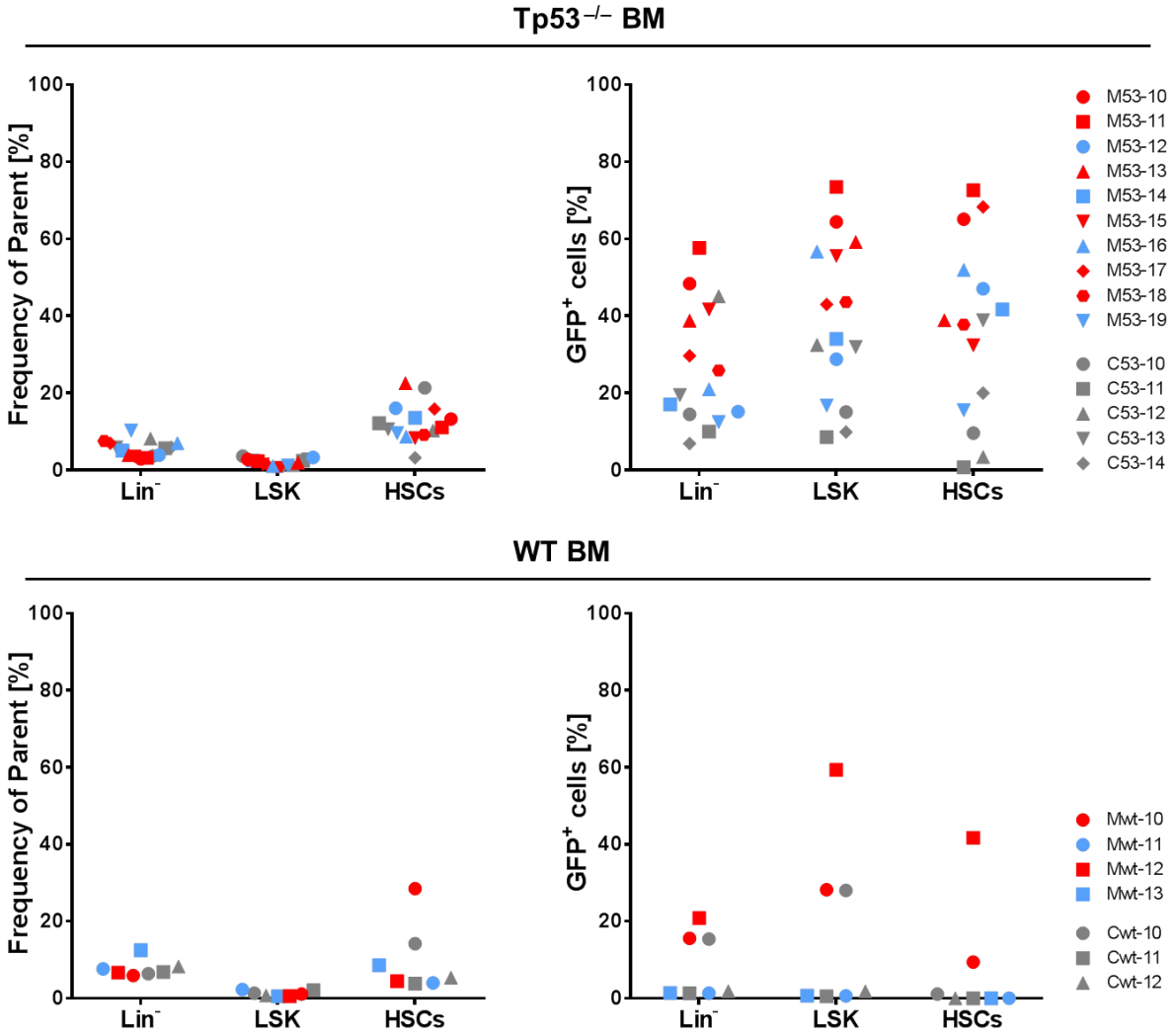

Figure 37: Inactivation of Tp53 reinforces the clonal dominance of GFP$^+$ cells within the LSK and HSC compartments of transplanted mice.
Flow cytometric analysis of hematopoietic progenitor cell populations in transplanted mice with GFP$^+$ cell expansion in the bone marrow. Frequencies of the indicated progenitor cell compartment in whole bone marrow (left, Parent of Lin$^-$: P1, parent of LSK: Lin$^-$, parent of HSCs: LSK (as in Figure 57, top)) and GFP$^+$ cell populations therein (right) are shown for mice transplanted with HSPCs encoding control shRNA (grey symbols), shRNA 405 (red symbols) or shRNA 409 (blue symbols) in Tp53$^{-/-}$ (top) and wildtype (WT, bottom) genetic background.

In summary, this experiment revealed that the inactivation of Tp53 reinforces the clonal dominance of bone marrow cells with reduced expression levels of Ctnna1. The loss of Tp53 enhances the repopulation and expansion potential of HSPCs with reduced Ctnna1 expression, especially in the HSC compartment of the bone marrow. However, the previously observed differentiation bias towards the myeloid lineage of the transplanted bone marrow

cells expressing shRNA 405 and the diminished bone marrow erythropoiesis caused by the expansion of GFP^+ cells in the bone marrow were not further enhanced when Tp53 was inactivated and, therefore, resulted from the expression of shRNA 405 alone.

4.6 Loss of Tp53 reinforces the neoplastic potential of bone marrow cells with reduced Ctnna1 expression upon secondary transplantation

4.6.1 Inactivation of Tp53 enhances bone marrow repopulation potential of cells with reduced Ctnna1 expression in secondary recipient mice without impacting peripheral hematological parameters

To test whether the clonal dominance of bone marrow cells with reduced Ctnna1 expression is reinforced by additional Tp53 inactivation, I performed secondary transplantations into sublethally irradiated recipients. Bone marrow cells from one mouse of each group from the previous experiment (control shRNA: C53-12, shRNA 405: M53-15, shRNA 409: M53-14) were transplanted into 10 sublethally irradiated recipient mice (group 405: 4 mice, group 409: 4 mice, control group: 2 mice, Figure 38).

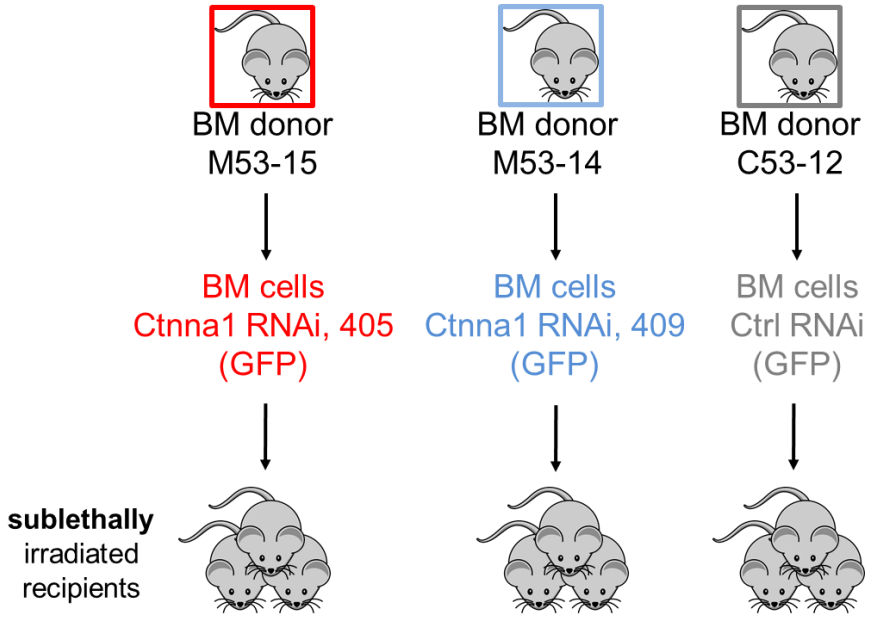

Figure 38: Design of the secondary transplantation experiment of $Tp53^{-/-}$ bone marrow cells from primary recipients.
One mouse of each group of mice transplanted with $Tp53^{-/-}$ HSPCs (M53-15, M53-14, C53-12, see Figure 31) was selected as primary bone marrow donor for secondary transplantations. All three donor animals showed an expansion of GFP^+ cells in the bone marrow. $5x10^6$ whole bone marrow cells were pooled with $2x10^5$ whole bone marrow cells from a wildtype animal and transplanted into ten sublethally irradiated recipient mice (4xM53-15, 4xM53-14, 2xC53-12). The experiment was terminated at 12 weeks after transplantation and bone marrow cells, splenocytes and peripheral blood cells were prepared and analyzed as described previously.

At 12 weeks after secondary transplantation I analyzed the frequencies of GFP^+ cells in the bone marrow, peripheral blood and spleen of the recipient mice. While the primary transplant donor mouse M53-15 (shRNA 405) showed a GFP^+ cell frequency of 59% in the

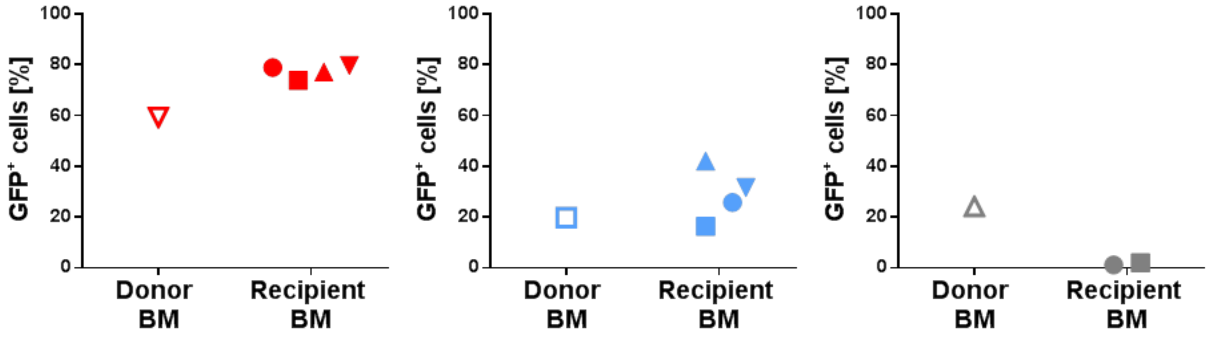

Figure 39: Tp53 inactivation in secondary transplanted bone marrow cells mediated successful engraftment of GFP$^+$ cells encoding shRNA 405 or 409.
Frequencies of GFP$^+$ bone marrow cells of the donor mice compared to the frequencies of GFP$^+$ cells found in the bone marrow of secondary recipient mice. Red: M53-15 as primary donor (shRNA 405), blue: M21 as primary donor (shRNA 409), grey: C23 as primary donor (control shRNA). See Figure 40 for full legend of the recipient mice.

bone marrow, the mean GFP$^+$ cell frequency in the bone marrow of secondary recipients was higher (77.5±2.5%, Figure 39, left). Accordingly, the secondary recipient mice of bone marrow cells from mouse M53-14 (shRNA 409) showed a mean GFP$^+$ cell frequency of 29 ± 13% in the bone marrow, which was higher than the respective GFP$^+$ cell frequency of the primary transplant donor mouse M53-14 (20%, Figure 39, middle). GFP$^+$ cells transplanted from control mouse C53-12 were not able to engraft in secondary recipients (Figure 39, right).

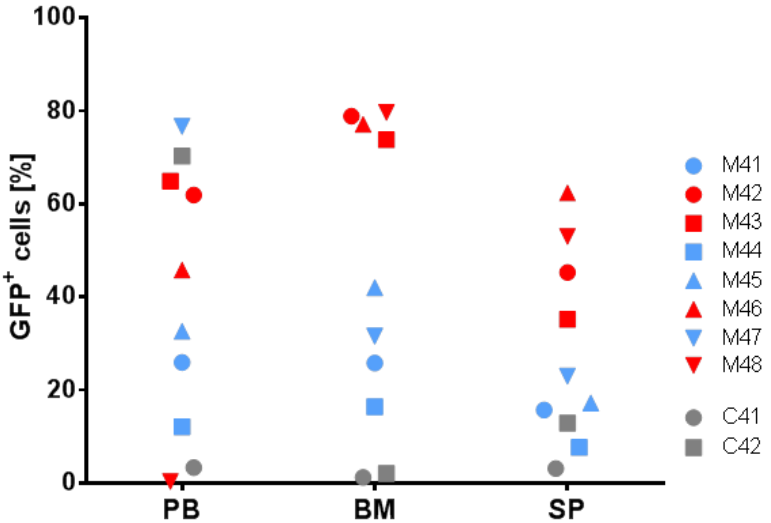

Figure 40: Frequencies of GFP$^+$ cells in peripheral blood, bone marrow and spleen of secondary recipient mice transplanted with Tp53$^{-/-}$ bone marrow cells from primary recipients.
The frequencies of GFP$^+$ cells as a measure for the proportion of cells with reduced Ctnna1 expression were analyzed by flow cytometry in mononuclear cells isolated from the peripheral blood (PB), the bone marrow (BM) and the spleen (SP) at 12 weeks after secondary transplantation. Red and blue symbols indicate mice transplanted with bone marrow of mice M53-15 (shRNA 405) and M53-14 (shRNA 409), respectively (termed "M4x"), grey symbols indicate mice transplanted with bone marrow of control mouse C53-12 (control shRNA, termed "C4x).

These results suggested a successful engraftment and an expansion of GFP$^+$ cells when Tp53$^{-/-}$ bone marrow cells encoding shRNA 405 or shRNA 409 were transplanted into secondary recipient mice. Strikingly, an engraftment of wildtype HSPCs encoding shRNA 409 in secondary recipients was not observed before (Figures 26 and 27), thus the inactivation of Tp53 had an additive effect on the self-renewing potential of bone marrow cells encoding shRNA 409. The loss of Tp53 alone did not account for the engraftment of bone marrow cells in sublethally irradiated secondary recipients, as the secondary transplanted GFP$^+$ bone marrow cells of control mouse C53-12 did not engraft. Thus, inactivation of Tp53 and downregulation of Ctnna1 had a synergistic effect on the self-renewal of bone marrow cells upon secondary transplantation.

GFP$^+$ cells were detected at in the bone marrow, peripheral blood and spleen of all mice transplanted with Tp53$^{-/-}$ bone marrow cells encoding either shRNA 405 or shRNA 409 from primary recipients (Figure 40). Previously, a characteristic pattern of GFP$^+$ cell distribution (high in BM, lower in PB and SP) was observed in mice transplanted with HSPCs encoding shRNA 405, indicating a block in hematopoietic cell maturation. Correspondingly, all mice of group 405 showed elevated frequencies of GFP$^+$ cells in the bone marrow (up to

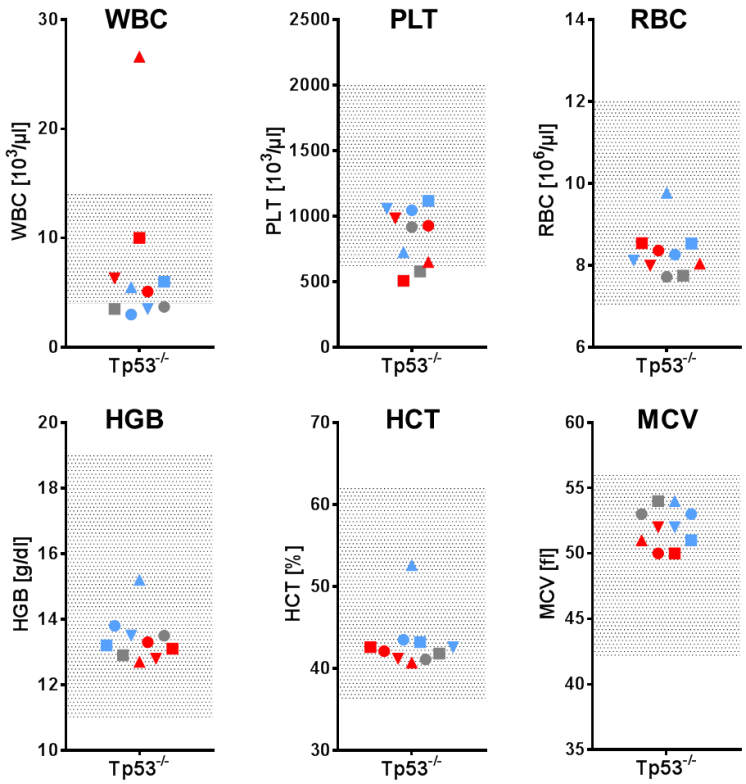

Figure 41: Secondary recipient mice transplanted with Tp53$^{-/-}$ bone marrow cells from primary donors did not show overt signs of hematological disease at 12 weeks post transplantation.
White blood cell (WBC) counts, platelet (PLT) counts, red blood cells (RBC) counts, hemoglobin (HGB) concentration, hematocrit (HCT) and mean corpuscular volume (MCV) of whole blood samples from secondary transplanted mice at 12 weeks after transplantation. Blue and red symbols indicate mice transplanted with bone marrow of mice M53-14 and M53-15, respectively, grey symbols indicate mice transplanted with bone marrow of control mouse C53-12 (see Figure 40 for full legend). Shaded areas indicate the normal range for each parameter (WBC: 4-14x10^3/µl, PLT: 600-2000x10^3/µl, RBC: 7-12x10^6/µl, HGB: 11-19 g/dl, HCT: 36-62%, MCV: 42-56 fl) for healthy C57BL/6 mice (from: Charles River Laboratories International, Inc., 2012).

80%) and less in the peripheral blood (up to 65%) and the spleen (up to 63%, Figure 40). However, this effect was not significant (BM vs. PB: P=0.1191, paired t-test, two-tailed P-value, α=0.05). Mice transplanted with bone marrow cells from mouse M53-14 (shRNA 409) showed GFP^+ cell frequencies of up to 77% in the peripheral blood, 42% in the bone marrow and 23% in the spleen (Figure 40). Remarkably, two mice of this group (M44 and M45) displayed the characteristic pattern of GFP^+ cell distribution as observed in mice from group 405.

Taken together, these results indicated that the inactivation of Tp53 had an additive effect on the engraftment ability of secondary transplanted bone marrow cells with reduced Ctnna1 expression, encoding either shRNA 405 or 409. The previously observed block in maturation of transplanted bone marrow cells encoding shRNA 405 was maintained upon secondary transplantation and also detected in two out of four secondary recipient mice transplanted with bone marrow from mouse M53-14 (shRNA 409). However, as cells of control mouse C53-12 did not engraft secondary recipients, this block in differentiation is due to reduced Ctnna1 expression levels and not enforced by Tp53 inactivation.

To test if the high frequencies of GFP^+ cells in the bone marrow caused a hematological disease in the secondary recipient mice, I measured the hematological parameters in their peripheral blood at termination of the experiment. Both mice of the control group and two out of four mice of group 409 showed minimally reduced WBC counts (Figure 41). One mouse of group 405 showed a high WBC count (Figure 41). This single value could result from the expansion of a single bone marrow cell clone due to an additional driver mutation. For all other mice, the WBC counts were normal (Figure 41). One mouse of group 405 and one mouse of the control group showed reduced PLT counts, while all other mice displayed normal PLT values. For all other parameter, the values of all mice were within their normal ranges (Figure 41). Thus, the recipient mice did not show any overt hematological dysregulations upon secondary transplantation of $Tp53^{-/-}$ HSPCs with reduced Ctnna1 expression. These results were somewhat surprising, as secondary transplantation of wildtype HSPCs encoding shRNA 405 caused obvious reduction of erythroid parameters in the peripheral blood of the recipient mice (Figure 25C-F), most likely due to the clonal dominance of GFP^+ cells in the bone marrow. This time, the clonal dominance was observed in all mice of group 405 and in two mice of group 409, yet no dysregulation in peripheral blood parameters was detected. However, this experiment was terminated at twelve weeks after secondary transplantation as opposed to 27 weeks in the preceding secondary transplantation assay. Thus, an effect of the clonal dominance of expanded secondary transplanted GFP^+ bone marrow cells with Tp53 inactivation and reduced Ctnna1 expression on the hematological parameters might have been observed at a later time point, when long-term repopulation of the secondary recipients was achieved.

4.6.2 Tp53$^{-/-}$ bone marrow cells with reduced Ctnna1 expression level maintain the differentiation bias towards the myeloid lineage upon secondary transplantation

Reduced Ctnna1 expression levels in Tp53$^{-/-}$ HSPCs mediated a differentiation bias of bone marrow cells towards the myeloid lineage as observed before for WT HSPCs. To determine whether this phenotype is maintained upon secondary transplantation of Tp53$^{-/-}$ bone marrow cells, I determined the frequencies of lymphoid and myeloid cells in the hematopoietic organs of the secondary recipients. Mice of group 405 showed a differentiation bias towards the myeloid lineage in whole bone marrow cells (65% myeloid, 11% lymphoid) compared to control mice (42% myeloid, 18% lymphoid; Figure 42A). Within the GFP$^+$ cell population, this phenotype was even more pronounced (77% myeloid, 7% lymphoid; Figure 42B). A similar manifestation was observed in the bone marrow of secondary recipient mice of group 409. In whole bone marrow, 49% of cells were myeloid and 18% of cells were lymphoid (Figure 42A). Within the GFP$^+$ bone marrow cells of these mice, the manifestation of this phenotype was strongly enhanced (67% myeloid, 11% lymphoid) compared to whole bone marrow (Figure 42B). However, the myeloid differentiation bias in the bone marrow of this group of mice was not as prominent as in the group transplanted with bone marrow from mouse M53-15 (shRNA 405). The myeloid differentiation bias was detected exclusively in the bone marrow of the recipient mice of groups 405 and 409, not in the peripheral blood or spleen. This suggested a block in maturation of myeloid bone marrow cells and a lack of transition of these cells to the periphery, as observed before (Figure 35).

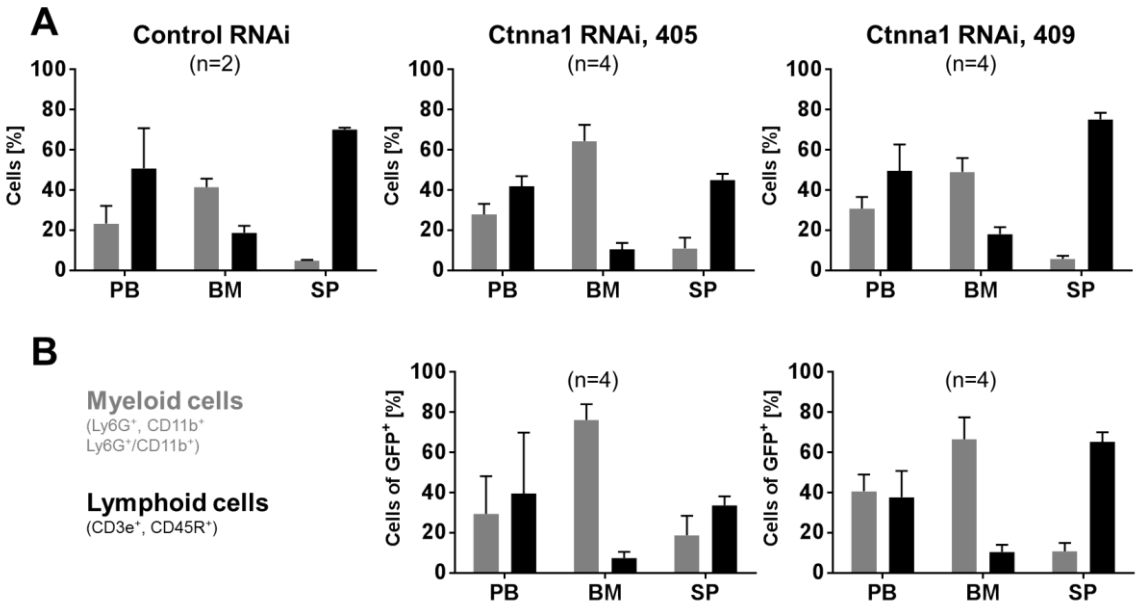

Figure 42: Bone marrow cells of secondary recipients encoding shRNA 405 or shRNA 409 were mostly differentiated within the myeloid lineage.
Flow-cytometric analysis of myeloid (grey bars) and lymphoid cells (black bars) in peripheral blood (PB), bone marrow (BM) and spleen (SP) of mice transplanted with Tp53$^{-/-}$ bone marrow cells from primary recipients encoding control shRNA (left), shRNA 405 (middle) or shRNA 409 (right). Top panels show myeloid and lymphoid cell frequencies in all cells, bottom panels show myeloid and lymphoid cell frequencies in GFP$^+$ cells of the indicated organs.

Next, I assessed the impact of secondary transplantation of $Tp53^{-/-}$ bone marrow cells with reduced Ctnna1 expression on erythropoiesis and measured the frequencies of $Ter119^-$ cells in the bone marrow of the secondary recipient mice. Exclusively mice transplanted with bone marrow from mouse M53-15 (shRNA 405) showed a pronounced elevation of $Ter119^-$ cells (77%) compared to control (49%; Figure 43). Mice transplanted with bone marrow cells from mouse M53-14 (shRNA 409) did only show a minor increase of the $Ter119^-$ cell frequency (53%) in the bone marrow compared to control mice (Figure 43). This indicated that inactivation of Tp53 did not further decrease the diminished bone marrow erythropoiesis caused by the expansion of bone marrow cells with reduced Ctnna1 expression in secondary transplanted mice.

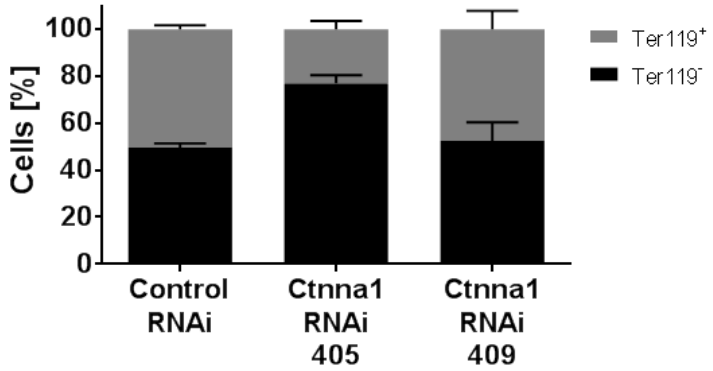

Figure 43: Reduced bone marrow erythropoiesis caused by the expansion of bone marrow cells expressing shRNA 405 was maintained in secondary recipient mice.
Mean frequencies of $Ter119^-$ (black bars) and $Ter119^+$ cells (grey bars) in the bone marrow of secondary recipients transplanted with bone marrow from mouse C53-12 (Control RNAi), M53-15 (Ctnna1 RNAi, 405) and M53-14 (Ctnna1 RNAi, 409).

4.6.3 The clonal dominance of bone marrow cells with reduced Ctnna1 expression within the stem and progenitor cell compartments is enhanced by the additional inactivation of Tp53 upon secondary transplantation

In previous transduction-transplantation experiments, the inactivation of Tp53 mediated a reinforced clonal dominance of bone marrow cells with reduced Ctnna1 expression in the stem and progenitor cell compartments of the bone marrow. To find out whether this phenotype is maintained upon secondary transplantation, I measured the frequencies of lineage negative cells, LSK cells and HSCs in the bone marrow and the fraction of GFP^+ cells within these progenitor cell subpopulations. Secondary transplantation of $Tp53^{-/-}$ bone marrow from primary recipients did not lead to increased frequencies of the stem and progenitor cell compartments in the entire bone marrow of secondary recipient mice (Figure 44, left). However, reduced Ctnna1 expression mediated by shRNA 405 conveyed a strong expansion of GFP^+ cells within the progenitor cell populations (34-75% in lineage negative cells, 90-94% in LSK cells and 53-80% in HSCs, Figure 44; right). In this group of mice, the frequency of GFP^+ cells within the LSK compartment was significantly increased

compared to the GFP$^+$ cells within the lineage negative cells and HSC compartments (LSK vs. Lin$^-$: P=0.0311, LSK vs. HSC: P=0.0104, paired t-test, two-tailed P-value, α=0.05). For mice of group 409, GFP$^+$ bone marrow cells expanded within the progenitor cell populations as well (18-25% in lineage negative cells, 42-65% in LSK cells and 18-74% in HSCs; Figure 44). Here, the frequency of GFP$^+$ cells was significantly increased within the LSK cell compartment compared to the frequency of GFP$^+$ cells within the lineage negative cells (LSK vs. Lin$^-$: P=0.033, paired t-test, two-tailed P-value, α=0.05). Strikingly, mice M44 and M45 of group 409 even showed an increased frequency of GFP$^+$ cells within the HSC compartment (Figure 44, right), indicating a similar clonal dominance phenotype of GFP$^+$ cells expressing shRNA 409 as observed before in mice transplanted with HSPCs encoding shRNA 405.

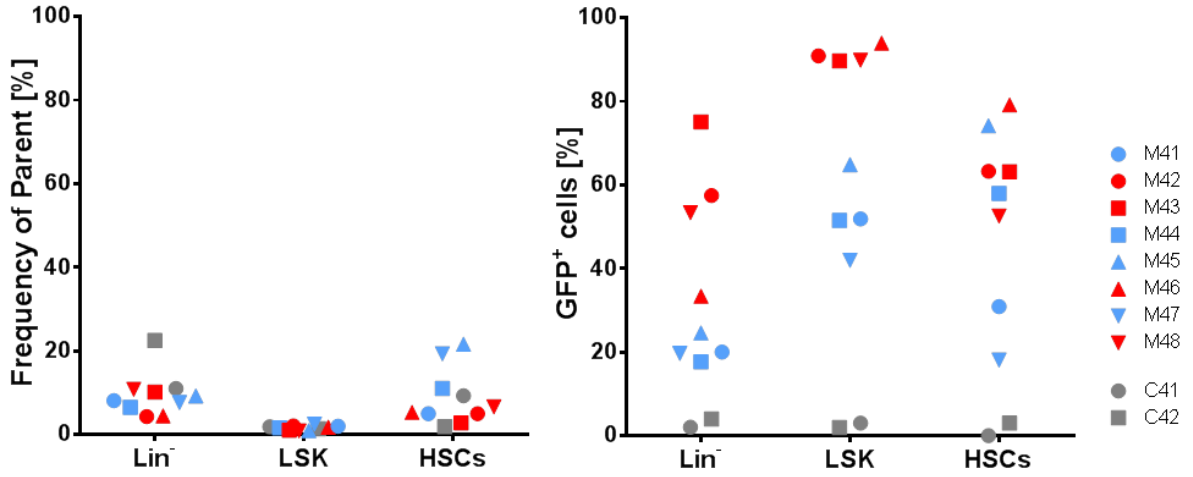

Figure 44: The clonal dominance of bone marrow cells with reduced Ctnna1 expression is maintained and reinforced upon secondary transplantation of Tp53$^{-/-}$ bone marrow cells.
Flow cytometric analysis of hematopoietic progenitor cell populations in the bone marrow of secondary recipient mice. Frequencies of the indicated progenitor cell compartment in whole bone marrow (parent of Lin$^-$: P1, parent of LSK: Lin$^-$, parent of HSCs: LSK (as in Figure 57, top)) and GFP$^+$ cell populations therein are shown for mice transplanted with bone marrow from mouse C53-12 (Control RNAi, grey symbols), M53-15 (shRNA 405, red symbols) and M53-14 (shRNA 409, blue symbols).

The clonal dominance observed in transplanted bone marrow cells with Tp53 inactivation and reduced Ctnna1 expression was maintained upon secondary transplantation into sublethally irradiated recipients. GFP$^+$ cells encoding either shRNA 405 or 409 were significantly increased within the LSK compartment in the bone marrow of secondary recipients. These results suggested the presence of neoplastic cells in the bone marrow of mice that received HSPCs encoding shRNA 405 or shRNA 409. Thus, the inactivation of Tp53 reinforced the clonal dominance phenotype of HSPCs with reduced Ctnna1 expression, particularly in the hematopoietic stem and progenitor cell compartments. As secondary transplanted Tp53$^{-/-}$ cells from control mouse C53-12 did not engraft and thus did not expand within these compartments, the clonal dominance is not caused by Tp53 inactivation alone. Its combination with the reduction in Ctnna1 gene dosage provided a synergistic effect on the potential of self-renewal of the transplanted cells.

4.7 Loss of Tp53 and reduced Ctnna1 expression leads to an earlier onset of death, most likely by peripheral blood cell dysplasia and bone marrow failure

4.7.1 Genetic inactivation of Tp53 in transplanted HSPCs significantly decreases overall survival of recipient animals

Expression of shRNA 405 combined with genetic inactivation of Tp53 in the bone marrow cells of primary and secondary recipient mice led to a reinforced clonal dominance of GFP^+ cells in the bone marrow. To determine the impact of reduced Ctnna1 expression levels with and without loss of Tp53 on the survival, I performed a competitive reconstitution experiment without a distinct termination time point and evaluated the survival of the recipient mice. The experiment comprised four groups of recipient animals: mice of two groups were transplanted with transduced HSPCs from $Tp53^{-/-}$ donors, encoding either control shRNA (7 mice) or shRNA 405 (8 mice). Mice of two control groups received transduced HSPCs from wildtype donors encoding control shRNA (7 mice) or shRNA 405 (7 mice). As before, the mice were monitored on a daily basis for their health. Upon signs of obvious illness, they were sacrificed and analyzed as previously described.

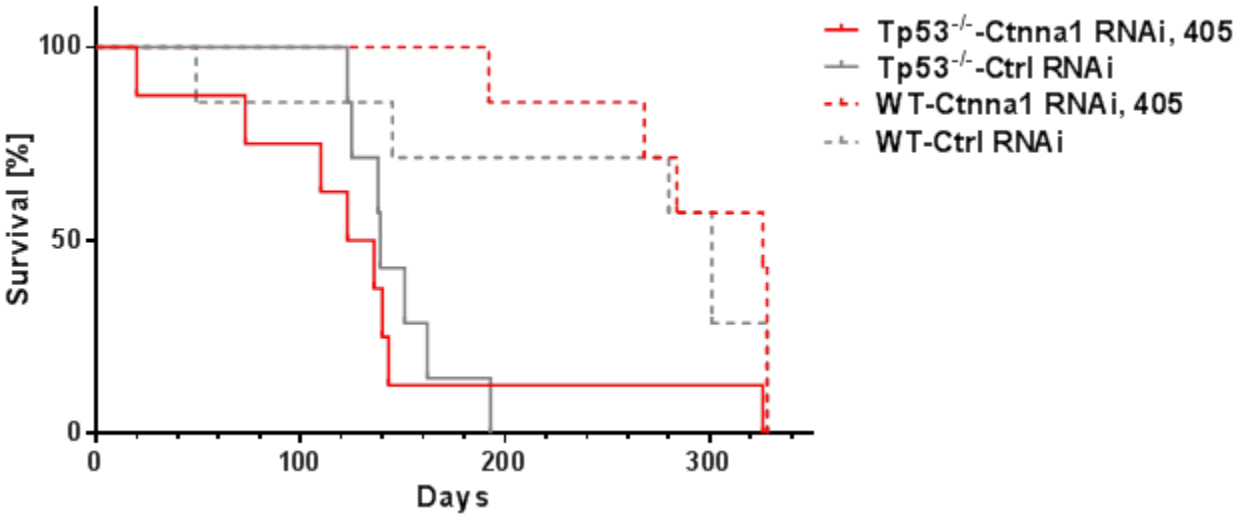

Figure 45: Genetic inactivation of Tp53 and reduced Ctnna1 gene dosage in the bone marrow of transplanted mice reduced the overall survival of the animals.
Kaplan-Meier survival curve of mice from two groups of mice transplanted with $Tp53^{-/-}$ HSPCs encoding control shRNA (7 mice, grey solid line) or shRNA 405 (8 mice, red solid line) and mice of two control groups transplanted with wildtype (WT) HSPCs encoding control shRNA (7 mice, grey dashed line) or shRNA 405 (7 mice, red dashed line). The survival of mice from group $Tp53^{-/-}$-Ctnna1 RNAi, 405 was significantly decreased compared to mice of the group WT-Ctnna1 RNAi, 405 (P=0.0033, Log-rank (Mantel-Cox) test).

The survival of the mice in each recipient group was observed and the experiment was terminated at 330 days after transplantation and all remaining mice were sacrificed. The median survival times of the mice of the groups were 129.5 days ($Tp53^{-/-}$-Ctnna1 RNAi, 405), 139 days ($Tp53^{-/-}$-Ctrl RNAi), 326 days (WT-Ctnna1 RNAi, 405) and 301 days (WT-Ctrl RNAi; Figure 45). Mice transplanted with $Tp53^{-/-}$ HSPCs encoding shRNA 405

showed a significantly shorter overall survival than mice transplanted with wildtype HSPCs encoding shRNA 405 (P=0.0033, two-tailed P-value, α=0.05, Log-rank (Mantel-Cox) test). However, independently from the genetic background, the overall survival of mice of the group transplanted with HSPCs encoding shRNA 405 was not significantly different from mice of the respective control group ($Tp53^{-/-}$: P=0.5671 and WT: P=0.5426, two-tailed P-value, α=0.05, Log-rank (Mantel-Cox) test).

These results showed a decrease in the overall survival due to the inactivation of Tp53. Reduced Ctnna1 expression levels alone in transplanted HSPCs did not cause differences in the survival of the mice compared to the respective control transplanted mice.

4.7.2 Recipient mice of HSPCs expressing shRNA 405 show pronounced peripheral blood cell dysplasia

Mice transplanted with $Tp53^{-/-}$ HSPCs encoding shRNA 405 showed a decreased survival often associated with visual signs of disease (ruffled fur, decreased motility, etc.). To investigate whether the mice suffered from peripheral blood cell dysplasia due to Ctnna1 gene dosage insufficiency, I analyzed the blood cell morphology in peripheral blood smears of the transplanted mice. In the blood of an age-matched wildtype mouse I found well-differentiated, mature cells of all lineages (Figure 46, 1-8; McGarry, 2010). In contrast, the blood smears of transplanted mice who received $Tp53^{-/-}$ or WT HSPCs encoding shRNA 405 were nearly devoid of mature lymphocytes. Instead, I almost exclusively found abnormal leukocytes with primarily monocytic features, often of different sizes and shapes of cells and nuclei (pleomorphism, pelgroid nuclei, Figure 46, 11-21; Sprussel et al., 2012). Furthermore, neutrophils showed hypersegmentation of their nuclei (Figure 46, 9-10) and erythrocytes were abnormally shaped (poikilocytosis), polychromatic or nucleated (Figure 46, 22-24; Lin et al., 2005). This strongly indicated a peripheral blood cell dysplasia, most likely caused by inefficient bone marrow hematopoiesis in the transplanted mice.

Next, I analyzed cytospins of bone marrow cells for the presence of dysplastic cellular features. GFP^- cells were comprised of progenitor cells from all hematopoietic lineages at physiological frequencies (Figure 47, right), as they were present in the bone marrow of an age-matched wildtype mouse (Figure 47, left). Conversely, the GFP^+ bone marrow cells from mice transplanted with HSPCs encoding shRNA 405 clearly showed a mainly granulocytic phenotype and a high frequency of myeloblasts (Figure 47, middle). These results confirmed the myeloproliferative phenotype of the GFP^+ bone marrow cell population detected previously by flow cytometry and revealed bone marrow cell dysplasia due to the expression of shRNA 405.

Taken together, additional inactivation of Tp53 accelerated the onset of death, because it reinforced the clonal dominance of HSPCs with reduced Ctnna1 expression by shRNA 405 in the bone marrow. However, all mice transplanted with HSPCs encoding shRNA 405 suffered from ineffective bone marrow hematopoiesis leading to dysplastic cells in the peripheral blood. The mice most likely became severely diseased due to progressive bone

marrow cell dysplasia ultimately leading to a failure of the hematopoietic system, accelerated by the additional loss of Tp53.

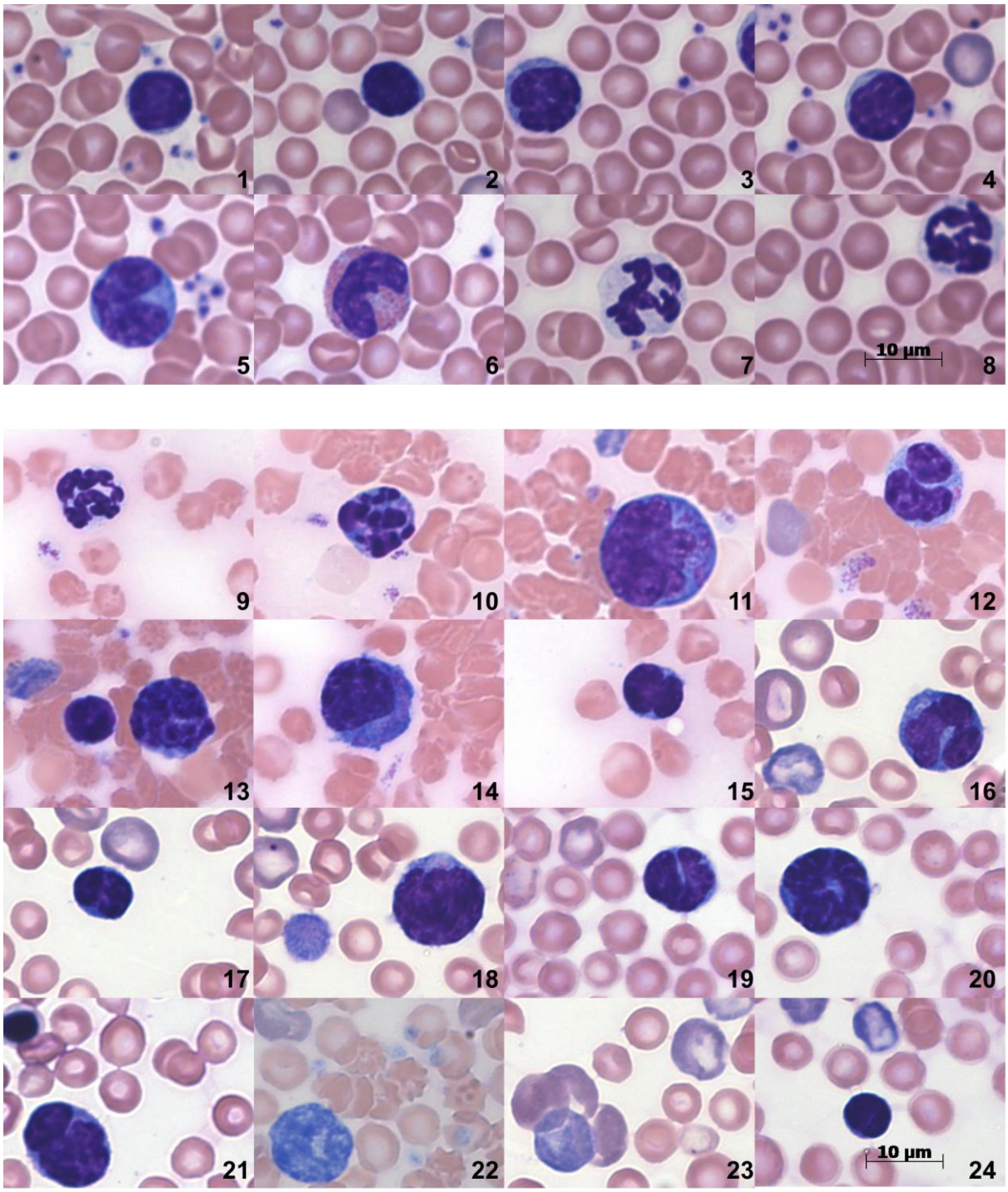

Figure 46: Reduced Ctnna1 expression in the bone marrow of transplanted mice led to peripheral blood cell dysplasia.
Peripheral blood smears of an age matched wildtype mouse (1-8) and recipients of HSPCs encoding shRNA 405 (9-24). 1-8: Mature blood cells of normal appearance: lymphocytes (1, 2), monocytes (3-5), basophils (6) and neutrophils (7, 8) with erythrocytes and thrombocytes. 9-24: Dysplastic blood cells: hypersegmented neutrophils (9, 10), cells with primarily monocytic features, with pleomorphic, sometimes pelgroid nuclei (11-21), abnormal, sometimes nucleated or polychromatic erythrocytes (22-24).

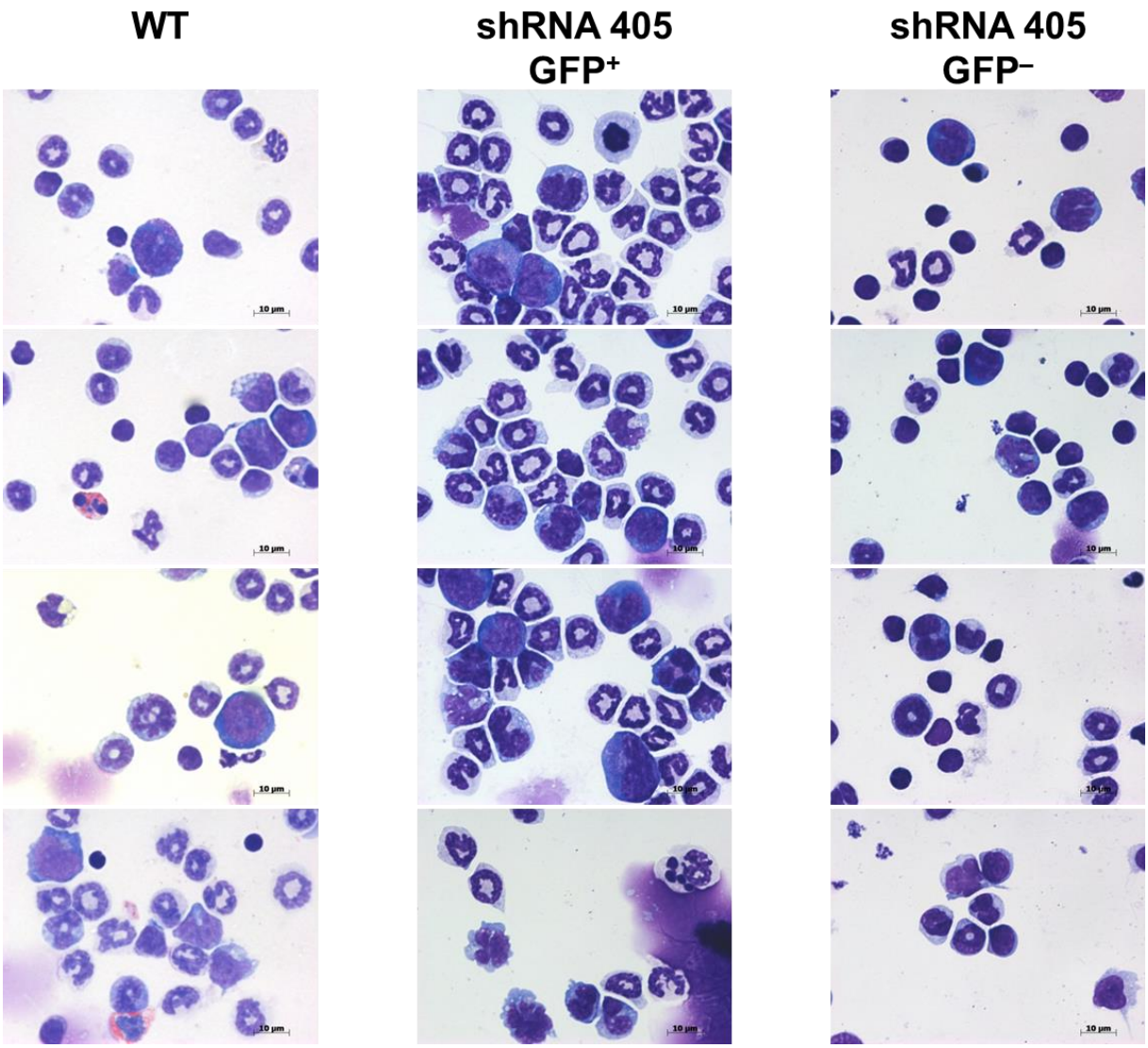

Figure 47: GFP$^+$ bone marrow cells expressing shRNA 405 were primarily composed of granulocytic progenitor cells and myeloblasts.
Left: Cytospin of bone marrow cells from an age matched wildtype (WT) mouse. Progenitor cells of all lineages were present at physiological frequencies. Middle: Cytospin of GFP$^+$ bone marrow cells from a representative mouse transplanted with HSPCs encoding shRNA 405, in which GFP$^+$ cells were expanded in the bone marrow. The cells were almost exclusively comprised of granulocytic progenitor cells, proerythroblasts and myeloblasts and devoid of lymphoid progenitors. This confirmed the myeloproliferative phenotype within the GFP$^+$ bone marrow cells expressing shRNA 405 as detected by flow cytometry. Right: Cytospin of GFP$^-$ negative cells from the same mouse transplanted with HSPCs encoding shRNA 405. Progenitor cells of all lineages were present at physiological frequencies.

4.8 Expression of shRNA 405 immortalizes primary murine bone marrow cells and confers a myeloproliferative phenotype *in vitro*

4.8.1 Primary murine bone marrow cells can be immortalized *in vitro* by the expression of shRNA 405

HSPCs encoding shRNA 405 targeting Ctnna1 showed a strong clonal dominance *in vivo* upon primary and secondary transplantation. This phenotype was associated with a differentiation bias of bone marrow cells towards the myeloid lineage and an expansion of

cells with reduced Ctnna1 expression within the stem and progenitor cell compartments of the bone marrow. To test whether reduced Ctnna1 expression also confers an advantage to cultured cells *in vitro*, freshly isolated, lineage negative wildtype and Tp53$^{-/-}$ HSPCs were transduced with a lentiviral vector encoding shRNA 405 (or control shRNA) plus GFP and monitored for their growth and the frequencies of GFP^{+} cells.

Non-transduced or control-transduced cells proliferated *in vitro* for approximately two weeks (Figure 48). In contrast, cells expressing shRNA 405 constantly expanded in culture. After 24 days (Tp53$^{-/-}$) or 31 days (wildtype) the proliferation and expansion of the cells could be attributed exclusively to the GFP^{+} cell population within the culture (Figure 48, bottom). The proportion of GFP^{+} cells increased immensely until they completely prevailed the GFP^{-} cells. Without Tp53, the growth of the cells expressing shRNA 405 was strongly enhanced, and, after 31 days in culture, 25fold more cells were detected compared to wildtype cells expressing shRNA 405 (Figure 48, top).

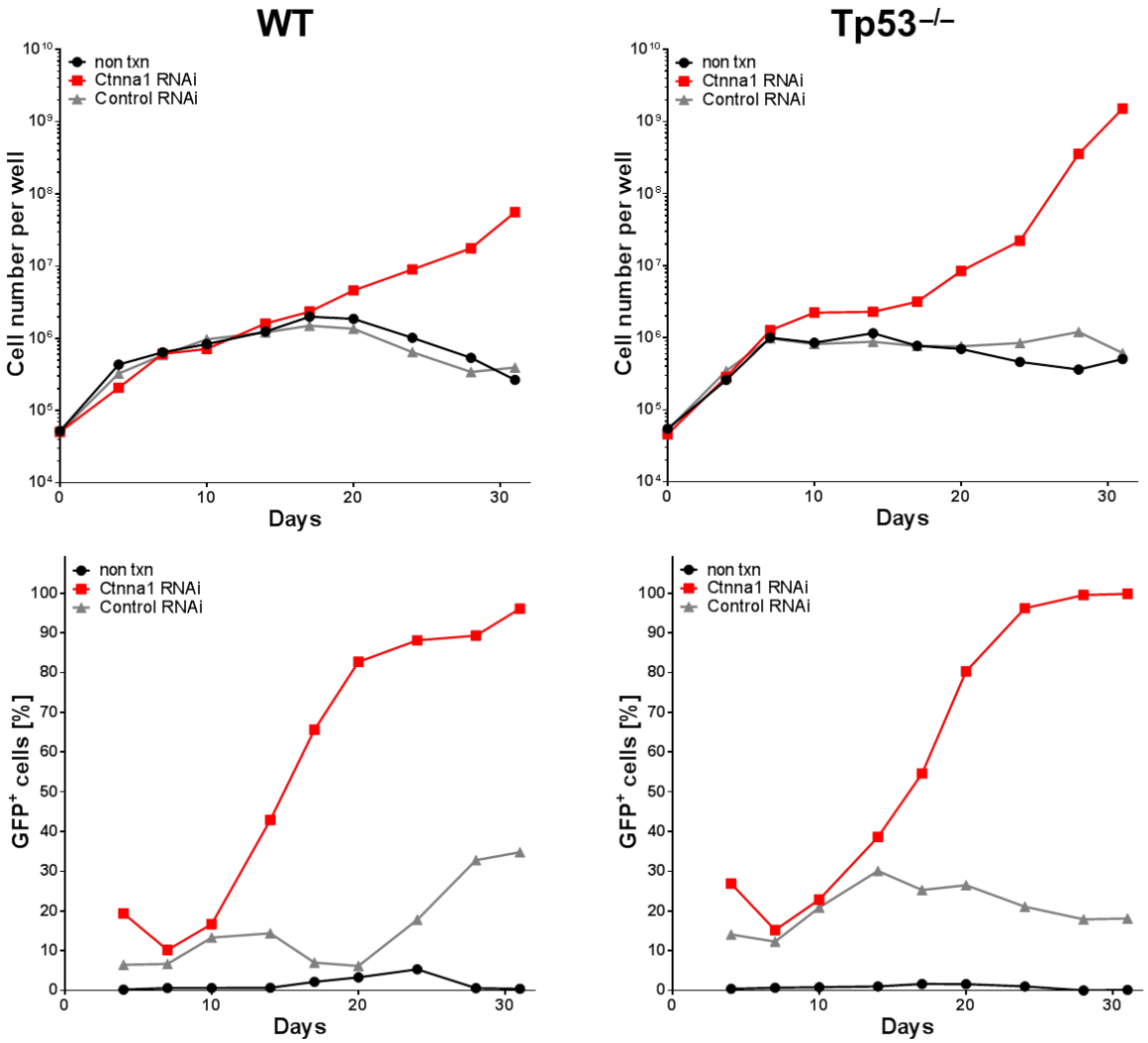

Figure 48: Expression of shRNA 405 immortalizes primary murine bone marrow cells *in vitro*.
Freshly isolated primary bone marrow cells from wildtype (WT, left) and Tp53$^{-/-}$ mice (right) were transduced with lentiviral vectors encoding shRNA 405 (Ctnna1 RNAi) or control (Control RNAi). 24 hours after transduction, 5x10^{4} cells were plated per well and their growth (top) and GFP^{+} cell frequency (bottom) was monitored for 31 days.

4.8.2 Most immortalized murine bone marrow cells expressing shRNA 405 show a myeloid immunophenotype while a lineage negative subpopulation is maintained

Primary murine bone marrow cells were immortalized *in vitro* by expression of shRNA 405. To determine the phenotype of the cells maintaining the culture, freshly isolated primary bone marrow cells of a wildtype donor were transduced with a vector encoding shRNA 405 and a Puromycin resistance gene. After Puromycin selection (2µg/ml) and cultivation for 7 weeks, I assessed the immunophenotype of the cells by flow cytometry. 86% of the cells were $Ly6G^+$ and/or $CD11b^+$ and, thus, differentiated to mature cells of the myeloid lineage (Figure 49, top). Within the $Ly6G^-$ and $CD11b^-$ cells, 8.5% of the cells were $CD45R^+$ (data not shown). $CD3^+$ cells were not detected. 8.2% of the cells were lineage negative containing two LSK subpopulations based on different expression levels of Kit and Sca1 (LSK^+ 3.2%, LSK^{++} 2.21%), but no HSCs (Figure 49, top right).

To identify the population of cells that maintained the culture I separated lineage negative from positive cells by flow cytometric cell sorting and cultivated them for 8 days. Next, I re-analyzed their immunophenotypes. The lineage negative sorted subpopulation gave rise to a distinct lineage positive cell population (85.3%), of which almost all cells (81%) were differentiated to mature cells of the myeloid lineage ($Ly6G^+$ and/or $CD11b^+$; Figure 49, middle left), while lymphoid cells ($CD3^+$ and $CD45R^+$) were not detected (data not shown). Furthermore, a lineage negative subpopulation was maintained (14.7%; Figure 49, middle left). LSK cells were not detected within the lineage negative population, however, the Kit^+ cell population was maintained (50%; Figure 49, bottom left). In contrast, after 8 days of culture, the lineage positive sorted subpopulation contained only 62.2% myeloid cells, which was comprised to 67% of $CD11b^{low}$ cells (Figure 49; middle right). 50% of the $Ly6G^-$ and $CD11b^-$ cells were $CD45R^+$ and therefore differentiated towards the B cell lineage (data not shown). Furthermore, the lineage positive sorted subpopulation did not produce a distinct lineage negative population or LSK cells therein. (Figure 49, bottom right). Importantly, lineage positive sorted cells did not proliferate during the monitored time after sorting, whereas lineage negative sorted cells did. 8 days after separation, only 40% of cells in the lineage positive sorted culture were still alive (data not shown). The lineage negative sorted cell culture contained a frequency of 70% viable cells, which was comparable to non-sorted cells cultivated for 8 weeks (75% viable cells; data not shown). These results revealed that the culture-maintaining cells are a population within the lineage negative cells.

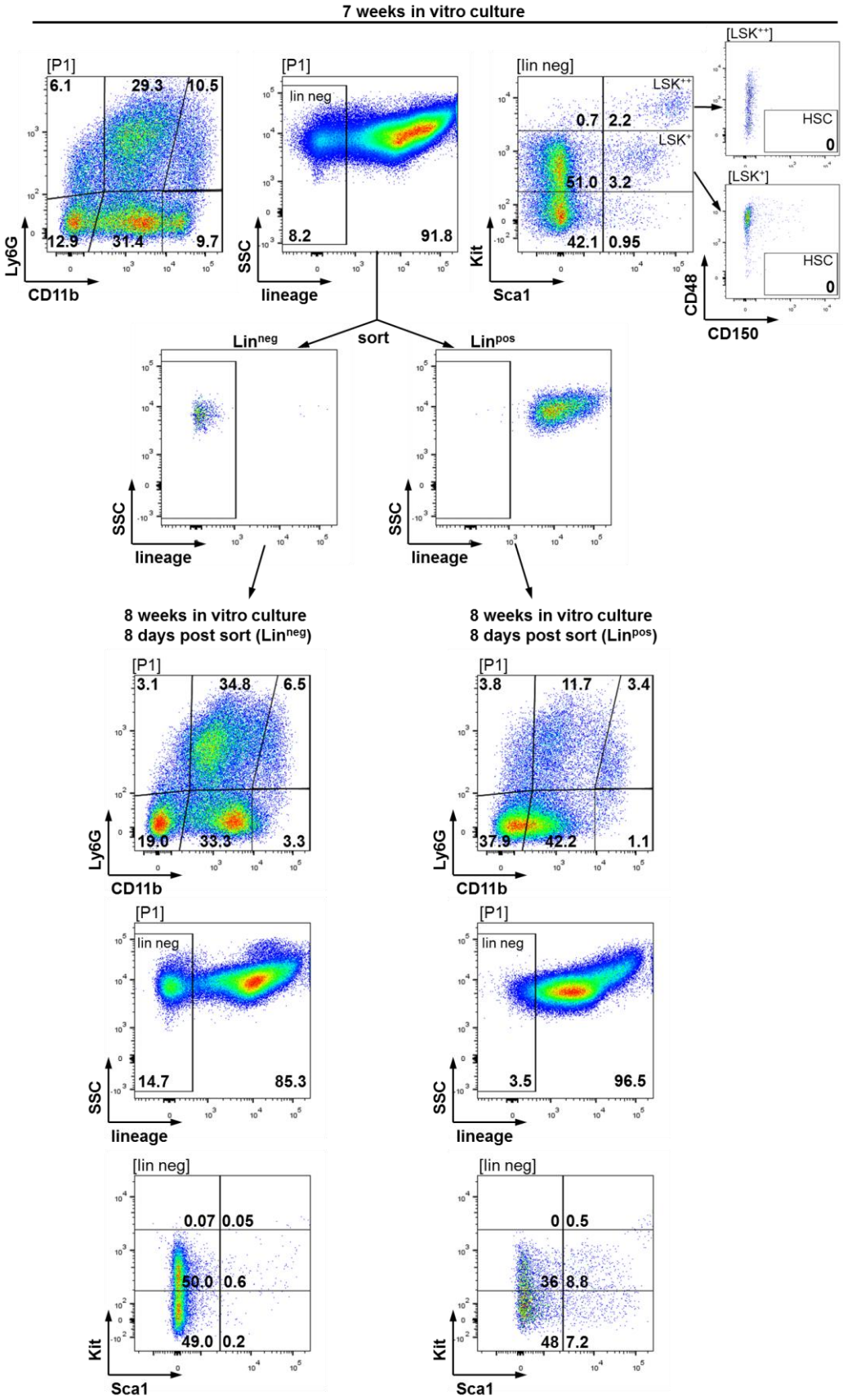

Figure 49: Lineage negative bone marrow cells are maintained upon immortalization by shRNA 405 and give rise to myeloid cells *in vitro*.

Top: 7 weeks cultivated immortalized primary bone marrow cells are mostly myeloid *in vitro* and maintain a lineage negative and LSK subpopulation, but no HSCs (top). Upon separation and cultivation of lineage positive and negative populations for 8 further days, only lineage negative cells gave rise to cells with the myeloid immunophenotype. However, the LSK population is lost (bottom). Frequencies in % of parent population, indicated on top of each dotplot.

4.8.3 Ectopic re-expression of Ctnna1 to different levels gradually reverts the growth phenotype of immortalized bone marrow cells *in vitro*

Immortalization of primary murine bone marrow cells was achieved by the knockdown of Ctnna1 expression by shRNA 405. However, vectors encoding other shRNAs targeting Ctnna1 were not able to confer this growth advantage to the cells *in vitro*. To determine whether the immortalization by expression of shRNA 405 is due to reduced Ctnna1 expression levels and not caused by off-target effects of shRNA 405, I ectopically re-expressed Ctnna1 to different levels in these immortalized cells. To re-express Ctnna1 to an expression level close to the endogenous one found in murine bone marrow cells, I cloned four re-expression vectors encoding Ctnna1 under the control of different promoters of various strengths.

Freshly isolated, lineage depleted primary bone marrow cells were transduced with vectors encoding shRNAs targeting Ctnna1 or Mybl2 (serving as differently immortalized control cells; Heinrichs et al., 2013) and a Puromycin selection marker. After selection, the

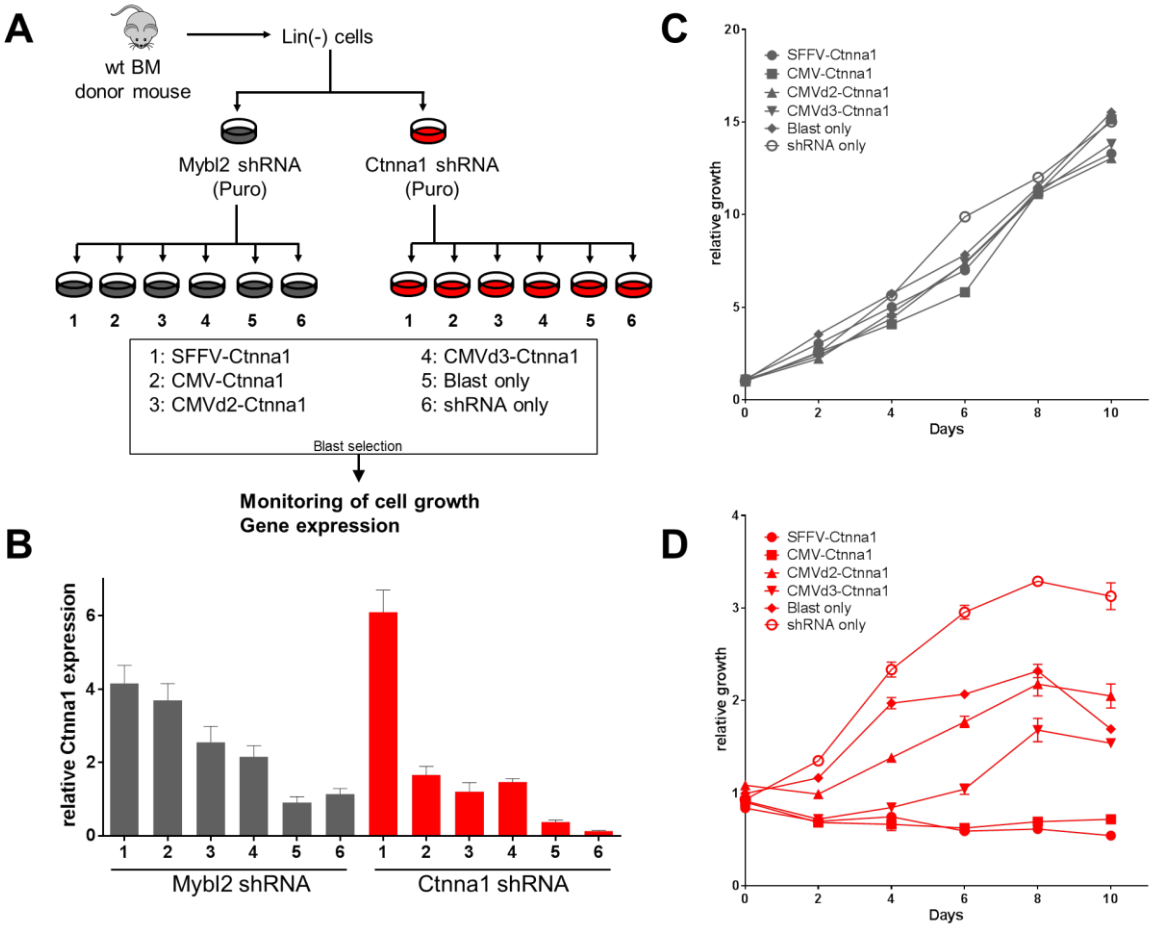

Figure 50: Increasing levels of ectopically expressed Ctnna1 gradually impaired the growth of shRNA 405-expressing immortalized bone marrow cells.
(A) Experimental design of re-expression experiment *in vitro*: Immortalized, Puromycin-selected primary bone marrow cells were transduced with four Ctnna1 re-expression vectors (Figure 55) mediating increasing Ctnna1 expression levels and cell growth and gene expression was measured. Mybl2 shRNA-immortalized cells served as control. (B) Total Ctnna1 expression level of transduced cells. (C) and (D) Relative growth of Mybl2 shRNA-immortalized cells (control) and shRNA 405-immortalized cells after re-expression of Ctnna1 to different levels. $0.4x10^6$ cells were seeded per well and the cell number was measured every two days.

cells were transduced with four different lentiviral re-expression vectors encoding Ctnna1 under the control of different promoters to achieve increasing gene dosage of ectopically expressed Ctnna1 (SFFV > CMV > CMVd2 > CMVd3). Cells transduced with a vector encoding only the Blasticidin resistance gene and cells transduced with the shRNA-encoding vector only served as internal control cell cultures (Figure 50A). After Blasticidin selection (6µg/ml), Ctnna1 expression levels were measured to ensure increasing ectopic Ctnna1 expression levels without massive Ctnna1 overexpression in cells immortalized by shRNA 405 (max. 6fold overexpression compared to Mybl2 shRNA-transduced cells; Figure 50B). Next, the cell growth was monitored and compared to the growth of control cells. Mybl2 shRNA-immortalized cells did not show an impairment of cell growth upon ectopic Ctnna1 re-expression revealing that Ctnna1 overexpression in primary bone marrow cells did not have a general negative effect on proliferation (Figure 50C). However, cells with reduced Ctnna1 levels mediated by the expression of shRNA 405 stopped proliferating in a gradual manner when Ctnna1 was re-expressed ectopically (Figure 50D and B). Indeed, this effect was dependent on the amount of re-expressed Ctnna1, i.e. the Ctnna1 gene dosage. Cells re-expressing Ctnna1 to the highest levels (Figure 50B, right panel, cultures 1 and 2) completely stopped proliferating (Figure 50D). Accordingly, re-expression of Ctnna1 to lower levels did not completely abolish the growth of the cells (Figure 50, B and D, cultures 3 and 4). Cells expressing shRNA 405 only or the control vector encoding the Blasticidin resistance gene expressed the lowest level of Ctnna1 and, thus, were not impaired in their growth at all (Figure 50, B and D, cultures 5 and 6).

These results indicated that reduced Ctnna1 expression levels were essential for the immortalization of bone marrow cells *in vitro* by expression shRNA 405. This experiment was repeated several times, also including variation of the experimental setup, e.g. the use of Doxycyclin-inducible re-expression vectors for Ctnna1. Unfortunately, these results could not be verified another time.

4.9 CTNNA1 expression leads to myeloid differentiation of the human HL60 cell line and thus abrogates their proliferative potential

4.9.1 Ectopic Expression of functional CTNNA1 stops proliferation of the human HL60 cell line

In primary cells the RNAi-mediated downregulation of Ctnna1 expression conferred a growth and survival advantage to the cells *in vitro*, indicating a tumor suppressor activity for α-Catenin. Next, I aimed to perform the reciprocal approach and re-expressed CTNNA1 in HL60 cells, an established human myeloid leukemia cell line derived from a patient with a 5q deletion encompassing the CTNNA1 gene. CTNNA1 expression was shown to be absent in these cells due to epigenetic silencing of the retained allele (Liu et al., 2007). To test whether ectopic re-expression of functional CTNNA1 in HL60 cells would perturb their proliferation,

I employed a Tetracycline-inducible re-expression system (Tet-ON System) to induce expression of wildtype CTNNA1 in HL60 cells by addition of Doxycycline to the medium. As a control, I used an N-terminally truncated form of CTNNA1 (CTNNA1ΔN$_{267}$), that lacks a functional β-Catenin-binding domain (Kobielak and Fuchs, 2004; Li et al., 2015).

For Doxycycline-inducible ectopic re-expression of CTNNA1 and CTNNA1ΔN$_{267}$ in the human HL60 cell line, cells were first transduced with a vector encoding the reverse Tetracycline-dependent transactivator (rtTA) M2 protein and Blue Fluorescent Protein (BFP). Subsequently, BFP^{+} sorted cells were transduced with vectors encoding CTNNA1 or CTNNA1ΔN$_{267}$ under a Doxycycline-inducible promoter coupled to a GFP-P2A-Puromycin resistance expression cassette via an IRES-element. This vector architecture enabled a selection by Puromycin for transduced cells with induced vector expression preventing the cells from silencing the ectopic CTNNA1 expression. Upon addition of Doxycycline and Puromycin to the medium, CTNNA1 expression was measured and cell growth was monitored. Transduced K562 cells, having regular CTNNA1 expression levels, served as controls.

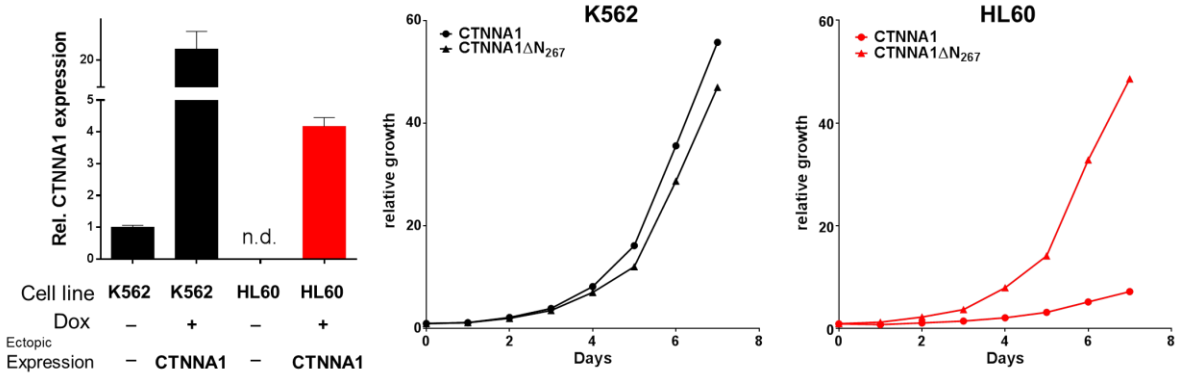

Figure 51: The growth of HL60 cells was impaired upon induced re-expression of CTNNA1, but not CTNNA1ΔN$_{267}$.
Left: Relative CTNNA1 expression level of K562 cells and HL60 cells with and without Doxycycline-induced CTNNA1 expression, n.d. – not detected. Middle and right: Relative growth of 0.3x10^{6} initially plated K562 and HL60 cells per well upon induced CTNNA1 or CTNNA1ΔN$_{267}$ expression (Doxycycline: 1 µg/ml, Puromycin 3 µg/ml).

Transduced K562 cells showed a 20fold CTNNA1 overexpression upon vector induction. As expected, normal, non-induced HL60 cells did not express CTNNA1 and upon addition of Doxycycline to the medium, CTNNA1 expression reached a level that was 4fold of the level in normal K562 cells (Figure 51, left). Transduced K562 cells did not show an impairment of cell growth upon vector induction, when CTNNA1 or CTNNA1ΔN$_{267}$ were overexpressed (Figure 51, middle). In contrast, transduced HL60 cells showed a massive impairment of cell proliferation when CTNNA1 expression was induced. Expression of CTNNA1ΔN$_{267}$ did not affect the cell proliferation (Figure 51, right). Thus, these results revealed a dependency of HL60 cell growth on the absence of CTNNA1 expression strongly suggesting a tumor suppressor role for CTNNA1 in these cells. Furthermore, it is likely that

an important functional domain is located within the deleted part of CTNNA1ΔN_{267}, since this mutant did not affect cell growth.

4.9.2 CTNNA1 expression in HL60 cells leads to a minor decrease in G1-S phase transition of the cell cycle

Re-expression of CTNNA1 in HL60 cells strongly impaired cell proliferation. Several causes could account for this effect, for instance a growth arrest, i.e. the accumulation of cells in one cell cycle phase. To test this hypothesis, I performed a cell cycle phase analysis by PI staining of transduced HL60 cells after induction of CTNNA1 expression. Normal HL60 cells showed a cell cycle profile without apoptotic cells, 51% of the cells in G1-phase, 34% in S-phase and 15% in G2-phase (Figure 52, left). The cell cycle profile of HL60 cells expressing CTNNA1 or CTNNA1ΔN_{267} was monitored every 2 days over 6 days after induction of expression.

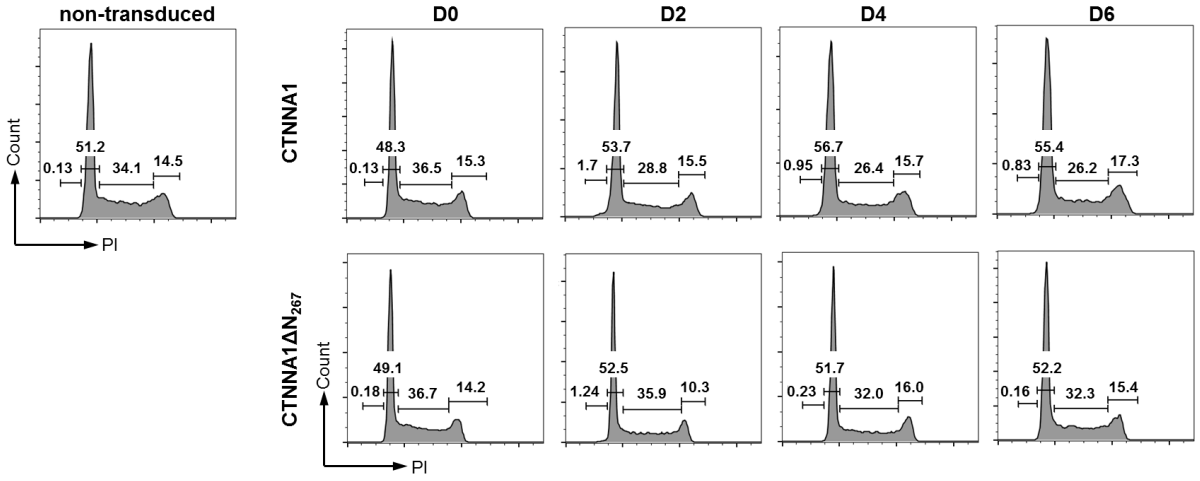

Figure 52: Expression of CTNNA1 mediated a minor block of G1-S transition in HL60 cells.
Cell cycle analysis via PI staining of $0.3x10^6$ HL60 cells. Left: Cell cycle profile of non-transduced HL60 cells. Right panel: Monitoring of cell cycle profiles of HL60 cells with induced vector expression of CTNNA1 (top) or CTNNA1ΔN_{267} (bottom) every 2 days after addition of Doxycycline (1 µg/ml) and Puromycin (3 µg/ml) to the medium.

Transduced HL60 cells expressing CTNNA1ΔN_{267} showed the same cell cycle profile as normal HL60 cells (Figure 52 bottom, mean values: G1: 51.9±1.6%, S: 34±1.5%, G2: 15±2.6%). However, expression of CTNNA1 caused only a minor accumulation of HL60 cells in G1-phase (54.5±3.7%) leading to a reduced frequency of cells in S-phase (27.6±4.8%) without affecting the frequency of cells in G2-phase (15.6±1%; Figure 52 top). Thus, a block in cell cycle progression upon expression of functional CTNNA1could not account for the massive stop in cell growth observed before.

4.9.3 CTNNA1 expression in HL60 cells mediates transcriptional upregulation of CD11b expression and induces myeloid differentiation

Triggering differentiation could account for the observed stop in proliferation of HL60 cells upon CTNNA1 expression without affecting the cell cycle progression. Differentiation of HL60 cells to cells of the myeloid lineage (monocytes, macrophages) can be induced by stimulation with different agents, such as ATRA (all-trans retinoic acid), DMSO (Dimethylsulfoxide), TPA (12-O-tetradecanoyl phorbol-13-acetate), PMA (Phorbol 12-myristate 13-acetate) or 1,25-D_3 (1α,25-dihydroxyvitamin D3). The maturation of the cells can be monitored by the expression of characteristic surface antigens (Boss et al., 1980; Sokoloski et al., 1993; Padilla et al., 2000; White et al., 2005; Borrell-Pages et al., 2014). To pursue this notion, I performed a comprehensive immunophenotyping analysis of HL60 cells upon induction of vector expression. First, I investigated which surface antigens characteristic for the myeloid lineage were differentially regulated when CTNNA1 was expressed in HL60 cells compared to non-transduced HL60 cells and cells expressing CTNNA1ΔN$_{267}$. After 3 days of vector expression, HL60 cells expressing functional CTNNA1 showed decreased expression of CD4 by MFI (36,095 rFU) compared to non-transduced (72,542 rFU) and CTNNA1ΔN$_{267}$-expressing cells (58,481 rFU). However, 100% of the cells were still CD4$^+$ (Figure 53A). Furthermore, they showed an increased expression of CD11b (74%), CD14 (26%), CD15 (97%) and CD49f (86%) compared to non-transduced (16% CD11b$^+$, 5% CD14$^+$, 96% CD15$^+$, 79% CD49f$^+$) and CTNNA1ΔN$_{267}$-expressing cells (40% CD11b$^+$, 8% CD14$^+$, 91% CD15$^+$, 80% CD49f$^+$; Figure 53A). Strikingly, the expression of CTNNA1 as well as CTNNA1ΔN$_{267}$ had an effect on the immunophenotype of the HL60 cells, most pronounced in the upregulation of CD11b, a marker protein found on monocytes, macrophages and granulocytes. Next, I determined in an independent experiment whether CD11b upregulation was time dependent and measured the frequency of CD11b$^+$ HL60 cells at days 0, 1, 2 and 3 after induction of vector expression. In both cases (CTNNA1 and CTNNA1ΔN$_{267}$ expression) the maximum increase of the frequency of CD11b$^+$ cells was observed during the first two days after vector induction (CTNNA1: D0 18%, D2 73%; CTNNA1ΔN$_{267}$: D0 17%, D2 55%; Figure 53B).

Next, I evaluated whether this effect is due to transcriptional upregulation of the expression of the ITGAM gene, which encodes the CD11b protein. I measured the expression of CTNNA1 and ITGAM and found that CTNNA1 expression was upregulated to the maximum of 3.5fold expression level compared to K562 control cells at one day after expression induction and was stable until day 3. However, ITGAM gene expression rose to 21fold expression level of non-transduced HL60 cells at day 1 and up to 29fold at day 2 after vector induction, before it decreased again to 23fold at day 3 (Figure 53C). These results indicated a time-dependent upregulation of the ITGAM gene expression upon CTNNA1 expression in HL60 cells. The upregulation of the ITGAM gene expression occurred in a one day delay after CTNNA1 expression was induced to the maximum. This suggests that

CTNNA1 could affect transcription and consequently initiate myeloid differentiation in HL60 cells. The induction of differentiation is most likely the reason for the observed stop in the proliferation of HL60 cells upon CTNNA1 expression, as self-renewal of cells associated with their proliferation and cell differentiation leading to maturation are differentially regulated processes in hematopoietic cells (Humphries et al., 1981; Nakahata et al., 1982).

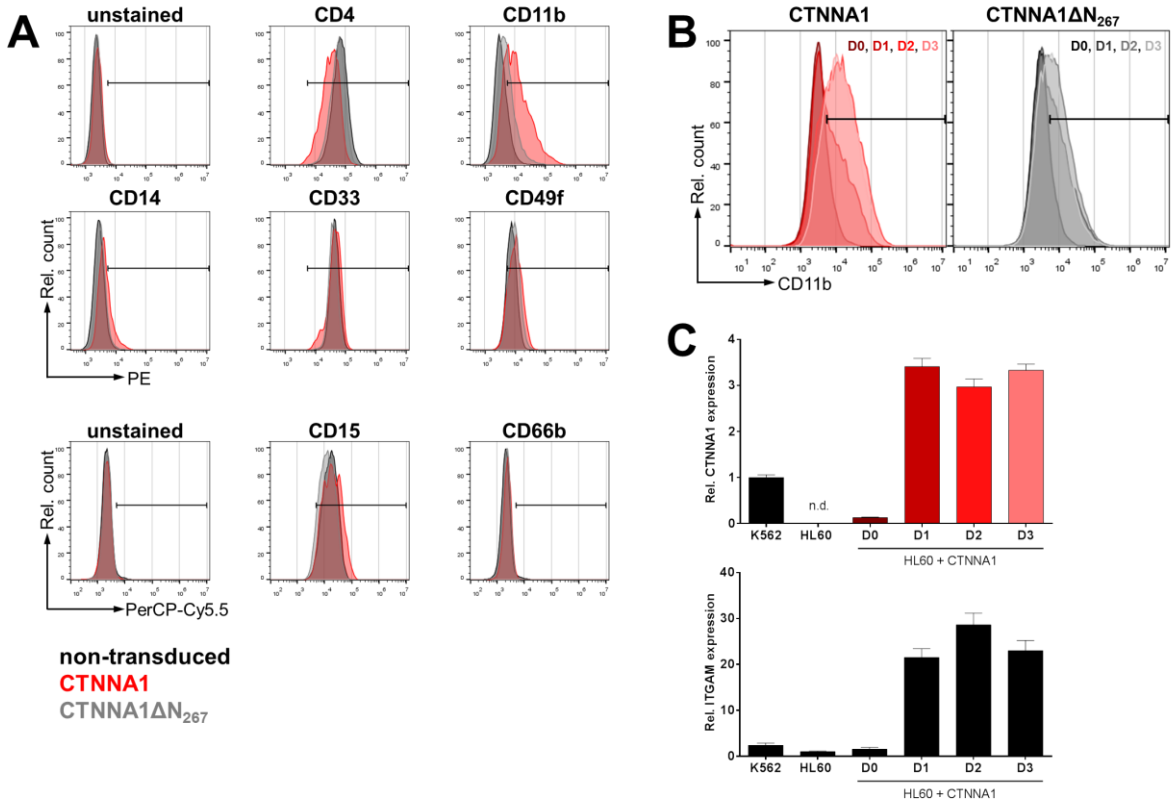

Figure 53: CTNNA1 expression in HL60 cells triggered cell differentiation towards the myeloid lineage. (A) Comprehensive immunophenotyping of HL60 cells at 3 days after vector induction (red and grey) compared to non-transduced cells (black). (B) Since CD11b showed the strongest regulation upon vector induction, the time course of CD11b expression was measured by flow cytometry in HL60 cells expressing CTNNA1 or CTNNA1ΔN$_{267}$. (C) Levels of CTNNA1 and ITGAM gene expression (QRT-PCR) in K562 and non-transduced HL60 cells compared to HL60 cells with induced CTNNA1 expression over 3 days.

The strongest effects of CTNNA1 expression on HL60 cells were observed two days after vector induction. Thus, RNA was isolated from cells of three independent experiments (CTNNA1 and CTNNA1ΔN$_{267}$, ±Doxycycline) of this time point and will be used for a microarray gene expression analysis to unravel the downstream effects of induced CTNNA1 expression in HL60 cells. These results will shed light on the mechanism of how CTNNA1 acts as a tumor suppressor in myeloid malignancies.

5 Discussion and Outlook

The CTNNA1 gene, encoding for α-Catenin, is located on chromosome 5q31. The heterozygous deletion of this region is the most frequent recurrent chromosomal aberration of bone marrow cells of patients with MDS (Horrigan et al., 2000). The expression of CTNNA1 was found to be significantly downregulated to 10-30% in leukemia-initiating cells (L-ICs) in 8 out of 11 patients with MDS with del(5q) compared to controls (Liu et al., 2007). These and additional studies designate CTNNA1 as a prime candidate functioning as a dosage-dependent tumor suppressor gene in MDS.

In this study, I analyzed the effects of a reduced gene dosage of α-Catenin mediated by RNAi in transplanted murine HSPCs. I performed an RNAi screen to test the knockdown efficiency of 24 shRNA sequences targeting the expression of Ctnna1. Out of these 24 shRNAs, eight showed a strong knockdown efficiency resulting in an Ctnna1 expression level of 28-49% in NIH-3T3 cells *in vitro* (Figure 4). Such a hit frequency was expected, since the knockdown efficiency of a processed siRNA molecule strongly depends on the sequence context within the target mRNA, the secondary structure of the mRNA and its potential sequence complementarity to unintended target sequences (Fire et al., 1998; Caplen et al., 2001; Elbashir et al., 2001; Jackson et al., 2003; Alagia and Eritja, 2016). Accordingly, I showed that, out of these eight shRNAs, only cells expressing shRNA 405 or 409 were dominantly expanding in the bone marrow of transplanted mice in a competitive reconstitution experiment *in vivo* (Figures 8 and 13). Moreover, only the expression of shRNA 405 mediated a myeloid expansion phenotype in the bone marrow of transplanted mice *in vivo* that was reproducible in all follow-up experiments (Figures 8, 10, 11, 12, 18, 20, 21 and 22). Mice with high frequencies of cells expressing shRNA 405 in the bone marrow showed peripheral blood cell dysplasia (Figure 46) and a myeloproliferative phenotype of bone marrow cells (Figure 47). *In vitro*, expression of shRNA 405 immortalized primary murine HSPCs (Figure 48) and conveyed the same myeloproliferative phenotype to the cells as observed *in vivo* (Figure 49). These results strongly supported my hypothesis: downregulation of Ctnna1 expression results in the loss of a tumor suppressor function in murine HSPCs.

Of note, every one of these eight shRNA sequences employed in the competitive reconstitution experiment mediated an Ctnna1 expression level of less than 50% in NIH-3T3 cells. However, only the expression of shRNA 405 triggered the anticipated MDS-like phenotype in the mice. Thus, the question arises why exclusively the expression of shRNA 405 mediated the clonal expansion of transduced bone marrow cells in the recipient animals. Peter Linsley and colleagues showed in a genome wide analysis of the efficacy and specificity of siRNA-mediated gene silencing that partial sequence identity of the siRNA sequence to a non-target sequence can mediate strong off-target effects (Jackson et al., 2003). These off-target effects are due to miRNA-like binding effects that lead to the simultaneous binding

of one miRNA to various target mRNAs (Lim et al., 2005). Clearly, as miRNA-target interactions are hardly predictable, every shRNA exhibits unpredictable off-target effects. In most instances, they are disadvantageous to the growth and survival of the cells and, thus, their expression could not mediate a clonal advantage to the transplanted HSPCs. Therefore, it is without surprise that not all of the eight vectors led to the phenotype observed by the expression of shRNA 405. Moreover, the strength of the on-target effect on Ctnna1 expression of these shRNA sequences might not have been sufficient to promote malignant transformation of the shRNA expressing cells *in vivo*.

The clonal expansion of HSPCs encoding shRNA 405 and the resulting myeloproliferative phenotype in transplanted mice was reproducible in subsequent competitive reconstitution experiments in this study (Figures 8, 18 and 32). The expression of shRNA 405 caused an average Ctnna1 expression level of 30% in transduced bone marrow cells (Figures 9, 19, 33 and 50B). This Ctnna1 expression level *per se* could have been sufficient for malignant transformation of murine HSPCs *in vivo*. However, only one, and not two, shRNA sequence was identified that promoted a clonal dominance upon expression in murine HSPCs. The expression of shRNA 405 could have possibly resulted in the advantageous combination of a positive on-target effect on Ctnna1 expression and, most importantly, a positive off-target effect that collaborated with reduced Ctnna1 expression levels, *in vivo* and *in vitro*. Thus, it remains unclear whether the effect of shRNA 405 expression on murine HSPCs exclusively depended on the reduced Ctnna1 expression level. Moreover, the question arises to what extent the positive impact of a proposed additional off-target effect contributed to the observed phenotype. This issue was addressed by the performance of an Ctnna1 re-expression experiment in immortalized primary bone marrow cells (Figure 50). Ectopic re-expression of Ctnna1 was expected to revert the clonal dominance phenotype of the cells given its dependence on reduced Ctnna1 expression levels. However, the ectopic re-expression of a gene at its physiological level is notoriously difficult. A massive overexpression of Ctnna1 and the potentially resulting toxicity were to be avoided by any means. Thus, I modeled different gene dosages by implementing the use of four different promoters (Figure 50B). I showed that re-expression of Ctnna1 to an up to 6fold level of control cells impaired the growth phenotype of cell expressing shRNA 405 in a dosage-dependent manner, while the growth of control cells was not impaired (Figure 50). This experiment strongly suggested a dependency of the immortalized cells on the reduced Ctnna1 expression level mediated by the expression of shRNA 405.

However, I was not able to validate these results in independent experiments using the same parameters as well as by employing different re-expression systems, such as the inducible Ctnna1 re-expression in immortalized bone marrow cells (data not shown). Thus, a key requirement for such a re-expression experiment is that the immortalized bone marrow cells are constantly depending on reduced Ctnna1 expression levels. Possibly, as the culture persists, the cells might progressively rely on the positive off-target effect mediated by

shRNA 405 expression and may acquire additional mutations, rendering their growth and survival independent from Ctnna1 gene dosage insufficiency. To successfully revert the growth phenotype it is therefore important to ectopically re-express Ctnna1 while the proliferation of the cells is still determined by reduced Ctnna1 levels, probably during early passages. Thus, further comprehensive analysis of the cellular phenotype *in vitro*, especially during early culture conditions, are required prior to Ctnna1 re-expression. This will lead to the identification of the cell population that depends on reduced Ctnna1 expression levels and thus maintains the growth of the culture. In addition, the employment of an inducible RNAi system will ensure the dependency of the observed phenotype on reduced α-Catenin expression levels.

Although the re-expression of Ctnna1 in primary murine bone marrow cells was challenging, I could show that expression of shRNA 405 caused a myeloproliferative phenotype and diminished erythropoiesis in the bone marrow of recipient mice upon transplantation. However, as mentioned above, gene dosage insufficiency of Ctnna1 alone was unlikely to mediate the observed phenotype. The expansion of cells encoding shRNA 405 was possibly due to the support of an off-target effect of the shRNA. Thus, the gene dosage insufficiency of Ctnna1 most likely confers a growth and survival advantage to the cells only in combination with further defined genetic events, such as the heterozygous loss of other genes located within the proximal CDR.

Indeed, the mono-allelic loss of more than one gene located in the proximal or distal CDRs of chromosome 5q suggests that the combination of gene dosage insufficiency of multiple tumor suppressor genes contributes to the pathogenesis of MDS. Thus, reduced gene dosage of CTNNA1 might collaborate with the gene dosage insufficiency of one or more other genes located within the proximal CDR. Such a collaboration of multiple haploinsufficient tumor suppressor genes has been shown already for the distal CDR. The lab of Todd Golub identified RPS14 as one of the haploinsufficient tumor suppressor genes in the distal CDR, accounting for the 5q– syndrome *in vivo* (Ebert et al., 2008). However, a phenotype entirely reflecting the clinical features of the 5q– syndrome in patients was not caused by RPS14 haploinsufficiency alone. Only the additional loss of miRNA-145, another gene encoded within the distal CDR (Kumar et al., 2011), induced thrombocytosis *in vivo*. Accordingly, the effect of the combination of Ctnna1 gene dosage insufficiency with reduced expression of other genes within the proximal CDR is of great interest. One of the most promising candidates for a collaboration with the CTNNA1 gene dosage insufficiency would be EGR1. In fact, the haploinsufficiency of EGR1 can promote the development of a myeloid disorder in mice (Joslin et al., 2007). However, it was not sufficient to reflect the entire natural history and the clinical features of MDS as observed in patients. Thus, we will employ the CRISPR/Cas9 technology to combine the heterozygous inactivation of genes located within the proximal CDR with reduced α-Catenin expression levels. The functional analysis

of their effects on murine HSPCs will identify advantageous combinations that could be tested additionally in the context of other frequent mutations identified in MDS, such as Tet2 or Dnmt3a inactivation.

While the interaction of genes within the proximal CDR is subject to follow-up studies, I modeled the statistically significant co-occurrence of 5q-deletions in MDS with the inactivation of TP53. Almost a fifth (18%) of MDS patients with del(5q) display mutations in the TP53 gene (Jadersten et al., 2011; Kulasekararaj et al., 2013). The co-occurrence of inactivating TP53 mutations with deletions of chromosome 5q is associated with adverse disease prognosis and an increased risk of leukemic evolution (Jadersten et al., 2011; Kulasekararaj et al., 2013; Papaemmanuil et al., 2013; Haferlach et al., 2014; Volkert et al., 2014). In the hematopoietic system, tightly regulated p53 signaling accounts for the quiescence and survival of HSPCs and ensures the preservation of a lifelong pool of HSCs (Liu et al., 2009; Pant et al., 2012). Loss of TP53 in MDS has been associated with aberrant self-renewal of cells, facilitating leukemic transformation and the progression to AML (Zhao et al., 2010; Xu et al., 2012; Stoddart et al., 2014a; Stoddart et al., 2014b). In fact, Stephen Nimer and colleagues reported that bi-allelic inactivation of Tp53 aggravated the disease phenotype of the NUP98-HOXD13 (NHD13) transgenic mouse model for MDS and accelerated the progression to AML (Xu et al., 2012).

In accordance with the data from this study, my results showed an additive effect of Tp53 inactivation to the clonal dominance phenotype of bone marrow cells expressing shRNA 405 (Figure 32), particularly in the hematopoietic stem and progenitor cell compartments (Figure 37). Furthermore, the reduction of Ctnna1 expression levels caused an earlier onset of death of the transplanted mice when Tp53 was inactivated (Figure 45). Most intriguingly, loss of Tp53 enabled cells encoding shRNA 409, reducing the Ctnna1 expression level to 60%, to engraft secondary recipient mice (Figure 32). Moreover, the engraftment of bone marrow cells encoding shRNA 405 and 409 in secondary recipient mice was enhanced when Tp53 was inactivated (Figures 26 and 39). This supported the notion that Tp53 inactivation reinforced self-renewal and long-term repopulation ability of the cells. However, Tp53 inactivation did not aggravate the myeloproliferative phenotype associated with a lack in maturation of bone marrow cells (Figure 35) and the diminished erythropoiesis that was detected in the bone marrow of primary or secondary recipient mice (Figure 36).

Five years ago, Ebert and colleagues demonstrated that the normal function of wildtype p53 can affect hematopoiesis (Dutt et al., 2011). The authors showed that RPS14 haploinsufficiency in murine HSPCs caused a defect in ribosomal biogenesis and resulted in the hyperactivation of the p53 pathway. This led to physiological p53 accumulation, cell cycle arrest and enhanced apoptosis in cells of the erythroid lineage resulting in a strongly diminished erythropoiesis. Other recent studies showed that accumulation of mutated p53 in hematopoietic progenitors of MDS patients accelerated disease progression and mediated a

worse prognosis (Kulasekararaj et al., 2013; Saft et al., 2014; Loghavi et al., 2015; Ok et al., 2015). Taken together, this shows that the physiological function of p53 can reinforce the disease progression as shown by Ebert and colleagues (Dutt et al., 2011), yet mutations of p53 play a key role in MDS development. The pathogenesis of MDS with mutated p53 strongly depends on the type of mutation in the p53 protein and their occurrence in the context of co-existing mutations (Kulasekararaj et al., 2013). However, aberrant accumulation of mutated p53 as well as inactivation of p53 function, as shown in my study or in the work from Stephen Nimer and colleagues (Xu et al., 2012), affect the homeostasis of the hematopoietic system.

As the results of my study strongly suggested a tumor suppressor function for α-Catenin and a reinforcement of the clonal dominance phenotype by the inactivation of Tp53 in murine HSPCs, the human HL60 cell line provided an excellent model for further investigation of the role of α-Catenin in myeloid malignancies. HL60 cells, a cell line derived from a patient with a myeloid malignancy, harbor a heterozygous deletion of chromosome 5q and do not express CTNNA1 (Liu et al., 2007). Furthermore, TP53 expression is inactivated in these cells (Wolf and Rotter, 1985). While re-expression of α-Catenin appeared to be challenging in immortalized primary cells, its tumor suppressor function could be clearly shown in the HL60 cell line. As demonstrated before by Tom Look's lab (Liu et al., 2007), I proved that induced ectopic re-expression of CTNNA1 to a 4fold level of control in the HL60 cells strongly perturbed their proliferation, while the growth of control cells was not affected (Figure 51). This finding was reproducible in three independent experiments. Thus, the proliferation of HL60 cells depends on the loss of CTNNA1 expression and strongly suggests a pivotal role of CTNNA1 as a tumor suppressor gene in myeloid malignancies.

The mechanism how α-Catenin acts as a tumor suppressor on a molecular level in myeloid malignancies is unknown. In contrast, its role in the pathogenesis of solid tumors originating from epithelial cells has been elucidated in the past years. It was shown that α-Catenin, as a structural element of adherens junctions, is crucial for the maintenance of cell polarity and the transmission of cell-cell contact inhibition signaling within cells of an epithelial tissue (Kobielak and Fuchs, 2004; Han and Yap, 2013). Yet, little is known on how the sensing of cell density and cell-cell contact inhibition of the adherens junctions translates into signaling for cell proliferation or apoptosis.

Recently, two studies proposed a tumor suppressor function of α-Catenin in the regulation of the Hippo signaling pathway in the skin (Schlegelmilch et al., 2011; Silvis et al., 2011). The Hippo signaling pathway senses cellular density within a tissue and restricts tissue size by limiting cell proliferation and promoting apoptosis (Schlegelmilch et al., 2011; Harvey et al., 2013). α-Catenin has been shown to be an upstream regulator of the Hippo signaling effector protein Yap1. Thus, I considered that the knockdown of Ctnna1 expression or its ectopic re-expression in primary murine bone marrow cells had an impact on Yap1 target gene expression. However, Yap1 was not expressed in the cells as determined by QRT-PCR

(data not shown). Thus, it is highly unlikely that the molecular mechanism how Ctnna1 acts as a tumor suppressor in hematopoietic cells depends on the regulation of the Hippo signaling pathway.

Two years ago, Li Ma and colleagues proposed a tumor suppressor role for CTNNA1 in regulating the NFκB signaling pathway (Piao et al., 2014). The authors showed that α-Catenin directly interacts with the IκBα protein in E-Cadherin negative basal-like breast cancer cell lines and thereby retains the NFκB transcription factor complex in the cytosol (Piao et al., 2014). The effect of CTNNA1 re-expression on NFκB signaling in HL60 cells has been investigated within the scope of a bachelor's thesis performed by Renata Spyra in our group in 2015. HL60 cells were transduced with a lentiviral NFκB reporter vector. This study showed that the NFκB activity was not altered by the re-expression of CTNNA1 in HL60 cells (unpublished data). However, in murine hematopoietic cells the effect of Ctnna1 on Nfκb signaling remains to be elucidated.

Within the past years yet another pathway has been associated with the function of α-Catenin: the Wnt signaling pathway. Jones and colleagues showed that α-Catenin could operate in HEK-293T cells as a central part of the β-Catenin destruction complex and additionally destabilize the binding of the transcription factor β-Catenin to the DNA. Thus, α-Catenin regulated Wnt target gene transcription in HEK-293T cells (Choi et al., 2013). Here, I re-expressed an N-terminal mutant of CTNNA1, which lacked amino acids 1-266 ($CTNNA1\Delta N_{267}$), in HL60 cells. The deletion of the N-terminal amino acids 1-266 encompassed the VH1 domain of the α-Catenin protein that contains the β-Catenin binding motif (Kobielak and Fuchs, 2004; Li et al., 2015). While its re-expression had no effect, the re-expression of wildtype CTNNA1 in HL60 cells mediated a strong inhibition of the cell proliferation (Figure 51). As the Wnt signaling pathway has been described as an inducer of cell proliferation in several cell lines by enhancing cell cycle progression (Davidson and Niehrs, 2010), my results initially indicated an CTNNA1-mediated inhibition of Wnt signaling that in turn repressed the cell cycle progression and thus the proliferation of HL60 cells. However, I could show that the impaired proliferation of HL60 cells upon CTNNA1 re-expression was not caused by an arrest in cell cycle progression (Figure 52) and rather resulted from enhanced differentiation towards the monocytic lineage (Figure 53). Moreover, cell cycle profiling did not indicate an accumulation of apoptotic cells (Figure 52), however, the rate of apoptosis was not validated in an independent assay. Yet, the results of my study do not exclude the possibility that α-Catenin acts as a negative regulator of Wnt signaling in hematopoietic cells. Wnt signaling has been implicated to be highly context dependent and subject to strict molecular control in hematopoietic stem cells (Reya et al., 2003; Staal et al., 2008; Gattinoni et al., 2009). It has been reported to promote self-renewal and multipotency of HSCs by limiting their proliferation and differentiation (Fleming et al., 2008; Staal et al., 2008). In accordance with these studies, the results of my study showed a stop in proliferation associated with enhanced differentiation of HL60 cells upon CTNNA1 re-expression. This

indicated an orchestration of signaling events, possibly including a repression of the Wnt signaling pathway. However, this notion requires further investigation including a comprehensive analysis of the Wnt signaling pathway in HL60 cells. Furthermore, the combination with the detailed analysis of the data from a microarray gene expression experiment will provide important insights into the change of gene expression and the regulation of key signaling pathways upon induced CTNNA1 re-expression in HL60 cells. These experiments will shed light on the molecular mechanism how α-Catenin functions as a tumor suppressor in myeloid malignancies.

6 Material and Methods

6.1 Material

6.1.1 Devices

Centrifuges	Eppendorf Centrifuge 5424
	Beckman Coulter Avanti J26-XP
	Eppendorf Centrifuge 5810R
Cytospin	Shandon Cytospin II, Thermo Scientific
Power Supply	Fisher Scientific FB300
Western Blot System	Hoefer SE250 System
Gel Electrophoresis Chambers	Peqlab Biotechnologies
Agarose Gel Documentation	red:: gel imaging system, protein simple, Biozym Scientific GmbH
Laminar Flow Hood	HERAsafe HS12, Heraeus, Thermo Scientific
CO_2 Incubator	Thermo Scientific HeraCell 240i
37°C Incubator	Thermo Scientific MaxQ 6000 Orbital Shaker
Heating Block	Peqlab 91-D1100
Thermo Shaker	TS-100, BioSan
Tube Rotator	VWR Tube Rotator
Horizontal shaker	VWR Rocking Platform
Spectrophotometer	PowerWave XS Microplate I, Biotek
	NanoDrop 2000, Thermo Scientific
Flow Cytometers	BD FACSAria I, IIIu
	Beckman Coulter Cytoflex
	Beckman Coulter Gallios
	Beckman Coulter FC500
Luminometer	Glomax Multi Detection System, Promega
qPCR cycler	CFX96 Real Time System C1000, BioRad Laboratories
PCR cycler	PTC-200 Thermal Cycler, MJ Research
Luminescence Detection	Fusion Fx7 System, Vilber Lourmat
Microscopes	Olympus CKX41, Olympus Corporation
	Axio Vert.A1, Zeiss
Sonicator	QSonica, Newtown

6.1.2 Laboratory and cell culture material

Syringe filters 0.2 µm, 0.45 µm	Minisart, Sartorius AG, Göttingen, Germany)
Syringe, 50 ml	Braun, Melsungen, Germany
40 µm Cell Strainer	BIOLOGIX Research, Münster, Germany
BD FACS Accudrop Beads	BD Bioscience, San Jose, CA, USA
Microscope slides	Marienfeld-Superior, Lauda Könighofen, Germany)
Cover slips	Roth, Karlsruhe
Shandon EZ Single Cytofunnels	Thermo Fisher Scientific, Waltham, MA, USA
Glass capillaries	Micro Hematocrit capillaries, Na-heparin, Brand, Wertheim, Germany
EDTA-Microvettes	Microvette 200 K3E, Sarstedt, Nümbrecht, Germany
Sterile filter pipette tips	Biozym, Hessisch Oldendorf, Germany
Ultra-High Performance Polypropylene Tubes, 50 ml	VWR, Radnor, PA, USA
Pipettes	Gilson Inc., Middleton, WI, USA
BD Falcon tubes	BD Bioscience, San Jose, CA, USA
Pipette tips and 1.5 ml/2 ml microcentrifuge tubes	StarLab, Hamburg, Germany

6.1.3 Chemicals, buffers, solutions and cell culture media

All chemicals were purchased from Sigma Aldrich (St. Louis, MO, USA) and Carl Roth (Karlsruhe, Germany), if not stated otherwise.

ACK Lysis Buffer	Lonza, Basel, Switzerland
ddH_2O	Milli-Q, Merck Millipore, Merck KGaA, Darmstadt, Germany
DMEM, 1x, 4.5g/l D-Glucose	Life Technologies, Carlsbad, CA, USA
D-PBS	Life Technologies, Carlsbad, CA, USA
EL Lysis Buffer	Qiagen, Hilden, Germany
Eukitt quick-hardening mounting medium	Fluka Analytical, St. Gallen, Switzerland
FBS	Biochrom AG, Berlin, Germany
HEPES Buffer, 1M	Life Technologies, Carlsbad, CA, USA
IMDM, 1x, 25mM HEPES	Lonza, Basel, Switzerland
L-Glutamine, 200mM	Life Technologies, Carlsbad, CA, USA
Penicillin/Streptomycin, 10000U/ml	Life Technologies, Carlsbad, CA, USA
RPMI 1640, 1x, L-Glutamine	Life Technologies, Carlsbad, CA, USA
TRIzol Reagent	Life Technologies, Carlsbad, CA, USA
X-Vivo15	Lonza, Basel, Switzerland

DNA loading dye, 6x	10 mM Tris/HCl, 0.005% SDS, 60 mM EDTA, 60% glycerol, 0.03% xylene cyanol FF
LB Medium	10 g tryptone, 5 g yeast extract, 5 g NaCl, add ddH_2O to 1 l
LB Agar	1 l LB Medium + 15 g Agar
MACS Buffer	D-PBS, 0.5% BSA, 2mM EDTA, sterile filtered and degassed
SDS Lysis Buffer (Ear Biopsies)	0.2 M NaCl, 0.1 M Tris/HCl pH 8, 5 mM EDTA, 0.5% (w/v) SDS
SDS Lysis Buffer (Protein)	50 mM Tris/HCl pH 7.5, 5 mM EDTA, 1% (w/v) SDS
SDS running buffer, 1x	0.125 M Tris, 0.96 M glycine, 0.5% (w/v) SDS
SDS sample buffer, 6x	70% (v/v) stacking gel buffer 4x, 30% (v/v) glycerol, 10% (w/v) SDS, 9.3% (w/v) DTT, 12% (w/v) bromphenol blue
Separating gel buffer, 4x	1.5 M Tris/HCl pH 8.8, 0.4% (w/v) SDS
Stacking gel buffer, 4x	0.5 M Tris/HCl pH 6.8, 0.4% (w/v) SDS
TAE Buffer, 50x	24.2% Tris, 5.71% glacial acetic acid, 0.05 M Na_2-EDTA pH 8.5
TBS-T	50 mM Tris, 150 mM NaCl, 0.05% (v/v) Tween20
TGM transfer buffer, 1x	0.25 mM Tris, 0.192 mM glycine, 10% (v/v) methanol
PI staining solution	0.2% sodium citrate, 0.05 mg/ml propidium iodide, 0.1% Triton X-100, 0.2 mg/ml RNase A
BW Buffer, 1x	10 mM Tris/HCl (pH 7.5), 1 mM EDTA, 2 M NaCl

Cytokines (recombinant murine Scf, recombinant murine Tpo, recombinant murine Flt3L) were purchased from PeproTech GmbH, Hamburg, Germany. They were dissolved in sterile PBS/0.2% BSA at 100 µg/ml stock solutions, diluted to 10 µg/ml working solutions and stored at -80°C.

Lyophilized oligonucleotides were purchased from Eurofins MWG Operon, Ebersberg, Germany. They were dissolved in ddH_2O at 100 µM (stock solutions) and diluted to 10 µM working solutions.

6.1.4 Reagent systems (Kits), enzymes and standards

QIAquick Gel Extraction and PCR Purification kits, the QIAprep Spin Miniprep kit, the QIAamp DNA Mini kit and the QuantiTect Reverse Transcription kit (all Qiagen, Hilden, Germany), Rapid DNA Ligation kit, SuperSignal West Pico Chemiluminescent Substrate (Thermo Fisher Scientific Inc., Waltham, MA, USA), CellTiter-Glo Luminescent Cell

Viability assay (Promega, Fitchburg, WI, USA), Lineage Cell Depletion kit, mouse (Miltenyi Biotec, Bergisch Gladbach).

All enzymes and their buffers were purchased from Thermo Fisher Scientific Inc. (Waltham, MA, USA), if not stated otherwise. RNase A (100mg/ml) and Proteinase K solution (Qiagen Hilden, Germany), rAPid Alkaline Phosphatase (Roche, Basel, Switzerland), AmpliTaqGold DNA Polymerase (LifeTechnologies Carlsbad, CA, USA), GeneRuler 1kb and PageRuler Pre-Stained Plus (Thermo Fisher Scientific Inc., Waltham, MA, USA).

6.1.5 PCR Primers, Oligonucleotides and shRNA sequences

Table 1: Cloning primers

Primer	Sequence (sense strand)
c-Ctnna1-FW1	CGCTGTCTAGAGCCACCATGACTGCCGTCCACGCAGG
c-405m-FW1	GTGCCCACAAGTCATCAATGCTG
c-405m-RV1	ATGACTTGTGGGCACAGCGCTTC
c-Ctnna1-RV1	CGGCAACGCGTTCAGATGCTGTCCATGGCTTTGAAC
c-hPGK-ClaI-FW1	CGCTATCGATTTGGGGTTGCGCCTTTTC
c-M2-MluI-RV1	AGCGACGCGTTTACCCGGGGAGCATGTC
c-NdeI-aC-FW1	GAACTGGCATATGCACTCAATAAC
c-NheI-aC-RV1	GGGGCGGAATTAGCTAGCTTAGATGCTGTC
c-NheI-IRES-FW1	GACAGCATCTAAGCTAGCTAATTCCGCCCC
c-n267-XbaI-FW1	TAAAGTCGACTCTAGAGCCACCATGGCCTCACAGCACCAG
c-aCcterm-RV1	AATTAGCTAGCTTAGATGCTGTCCATAG

Table 2: Primers for shRNA sequence identification by QPCR

Primer	Sequence (sense strand)
405-FW1	AGGCGCTGTGTCCTCAGGTTATCTT
408-FW1	AGGGATGAGACGCAGACCAAGATTT
409-FW1	AGGACGACTCTGACTTCGAGACTTT
410-FW1	AGGACATTACTTCCATCGATGACTT
412-FW1	AGGTAGCAGATTTCAGACTCAACTT
413-FW1	AGCAGGGAGGTAGCAGATTTCAGTT
418-FW1	AGGCCTGATGACTGCATAGGGTTTT
420-FW1	AGCCTACGTGGCTTCCACCAAATTT
hp-RV2	ACTATTCTTTCCCCTGCACTGTACC

Table 3: Primers for expression analysis by QRT-PCR

Primer	Sequence (sense strand)	Target gene
Ctnna1-FW1	ACTTTGATGTCAGAAGCAGGACC	Ctnna1
Ctnna1-RV1	CACCTGTTCTGCAATCTTTGCTTT	
Ctnna1-FW3	CTGAAGTGCCTGCTTTCTAGGTA	Ctnna1
Ctnna1-RV3	GGCCACCCTTGGTCATTTAATTC	
Ctnna1-FW5	CTTCAAATGGGACCCCAAAAGTC	Ctnna1
Ctnna1-RV5	ACTATTGGTGTTTACCAGGGTTGT	
Ubqln1-FW1	GCACCTAGCACTGCACCTAGTGA	Ubqln1
Ubqln1-RV1	TGAAATCTGACTTCTGGACTCTGC	
Vps39-FW1	GAGGAGAAGGTGTGCATGGTATG	Vps39
Vps39-RV1	GGTGTCGGCTGAGTTTACCTCTT	
Papola-FW1	AGACAAGTGCGGTTCAATCAGAA	Papola
Papola-RV1	AACAGGAATAGGATTTGCAGGGA	
CTNNA1-FW5	CAAAAGTCACAGGGTATGGCTTC	CTNNA1
CTNNA1-RV5	GGTCTGTGTCTCATCCTGTTTCT	
UBQLN1-FW1	CACTGAACCTGGACATCAGCAGT	UBQLN1
UBQLN1-RV1	CAAGTTTGCTTCACGGTTCAAAA	
VPS39-FW1	TCATCACAGAGGAGAAGGTGTGC	VPS39
VPS39-RV1	TCAGCTGGGTTTACCTCTTTGGA	
PAPOLA-FW1	GGAGTCAAGAGGACATCCTCACC	PAPOLA
PAPOLA-RV1	TCATGTCCACTCAAAGCAAGACA	
ITGAM-FW1	TAATGATCAGGTGGTGAAAGGCA	ITGAM
ITGAM-RV1	AGTCACAACACTCTGGATCTGTC	

Table 4: Primers for LAM-PCR.

*:5’ end biotinylation

Primer	Sequence (sense strand)	Reference
LC-RV1	GACCCGGGAGATCTGAATTC	Schmidt et al., 2007
LC-RV2	AGTGGCACAGCAGTTAGG	Schmidt et al., 2007
LC-RV3	TGAATTCAGTGGCACAGCAG	
LTRIA-bio	*GAGCTCTCTGGCTAACTAGG	Schmidt et al., 2007
LTRIB-bio	*GAACCCACTGCTTAAGCCTCA	Schmidt et al., 2007
LTRII-bio	*AGCTTGCCTTGAGTGCTTCA	Schmidt et al., 2007
LTRIII	AGTAGTGTGTGCCCGTCTGT	Schmidt et al., 2007
HIV1_LTR-FW1bio	*TGGCTAACTAGGGAACCCACTGC	
HIV1_LTR-FW2	TGTGTGCCCGTCTGTTGTGTGAC	
HIV1_LTR-FW3	CCCTCAGACCCTTTTAGTCAGTGTGG	

Table 5: Linker oligonucleotides for LAM-PCR

Oligonucleotide	Sequence (sense strand)	Reference
LC1	GACCCGGGAGATCTGAATTCAGTGGC ACAGCAGTTAGG	Schmidt et al., 2007
LC2	AATTCCTAACTGCTGTGCCACTGAAT TCAGATC	Schmidt et al., 2007

Table 6: shRNA sequences
shRNAs 400-423: targeting Ctnna1 expression; shRNAs C, D, J – scrambled control shRNAs

shRNA	Sequence (sense strand)	shRNA	Sequence (sense strand)
400	CCGAGGCAAAGGTCCACTCAA	414	CACCTTAGACGGTCTGGAGAA
401	CGCTCTCAACAACTTTGATAA	415	GCTGAAGTGCCTGCTTTCTAG
402	GCCAACAAACTGATTGAGGTT	416	CGCATGGCTACAGTTACTAAT
403	GCCAGGAGTTTACACAGAGAA	417	CCCTGTTATTCCAGCTTGAAA
404	CTACGAGCCAGGAGTTTACAC	418	GCCTGATGACTGCATAGGGTT
405	GCGCTGTGTCCTCAGGTTATC	419	CCAGCTCAACATCTGCAGCAA
406	GTCATGGACCACGTATCAGAT	420	CCTACGTGGCTTCCACCAAAT
407	GCAGCCCGAGTCATTCATGTA	421	CCTACGTGGCTTCCACCAAAT
408	GGATGAGACGCAGACCAAGAT	422	CCAGTCACATGCTTCACTCAA
409	GACGACTCTGACTTCGAGACT	423	GCTGGATGCTGAAGTGTCCAA
410	GACATTACTTCCATCGATGAC	C	CGCGATCGTAATCACCCGAGT
411	GTGGCCCAGTGTAAATCACAG	D	CAACAAGATGAAGAGCACCAA
412	GTAGCAGATTTCAGACTCAAC	J	CTTCGAAATGTCCGTTCGGTT
413	CAGGGAGGTAGCAGATTTCAG		

6.1.6 Software Tools

Graphs corresponding statistics were obtained with GraphPad Prism (Graph Pad Software, San Diego, CA, USA; version 5.04 for Windows). Flow cytometry data was analyzed using FlowJo (Tree Star Inc., Ashland, OR, USA). All figures were prepared using Microsoft PowerPoint. Geneious (Biomatters, Auckland, New Zealand) was used for plasmid and primer design as well as determination of restriction sites. QPCR data was obtained from BioRad CFX Manager 3.0 (BioRad Laboratories, Hercules, CA, USA). Calculations were performed using Microsoft Excel.

6.1.7 Antibodies

Table 7: Antibodies for Western Blot

Reactivity	Antigene	Clone	Clonality	Distributor
rb-α-ms	Alpha-1 Catenin	EP1793Y	monoclonal	Epitomics
HRP-gt-α-rb	Rabbit IgG		polyclonal	Thermo Fisher Scientific

Table 8: Antibodies for flow cytometry

Reactivity	Antigene	Clone	Conjugation	Distributor
α-ms	CD5	n/a	Biotin	Miltenyi Biotec (lineage cell depletion Kit, Ab-cocktail)
α-ms	CD11b (Mac-1)	n/a		
α-ms	CD45R (B220)	n/a		
α-ms	Ly6G/C (Gr-1)	n/a		
α-ms	Ter119	n/a		
α-ms	Ly6A (Sca-1)	D7	PE-Cy7	eBioscience
α-ms	CD117 (Kit)	2B8	APC	eBioscience
α-ms	CD48	HM48-1	PerCP-Cy5.5	BioLegend
α-ms	CD150	TC15-12F12.2	Brilliant Violet 421	BioLegend
α-ms	CD11b (Mac-1)	M1/70	APC	eBioscience
α-ms	CD11b (Mac-1)	M1/70	PerCP-Cy5.5	eBioscience
α-ms	Ly6G (Gr-1)	RB6-8C5	eFluor450	eBioscience
α-ms	Ly6G (Gr-1)	RB6-8C5	PE	eBioscience
α-ms	CD3e	145-2C11	PerCP-Cy5.5	eBioscience
α-ms	CD3e	145-2C11	Biotin	eBioscience
α-ms	CD45R (B220)	RA36B2	PE-Cy7	eBioscience
α-ms	CD45R (B220)	RA36B2	Biotin	eBioscience
α-ms	Ter119	TER-119	APC	eBioscience
α-ms	Ter119	TER-119	Biotin	eBioscience
α-ms	CD71	R17217	Biotin	eBioscience
α-biotin	SA		APC-eFluor780	eBioscience
α-biotin	SA		PE-Cy7	eBioscience
α-biotin	SA		PE	Miltenyi Biotec
α-hu	CD4	RPA-T4	PE	BD Biosciences
α-hu	CD11b (MAC-1)	Bear1	PE	Beckman Coulter
α-hu	CD14	M5E2	PE	BD Biosciences
α-hu	CD15	HI98	PerCP-Cy5.5	BD Biosciences
α-hu	CD33	HIM3-4	PE	EXBIO
α-hu	CD49f	GoH3	PE	BD Biosciences
α-hu	CD66b	G10F5	PerCP-Cy5.5	BioLegend
	Isotype (IgG1κ)	MOPC-21	PE	BD Biosciences

6.2 Methods

6.2.1 Animal experiments

6.2.1.1 Genotyping of mouse strains

To ensure the desired transmittance of transgenes after crossbreeding, genotyping was performed using PCR amplification. To obtain tissue for DNA extraction, ear biopsies were taken from each mouse to be genotyped. The biopsies were kept overnight in 200 µl SDS-Lysis buffer with Proteinase K (0.5 mg/ml) at 800rpm, 55 °C. After centrifugation (15min, max. speed), 200 µl supernatant were transferred and mixed with Isopropanol (v/v), inverted multiple times and centrifuged (1 min, max. speed). The supernatant was discarded and the pellet was washed in 600 µl 70% Ethanol, inverted multiple times and centrifuged (1 min, max. speed). The supernatant was discarded and the pellet was dried at 37 °C for 30 min before it was resuspended in 60 µl ddH_2O and the DNA content was measured photometrically with the NanoDrop.

The genotyping PCR assays of both strains used in this thesis, p53-KO (B6.129S2-Trp53^{tm1Tyi}/J (Jacks et al., 1994)) and R26-M2rtTA knock-in (B6.Cg-Gt(ROSA)26Sor$^{tm1(rtTA*M2)Jae}$/J (Hochedlinger et al., 2005)), were performed using a common forward primer combined with two reverse primers (mutant and wildtype) to obtain PCR products of different sizes depending on the genotype. Primer sequences and genotyping PCR protocols were obtained from The Jackson Laboratories (p53-KO: www.jax.org/strain/002101; R26-M2rtTA knock-in: www.jax.org/strain/006965).

6.2.1.2 Isolation of primary murine bone marrow cells

Mice were sacrificed and femur, tibia, and hips were dissected. Connective and muscle tissue were removed with sterile cotton cloths before the bones were crushed in a mort. Bone marrow cells were suspended in MACS Buffer and subsequently filtered through a cell strainer with 40 µm pore size to obtain a single cell suspension. If needed for analysis by flow cytometry, an aliquot of untreated full bone marrow cells was kept in a separate tube before the erythrocytes were lysed with ACK Lysis Buffer (Lonza) for 8 min on ice. Cells were washed, spun down at 300 g for 6 min and resuspended in MACS Buffer for subsequent procedures.

6.2.1.3 Preparation of lineage negative murine bone marrow cells

To enrich freshly prepared bone marrow cells for the lineage negative cell population containing the hematopoietic stem and progenitor cell compartment, a negative selection by MACS (magnetic cell separation) was performed using the Lineage Cell Depletion Kit, Mouse (Miltenyi Biotec), according to the manufacturer's protocol. Briefly, the isolated bone marrow cells were stained with a mixture of biotinylated antibodies against lineage markers (CD5, CD45R, CD11b, Gr1, Ter-119, 7-4). Next, the labeled cells were coupled to Streptavidin-conjugated magnetic micro-beads and ran through a separation column in a

magnetic field (lineage depletion). Unlabeled cells passed the column in an "untouched" manner and were collected in a clean sterile tube. The purity of the enriched lineage negative cell population was assessed by flow cytometry. Aliquots of cells labeled with the antibody mixture before and after magnetic cell separation were stained with PE-coupled Streptavidin (10 µl per 10^7 cells) in 100 µl MACS Buffer for 15 min at 4 °C in the dark. After the cells were washed, the frequency of remaining lineage positive cells was assessed by flow cytometry. Usually, enrichment to 85%-95% of lineage negative cells was reached with a starting frequency of about 5%-10%. After enrichment, lineage negative cells were kept in X-Vivo 15 medium supplemented with cytokines (80 ng/ml Scf, 40 ng/ml Tpo, 40 ng/ml Flt3L), 100 U/ml Pen/Strep, 2 mM L-Glutamine and 10% h.i. FBS for 24 hours.

6.2.1.4 Irradiation of recipient animals and transplantation of donor bone marrow cells

72 hours prior to transplantation, 4-5 donor mice were sacrificed and their bone marrow was isolated. Lineage negative cells were obtained by MACS and cultivated for 24 hours. Next, the cells were transduced with lentiviral particles to obtain 5-10% genetically modified cells. Transduced cells were cultivated in X-Vivo 15 medium supplemented with cytokines (80 ng/ml mScf, 40 ng/ml mTpo, 40 ng/ml mFlt3L), 100 U/ml Pen/Strep, 2 mM L-Glutamine and 10% h.i. FBS for further 48 hours.

24 hours prior to transplantation, donor animals were irradiated at the Institute of Medical Radiation Biology. Lethal irradiation was achieved with whole body X-Ray irradiation at a dose of 9.5 Gy. For sub-lethal irradiation an irradiation dose of 4.5 Gy was applied to the mice. Irradiated mice were fed drinking water supplied with 0.02% Enrofloxacin (Baytril) for two weeks post transplantation to prevent infections.

At the day of transplantation, one mouse was sacrificed to provide non-lineage depleted bone marrow helper cells to support the bone marrow reconstitution in the lethally irradiated recipient animals. Per recipient animal, $1x10^5$-$2x10^5$ lineage depleted, genetically modified bone marrow cells were prepared and pooled with $2x10^5$ bone marrow helper cells in a volume of 50 µl PBS per transplantation. The cells were transplanted into anaesthetized irradiated recipient mice by retro-orbital injection. For sub-lethally irradiated recipients, no helper bone marrow cells were added. Instead, $5x10^6$ full bone marrow cells from the donor mouse were transplanted directly without lineage depletion.

Transplanted animals were monitored consistently (every 1-2 days) for their health and sacrificed if they showed signs of illness. Mice were sacrificed at 2-6 months after transplantation, depending on the experimental design.

6.2.1.5 Blood sampling

For regular blood sampling during reconstitution experiments tail vein bleeding was performed. Mice were put under red light for 1min to increase their blood pressure. The tail vein was carefully incised with a scalpel and approx. 200 µl blood were drawn with a heparin coated glass capillary into an EDTA-containing blood monovette.

For blood sampling upon experiment termination, a retro-orbital sinus bleeding was performed. Mice were anaesthetized and approx. 200 µl blood were drawn directly with a heparin coated glass capillary from the retro-orbital venous sinus into an EDTA-containing blood monovette. Mice were sacrificed while still in anesthesia for further organ preparation.

6.2.1.6 Assessment of Complete Blood Counts

Complete blood counts were assessed from 12 µl EDTA-blood sample on a scil VetABC Hematology Analyzer at the animal facility, UK Essen, according to the manufacturer's protocol.

6.2.1.7 Isolation of primary murine peripheral blood mononuclear cells

For erythrocyte lysis, 80 µl EDTA-blood was resuspended in 1.8 ml EL erythrocyte lysis buffer (Qiagen) and incubated for 10 min at room temperature. Cells were washed with PBS, spun down at 300 g for 6 min and resuspended in MACS buffer for subsequent procedures.

6.2.1.8 Isolation of primary murine splenocytes

Mice were sacrificed and after removal of the bones the ventral cavity was opened to remove the spleen carefully by cutting surrounding connective tissue. The spleen was homogenized by mashing the cells through a 40 µm cell strainer with a syringe plunger. The cell strainer was washed several times with MACS buffer to elute all remaining cells into the tube. If needed for analysis by flow cytometry, an aliquot of untreated splenocytes was kept in a separate tube before the erythrocytes were lysed with ACK Lysis Buffer (Lonza) for 8 min on ice. Cells were washed, spun down at 300 g for 6 min and resuspended in MACS Buffer for subsequent procedures.

6.2.1.9 Blood smears, cytospins and histological staining

For evaluation of blood cell and bone marrow cell morphologies in the mice, histological May-Gruenwald-Giemsa staining was performed on peripheral blood smears and cytospins of the bone marrow. For blood smears, 4 µl EDTA-blood were spread on a microscopic glass slide and air-dried. Bone marrow cells were sorted flow-cytometrically to obtain GFP^+ and GFP^- cell populations. $0.15x10^6$ cells were centrifuged (5 min, 1200 rpm) on microscopic glass slides and air dried. Staining was performed for 3 min in May-Grünwald solution, washed for 1 min in ddH_2O, stained for 20 min in 1x Giemsa solution and rinsed twice with ddH_2O. Dried slides were mounted with coverslips using Eukitt mounting medium.

6.2.2 Cell culture

6.2.2.1 Human cell lines

HEK-293T cells

This epithelial cell line has been originally derived from human embryonic kidney cells obtained in 1973 by Alex van der Eb's laboratory. The cells have been transformed with

sheared Adenovirus 5 DNA (Graham et al., 1977) and express the SV40 Large T Antigen (Fu and Manley, 1987). They were cultured in DMEM supplemented with 10% h.i. FBS. For passaging, they were shortly treated with 1x Trypsin-EDTA and replated at $0.5x10^6$ cells/ml. They were used for the production of lentiviral supernatants.

K562 cells

This suspension cell line has been established from a 53-year old female with CML in blast crisis (Lozzio and Lozzio, 1975). They were cultured in RPMI supplemented with 10% h.i. FBS and were used for titration of lentiviral supernatants and as a control cell line in re-expression experiments. K562 cells were passaged every 2-3 days at a 1:5 ratio.

HL60 cells

This promyelocytic leukemia cell line has been established from a 36-year old female (Gallagher et al., 1979). The cells were cultured in RPMI supplemented with 10% h.i. FBS. Since they harbor a deletion of one chromosome 5q and an epigenetic suppression of the other allele (Ulger et al., 2003; Liu et al., 2007), they were used for CTNNA1 re-expression experiments. HL60 cells were passaged every 2-3 days at a 1:4 ratio.

6.2.2.2 Murine cell lines

NIH-3T3 cells

This fibroblast cell line has been established from BALB/c mouse embryonic fibroblasts in the 1960s (Aaronson and Todaro, 1968). They were cultured in DMEM supplemented with 10% h.i. FBS. For passaging, they were shortly treated with 1x Trypsin-EDTA and replated at $0.5x10^6$ cells/ml. The cells were used for the test of the knockdown efficiency of lentiviral vectors encoding shRNAs targeting Ctnna1.

Primary bone marrow cells

After lineage depletion, freshly isolated bone marrow cells were cultivated in X-Vivo 15 medium supplemented with cytokines (80 ng/ml Scf, 40 ng/ml Tpo, 40 ng/ml Flt3L), 100 U/ml Pen/Strep, 2 mM L-Glutamine and 10% h.i. FBS for 24 hours before they were transduced with lentiviral supernatants to deliver an immortalizing genetic alteration. For long-term culture, the cytokine concentration of the medium was scaled down to 20 ng/ml Scf, 10 ng/ml Tpo, 10 ng/ml Flt3L. The cells were kept at a density of $1x10^6$ cells/ml and medium was replaced every 2 days.

6.2.2.3 Monitoring cell growth

Cell growth was monitored via the CellTiter-Glo Luminescent Cell Viability Assay (Promega). The assay quantifies the amount of ATP released from lysed cells by the oxidation of luciferin in the presence of O_2, Mg^{2+} and ATP. Catalyzed by the Ultra-Glo recombinant luciferase, the oxidation results in oxyluciferin and thus in a stable luminescent signal that is proportional to the amount of viable cells. For a standard assay setup to monitor the growth of primary bone marrow cells, $0.25x10^6$ cells/well were plated in a 24-well plate in 800 µl medium. Per measurement, 50 µl of cell suspension plus 5 µl 1 M HEPES buffer solution

were thoroughly resuspended with 100 µl of CellTiter-Glo Reagent in a well of an opaque 96-well microplate suitable for luminescence measurement. The plate was incubated for 10 min at room temperature and luminescence was measured on the GloMax-Multi Detection System with 1s integration time in a predefined CellTiter-Glo protocol (Promega). Every measurement was performed in triplicates and at suitable time intervals. All measurement values of an individual cell suspension were normalized on the respective starting value.

Another method for monitoring cell growth was the manual counting of cells in the Cytoflex flow cytometer (Beckman Coulter), which accurately counts absolute events in a population and measures the acquired sample volume. If this method was used, a defined amount of cell suspension was counted in suitable time intervals. The total cell number per well was calculated according to the total volume per well.

6.2.3 Molecular biology methods

6.2.3.1 Polymerase Chain Reaction (PCR)

The Polymerase Chain Reaction (PCR) is used to enzymatically amplify short DNA fragments from a DNA template (Saiki et al., 1988). It is also a useful tool to introduce specific mutations into a DNA sequence of interest or to fuse two DNA fragments.

If not stated otherwise, PCR was performed in a PTC-200 Thermal Cycler and contained 1x Buffer for appropriate PCR conditions, 10-100 ng Template DNA, 0.5 µM forward and reverse primer each, 0.2 mM dNTPs, 1-5 U DNA Polymerase and ddH_2O. For genotyping the *Taq* polymerase system (Qiagen) was used according to protocol. For cloning, the Phusion Hot Start II Polymerase system (Thermo Scientific) was used according to protocol due to its high fidelity and proof-reading activity.

6.2.3.2 Agarose Gel Electrophoresis

A 1-2% agarose gel was prepared depending on the size of the DNA fragments to be separated. The appropriate amount of agarose was heat-dissolved in 1x TAE buffer. Ethidium bromide (0.07%), a DNA intercalating agent allowing the detection of DNA by UV light, was added and the gel was casted. The gels were run in 1x TAE-buffer at 90-120V for 45-60 min, the DNA fragments were detected by UV light, and photographed for documentation. In case of a preparative gel, the gel blocks containing the desired DNA fragments were cut out with a scalpel.

6.2.3.3 DNA purification

PCR products larger than 100 bp were purified using the QIAquick PCR Purification Kit (Qiagen) employing the silica-membrane-based column purification according to the manufacturer's instructions. Purification of DNA bands from agarose gel blocks was performed using the QIAquick Gel Extraction Kit (Qiagen) according to the manufacturer's instructions. The concentration and the purity of the obtained DNA were determined with a spectrophotometer (NanoDrop).

6.2.3.4 RNA extraction

Total RNA was extracted using TRIzol Reagent, a monophasic solution of phenol, guanidine isothyocyanate and other components permitting the isolation of total RNA. TRIzol Reagent inhibits RNase activity while disrupting the cells and dissolving the cellular components during homogenization of the sample (Chomczynski and Sacchi, 1987; Chomczynski, 1993). Up to $5x10^6$ cells were resuspended in 1 ml of TRIzol Reagent and 200 µl Chloroform per ml TRIzol was added. After centrifugation for 12 min at 12000 g at 4° C the homogenate was separated into a clear aqueous upper layer (containing the RNA), an interphase and an organic lower layer containing DNA and protein. The upper layer was transferred into a new tube and RNA was precipitated with 5µg glycogen and isopropanol (v/v), centrifuged at fullspeed for 12 min at 4 °C. The supernatant was discarded and the pellet was washed with 1 ml 80% Ethanol. After centrifugation (30 sec, fullspeed, RT), the ethanol was discarded, the pellet was air-dried, and resuspended in 25-50 µl of RNase free ddH_2O. The RNA content was measured at the NanoDrop.

6.2.3.5 cDNA synthesis (Reverse transcription)

For the reverse transcription to enzymatically generate cDNA (complementary DNA) from RNA the QuantiTect Reverse Transcription Kit (Qiagen, Hilden) was used according to the manufacturer's instructions. Briefly, genomic DNA was eliminated from 100-500 ng purified RNA with gDNA wipeout buffer. Next, reverse transcription was performed using a pre-mixed blend of Oligo-dT- and random primers allowing high cDNA yields from all regions of the RNA transcript. The enzymatic mix performing the reverse transcription was composed of two recombinant reverse transcriptases (Omniscript and Sensiscript, Qiagen, Hilden) and a strong RNase inhibitor.

6.2.3.6 Preparation of genomic DNA from cultivated cells

Up to $5x10^6$ cultivated cells were harvested and centrifuged. The supernatant was discarded and the pellet was frozen at -80 °C. Genomic DNA was extracted using the QIAamp DNA Mini Kit according to the manufacturer's instructions.

6.2.3.7 Quantitative PCR (QPCR)

Quantitative PCR (QPCR) was performed to determine the relative copy number of a specific amplicon in genomic DNA or cDNA. This method was used for the titration of lentiviral supernatants by quantifying the amount of integrated viral genome in the host genome after transduction, identification of the integrated shRNA in the DNA of clonally expanded bone marrow cells or determination of the relative expression levels of genes (QRT-PCR).

Briefly, a SYBR Green based assay was performed in triplicates on a CFX96 Real Time System (Bio-Rad Laboratories Inc.) in a 20 µl reaction volume (1x MasterMix (1x PCR Gold Puffer; 2.5 mM $MgCl_2$; 0.3 mM dNTPs, Life Technologies), 0.25 µM forward primer, 0.25 µM reverse primer, 0.25x SYBR Green (Life Technologies), 0.03 U AmpliTaq Gold

DNA Polymerase (Life Technologies), 1 µl Template DNA (cDNA or 25 ng genomic DNA). Upon intercalating into double-stranded DNA, SYBR green fluoresces. The fluorescence intensity was measured after each PCR amplification cycle and was used to quantitate the amount of template DNA. With the formula $Nn = No * 1.95^{Ct}$ (N_n – number of molecules at detection threshold, N_0 – number of molecules in template DNA, 1.95 – estimated primer efficiency, C_t – number of amplification cycles to detection threshold) the number of template DNA molecules in the sample was calculated for each used primer pair. If the primer pair efficiency was known, it was implemented into the formula instead of the shown estimation.

6.2.4 Molecular Cloning

6.2.4.1 Restriction enzyme digestion of DNA

Plasmids and PCR products were digested using FastDigest restriction enzymes (Thermo Scientific) at 37 °C. The amount of enzyme and the time of incubation were adjusted to the amount of DNA to be digested. Digestion buffers were used according to the manufacturer's instructions. For analytical approaches 0.5-2 µg DNA were digested. For preparative digestions 5-6 µg DNA were used. All preparative digestions providing the plasmid backbone in subsequent cloning reactions were treated with 1 U of Alkaline Phosphatase for the last 10 min of the digestion reaction to remove 5'-phosphate groups to prevent a religation of the plasmid in the ligation reactions. Digested products were directly column-purified or separated by agarose gel electrophoresis and subsequently gel-purified.

6.2.4.2 Ligation of DNA fragments and transformation of bacteria

35-80 ng of dephosphorylated plasmid backbone and 3-4 fold molar excess of the desired insert were ligated in a 10 µl reaction volume using the T4 DNA ligase in a buffer allowing rapid ligation. A ligation reaction without insert served as control. The reaction was incubated at room temperature for 10 min, gently stirred into 50-100 µl of chemically competent bacteria, and incubated on ice for 20 min. The bacteria were heat shocked at 42 °C for 45 sec followed by addition of 250 µl of LB medium for recovery at 37 °C for 45 min. The bacteria suspensions were plated on agar plates containing ampicillin (100 µg/ml). The agar plates were incubated overnight at 37 °C.

6.2.4.3 Preparation of plasmid DNA

Individual bacterial colonies were picked and transferred to a liquid culture of 4 ml LB medium containing ampicillin (100 µg/ml) and incubated at 37 °C overnight while shaking at 250 rpm. After sedimentation of the bacteria (2500 g, 10 min, RT) plasmid DNA was purified using the QIAprep Spin Miniprep Kit (Qiagen) according to the manufacturer's instructions. For higher yields of plasmid DNA, 4 ml LB medium cultures were inoculated into 100 ml LB medium containing ampicillin (100 µg/ml) and incubated at 37 °C overnight on a shaker (250 rpm). The bacteria were pelleted by centrifugation (3500 g, 20 min, 4 °C) and plasmid DNA was purified using the QIAGEN Plasmid *Plus* Maxi Kit (Qiagen) according to the

manufacturer's instructions. If necessary, eluted plasmid DNA was sequenced by Sanger sequencing (Sanger et al., 1977).

6.2.4.4 Annealing of oligonucleotides

Complementary ssDNA oligonucleotides were annealed and phosphorylated in a 20 µl reaction (1 µl 10 µM Oligo1, 1 µl 10 µM Oligo2, 1x Ligation buffer (Thermo Fisher Scientific), 5 U T4 Polynucleotide Kinase (Thermo Fisher Scientific)) for 1 hour at 37 °C to generate dsDNA oligonucleotides for cloning.

6.2.4.5 Blunting of DNA fragments

1 µg DNA with 5' and 3' overhanging ends was blunted in a 20 µl reaction in 1x T4 polymerase reaction buffer, 0.125 mM dNTPs, 1 U T4 DNA Polymerase for 10 min at room temperature. The reaction was inactivated by heating to 75 °C for 10 min.

6.2.4.6 Cloning of RNAi vectors

Prior to modeling gene dosage insufficiency *in vivo*, 24 shRNA sequences targeting the Ctnna1 mRNA were designed for *in vitro* testing. The annealed oligonucleotides (Figure 54A) were ligated directly into a lentiviral pLKO.1 vector backbone (Stewart et al., 2003) opened by restriction digestion with AgeI/EcoRI (Figure 54B and C). For *in vivo* approaches, the Puromycin resistance CDS was replaced by GFP CDS for selected vectors by BamHI/KpnI restriction digestion (Figure 54D) to obtain pLKO.G-shRNA vectors.

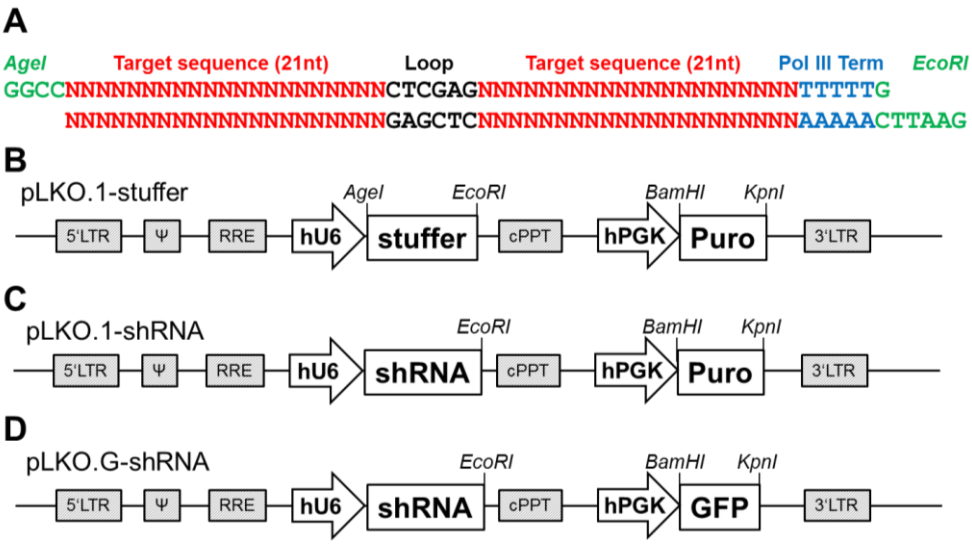

Figure 54: Lentiviral vector designs used for Ctnna1 knockdown in vitro and *in vivo*.
(A) Structure of shRNA-specific cloning oligonucleotide. (B) pLKO.1 vector used for vector backbone preparation containing a stuffer sequence downstream of the U6 promoter. (C) pLKO.1 vector with shRNA construct, used for in vitro testing. (D) pLKO.G: Variant of pLKO.1 with GFP as selection marker, used for transduction/transplantation experiments *in vivo*. Grey box: lentiviral vector backbone element, white arrow: promoter, white box: CDS

6.2.4.7 Cloning of expression vectors

To re-express ectopic Ctnna1 in shRNA 405 expressing murine bone marrow cells, four silent single nucleotide mutations were introduced at the shRNA 405 binding site of the Ctnna1 CDS by Fusion PCR. The amplified mutant Ctnna1 CDS was inserted via XbaI/MluI restriction digestion into a lentiviral pLE-vector backbone (originating from pRRLSIN.cPPT.PGK-GFP.WPRE (Dull et al., 1998; Zufferey et al., 1998; Zufferey et al., 1999; Zennou et al., 2000), modified by S. Heinrichs). Promoters mediating different Ctnna1 expression levels were subsequently introduced by HpaI/XbaI restriction digestion. Four lentiviral re-expression vectors were produced: pLE11-Ctnna1 (SFFV-promoter), pLE14-Ctnna1 (CMV-promoter), pLE14d2-Ctnna1 and pLE14d3-Ctnna1 (CMV promoters with different internal deletions mediating attenuated transgene expression). A lentiviral control vector without transgene expression encoding only the Blasticidin resistance CDS under the control of the human PGK promoter (pLE-Blast) was cloned by XbaI/MluI restriction digestion followed by blunting of the DNA fragments and re-ligation of the vector.

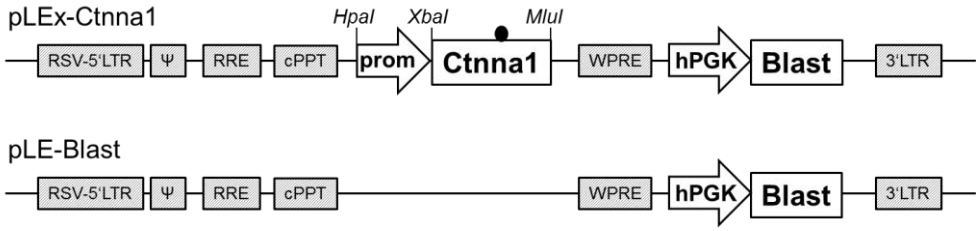

Figure 55: Lentiviral vector designs for constitutive ectopic Ctnna1 re-expression in murine bone marrow cells.
pLEx-Ctnna1: To abrogate binding of shRNA 405, four silent single nucleotide mutations were introduced by PCR into the Ctnna1 CDS (black circle). Ctnna1 CDS was expressed under the control of four different promoters of different strengths (SFFV>CMV>CMVd2>CMVd3) to reach Ctnna1 re-expression to different levels. pLE-Blast served as control vector encoding only the Blasticidin resistance gene without an upstream re-expression cassette. Grey box – lentiviral vector backbone element, white arrow – promoter, white box – CDS

6.2.4.8 Cloning of inducible re-expression vectors (TET-ON-System)

The rtTA-M2 CDS under the control of the human PGK promoter was PCR-amplified from pHK130 (Dr. Hannes Klump, Transfusion Medicine, Essen) and inserted by ClaI/MluI digestion into a lentiviral pLE-vector backbone containing IRES-BFP (pLE52-M2, Figure 56). CTNNA1 CDS was amplified by fusion PCR and inserted by SpeI/SgsI digestion

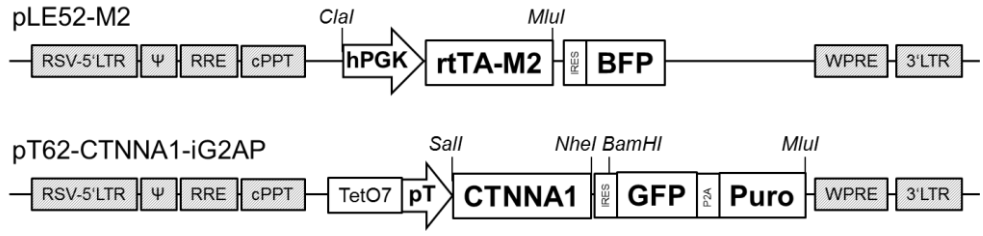

Figure 56: Lentiviral vector design for doxycycline-inducible CTNNA1 re-expression in the human HL60 cell line.
HL60 cells were transduced with pLE52-M2 to introduce the rtTA-M2 protein into the HL60 cells. Sorted BFP^+ cells were then transduced with pT62-CTNNA1-iG2AP encoding CTNNA1 or CTNNA1ΔN_{267} coupled to GFP-2A-Puro under a Tetracycline-inducible promoter (pT). This vector architecture prevented vector-silencing due to Puromycin-mediated selective pressure. Grey box: lentiviral vector backbone element, white arrow: promoter, white box: CDS

into a lentiviral vector backbone opened by XbaI/MluI (compatible end ligation) containing a 7x Tetracycline-responsive element (TetO7) upstream of a Tetracycline-inducible promoter (pT). This intermediate cloning product contained an IRES element coupled to a BFP CDS downstream of the CTNNA1 CDS. The BFP reporter was exchanged by a fusion PCR-amplified IRES-GFP-P2A-Puromycin element by BamHI/MluI digestion (pT62-CTNNA1-iG2AP, Figure 56). To obtain analogous lentiviral vectors encoding mutant CTNNA1, the CTNNA1 expression cassette was exchanged by the insertion of fusion PCR-amplified CTNNA1ΔN_{267} (N-terminal deletion of aa1-266) CDS via SalI/NheI digestion.

6.2.5 Lentiviral vectors

Genetic manipulation of cells was accomplished by the stable integration of genetic material into the host cell genome employing lentiviral particles derived from the Human Immunodeficiency Virus-1 (HIV-1). These particles are replication deficient (SIN lentiviral vector) and pseudotyped by the envelope glycoprotein of the vesicular stomatitis virus (VSV-G) to transduce dividing as well as non-dividing cells (Naldini et al., 1996; Zufferey et al., 1997; Miyoshi et al., 1998). A second generation packaging system was used to produce cell culture supernatants containing lentiviral particles. It combines a packaging plasmid (pCMV-dR8.91(Zufferey et al., 1997)), an envelope plasmid (pMD2.G (Addgene #12259, Didier Trono)), and the transfer plasmid encoding the viral genome along with the desired transgenes.

6.2.5.1 Production of lentiviral particles

Cell culture supernatants containing lentiviral particles were produced by co-transfection of packaging plasmid, envelope plasmid and transfer plasmid into HEK293T cells. 24 hours prior to transfection, the cells were seeded at a density of $16x10^6$ cells/flask in two 175 cm^2 cell culture flasks in order to reach an optimal confluency of 70%-90% at the time of transfection. For transfection 6 mL of serum-free DMEM were mixed with 280 µl of PEI (1 mg/ml), 45 µg pCMV-dR8.91, 7 µg pMD2.G, and 45 µg of the transfer plasmid. The mixture was incubated for 30 min at RT before it was added to the medium of the HEK-293T cells. 10-16 hours post transfection the transfection medium was replaced with fresh medium. 24 hours and 48 hours after medium replacement, supernatants of the cells were harvested, supplemented with 40 mM HEPES buffer, and kept on ice. The harvested supernatants containing the viral particles were pooled, filtered through a 0.45 µm filter and spun at 19000 g for 90 min at 4 °C to sediment the viral particles. The pellet was resuspended in 1 ml IMDM medium supplemented with 2 mM L-Glutamine, incubated on ice for 1 hour, aliquoted at feasible amounts, and frozen at -80 °C.

6.2.5.2 Transduction of cells with lentiviral particles

Transduction of K562 cells for viral titer determination

$0.5x10^6$ K562 cells were transduced with 10 µl concentrated lentiviral supernatant in 500 µl medium (RPMI, 10% h.i. FBS, 4 µg/ml Polybrene, 30 mM HEPES) by spin transduction (90 min, 1000 g, 25 °C) in a 24-well plate. After transduction, cells were washed in PBS and resuspended in 500 µl serum-free DMEM with 50 U/ml Benzonase and incubated 20 min at 37 °C on a tumbler to digest residual plasmid DNA. Cells were washed in PBS and cultivated in 2.5 ml fresh RPMI, 10% h.i. FBS in a 12-well plate. 48 hours after transduction, 1.4 ml of cell suspension was harvested (approx. $1x10^6$ cells), spun down and the pellet was frozen at -80 °C for subsequent gDNA extraction and viral titer determination.

Transduction of primary murine bone marrow cells for *in vivo* or in vitro approaches

Up to $0.3x10^6$ bone marrow cells were transduced with an adjusted volume of concentrated lentiviral supernatant in 180 µl medium (X-Vivo, 10% h.i. FBS, 100 U/ml Pen/Strep, 2 mM L-Glutamine, 40 ng/ml Scf, 20 ng/ml Tpo, 20 ng/ml Flt3L, 4 µg/ml Polybrene, 30 mM HEPES) by spin transduction (90 min, 1000 g, 25 °C) in a 48-well plate. After transduction, cells were post-incubated at 37 °C for 3 hours and then washed with PBS. The transduced cells were cultivated in X-Vivo, 10% h.i. FBS, 100 U/ml Pen/Strep, 2 mM L-Glutamine, 20 ng/ml Scf, 10 ng/ml Tpo, 10 ng/ml Flt3L for at least 24 hours before subsequent analysis.

6.2.5.3 Linear amplification-mediated PCR (LAM-PCR)

Lentiviral vectors do not integrate into specific sites of the host genome and their integration may cause unwanted side effects independently from the delivered transgene (insertional mutagenesis). It is crucial to identify the insertion site of the vector in the host genome to rule out cellular deregulation caused by insertion. Linear amplification-mediated PCR (LAM-PCR) is a highly sensitive method to identify vector-genome junctions emanating from the known vector sequence. In brief, the LAM-PCR consists of five main steps: linear pre-amplification of the vector-genomic fusion sequence by extension of one primer annealing to the known vector sequence, immobilization of the ssDNA, double-stranded DNA synthesis and enzymatic digestion of the dsDNA, ligation of a known linker sequence to the 3' end of the unknown genomic target DNA, and nested PCR with linker- and vector-specific primer sequences (Schmidt et al., 2002; Schmidt et al., 2007; Appelt et al., 2009; Schmidt et al., 2009; Bartholomae et al., 2012).

The following protocol has been adapted from Schmidt and colleagues (Schmidt et al., 2007):

1. Linear PCR using biotinylated primers: 50 µl reaction composed of 1x reaction buffer (Qiagen), 0.02 µM LTRIa-primer, 0.2 mM dNTPs (Life Technologies), 100 ng template DNA, 1.25 U *Taq* polymerase (Qiagen), ddH_2O. Program: 1. 95 °C, 5 min; 2. 95 °C, 1 min; 3. 60 °C, 45 sec; 4. 72 °C, 1 min 30 sec; step 2-4 for 49 additional cycles; 5. 72 °C, 10

min. After the first 50 cycles of linear PCR, 2.5 U of *Taq* polymerase were added directly into the reaction and another 50 cycles were performed.

2. Capture of amplified biotinylated DNA fragments on Streptavidin-labeled magnetic beads: 200 µg beads (DynaBeads M-280) were washed once in 1x BW-buffer and twice with PBS/0.1% BSA before they were resuspended in 2x BW-buffer. PCR product was added in a 1:1 ratio (v/v) and incubated overnight on a shaker at 500rpm.

3. Synthesis of double-stranded DNA and restriction digest: DNA-bead complexes were washed once in ddH_2O and resuspended in 20 µl hexanucleotide priming mixture (1x Klenow buffer, 1x hexanucleotide primer mix (5 µM), dNTPs (50 µM), 0.2 U Klenow polymerase (all Life Technologies), ddH_2O) and incubated at 37 °C for 1 hour to generate double stranded DNA. The bead-DNA complexes were washed in ddH_2O and resuspended in 20 µl restriction digest mixture (1x restriction enzyme buffer, 5U enzyme, ddH_2O). Two enzymes were used: *TasI* and *Hin1II* (Thermo Fisher Scientific). Both are "four-cutters", yielding an average amplicon length of approx. 128 bp.

4. Ligation of known linker oligonucleotide: Unidirectional double stranded linker cassettes for *TasI* digestion were generated in a 50 µl ligation mixture (1x Fast Link Ligation Buffer (Epicentre), 1.25 µM LC1 Oligo, 1.25 µM LC2 Oligo, ddH_2O). For *Hin1II* digestion, oligonucleotides LC1B and LC2B were used. The reaction was incubated at 94 °C for 10 min, cooled down to 35 °C at a rate of 0.1 °C/s in a thermocycler, aliquoted à 9 µl and stored at -20 °C for one time use. The final concentration of the linker cassette aliquots was 1.25 µM. Ligation of the linker cassette to the DNA was performed in a 10 µl reaction (1x Fast Link Ligation Buffer, 1 mM ATP, 2 U Fast Link Ligase (all Epicentre), 0.25 µM linker cassette, ddH_2O) for 10 min to 1 hour at room temperature. The bead-DNA complexes were collected and resuspended in 0.1 M NaOH for 10 min at 500 rpm for separation of the dsDNA to obtain the non-biotinylated ssDNA strand. The beads were collected and the supernatant containing the denatured ssDNA served as template.

5. Nested PCR amplification of unknown sequence: The integrated vector sequence was amplified in two subsequent PCR reactions. First, denatured ssDNA was amplified in a 50 µl reaction (PCRI) consisting of 1x PCR-Buffer (Qiagen), 0.5 µM vector-specific biotinylated primer LTRII, 0.5 µM linker-specific primer LC-RV1, 0.5 mM dNTPs (Life Technologies), 2.5 U Taq polymerase (Qiagen), 2 µl ssDNA, ddH_2O. Program: 1. 5 min, 95 °C, 2. 1 min, 95 °C, 3. 45 sec, 60 °C, 4. 90 sec 72 °C, 5. steps 2-4 for 34 additional cycles, 6. 10 min, 72 °C. For enrichment, the biotinylated PCR product was immobilized on Streptavidin-beads and the non-biotinylated ssDNA strand was obtained as described before. Next, the ssDNA was amplified in a 50 µl reaction (PCRII) consisting of 1x PCR Buffer (Qiagen), 0.5 µM vector-specific primer LTRIII, 0.5 µM linker-specific primer LC-RV2, 0.5 mM dNTPs (Life Technologies), 2.5 U Taq polymerase (Qiagen), 1 µl Template ssDNA from PCRI, ddH_2O employing the same program as in PCRI. The amplified PCR product was

loaded on a 2% agarose gel and specific bands were isolated, DNA was purified and sequenced by Sanger sequencing (Sanger et al., 1977).

6.2.6 Flow Cytometry

Flow cytometry is the standard method to analyze physical properties of a large number of cells on a single cell level. Antibodies conjugated to specific fluorophores can be used to detect surface antigens of cells (e.g. immunophenotyping) or intracellular structures. Furthermore, the expression of intracellular fluorescent reporter proteins, such as GFP (green fluorescent protein), can be measured as well. In the flow cytometer the cells are separated in a capillary by a fluidic stream. Single cells separately pass the light path of an excitation laser beam and the emitted light of the coupled fluorophores and scattered incident light are detected in photomultiplier tubes (PMTs) amplifying the signal. The scattered incident light provides information about the cell size (axial light scattering, forward scatter) and granularity (perpendicular light scattering, side scatter). Incident light is usually filtered by a 488 nm long pass filter before reaching the PMTs assigned for fluorescence signal detection (Traganos, 1984; Alexander et al., 2009; Pierzchalski et al., 2011). Data acquired by flow cytometry was analyzed with the software package FlowJo (Tree Star Inc., Ashland, OR, USA).

Some flow cytometers are able to specifically sort single cells or cell populations with a distinct fluorescence signal according to the user-defined sorting parameters (fluorescence activated cell sorting – FACS) into a collection tube or cell culture plate. FACS is an efficient method to obtain highly purified cell populations allowing further analysis of defined subpopulations (Julius et al., 1972; Ibrahim and van den Engh, 2007).

6.2.6.1 Immunophenotyping

Extracellular labeling of surface antigens of isolated primary murine bone marrow cells with fluorophore-conjugated antibodies was used to determine their phenotype ex vivo and in vitro. Based on the expression of characteristic surface antigens hematopoietic stem and progenitor cells can be distinguished from lineage restricted or differentiated bone marrow cells. To discriminate differentiated (lineage positive) bone marrow cells from more immature hematopoietic stem and progenitor (lineage negative) cells, the cells were stained with an antibody cocktail containing biotin-conjugated monoclonal antibodies against CD5, CD11b/Mac1, CD45R/B220, Ly6G/Gr1, and Ter119. Labeling was performed for 20 min at 4 °C in the dark in 100 µl MACS Buffer using 10 µl of Antibody cocktail per 10^6 cells. In a second step the cells were stained in 100 µl MACS Buffer for 30 min at 4 °C in the dark with a titrated amount of streptavidin-conjugated fluorophore to detect the biotinylated antibodies. To remove excess antibodies, cells were washed with MACS Buffer after every staining step. To further characterize bone marrow cell subpopulations, cells were also stained with titrated amounts of fluorophore-conjugated anti-mouse antibodies against Ly6A/Sca1, CD117/Kit, CD48, CD150, CD11b/Mac1, Ly6G/Gr1, CD45R/B220, CD3e, CD71, and Ter119 (Figure

57). Immunophenotyping of HL60 cells upon re-expression of CTNNA1 or CTNNA1ΔN$_{267}$ was performed by staining with anti-human antibodies against CD4, CD11b, CD14, CD15, CD33, CD49f and CD66b.

If not stated otherwise, cells were stained in 100 µl MACS Buffer for 30 min at 4 °C in the dark and washed with MACS Buffer after staining to remove excess antibodies. For flow cytometric measurement, cells were resuspended in 200-800 µl MACS Buffer.

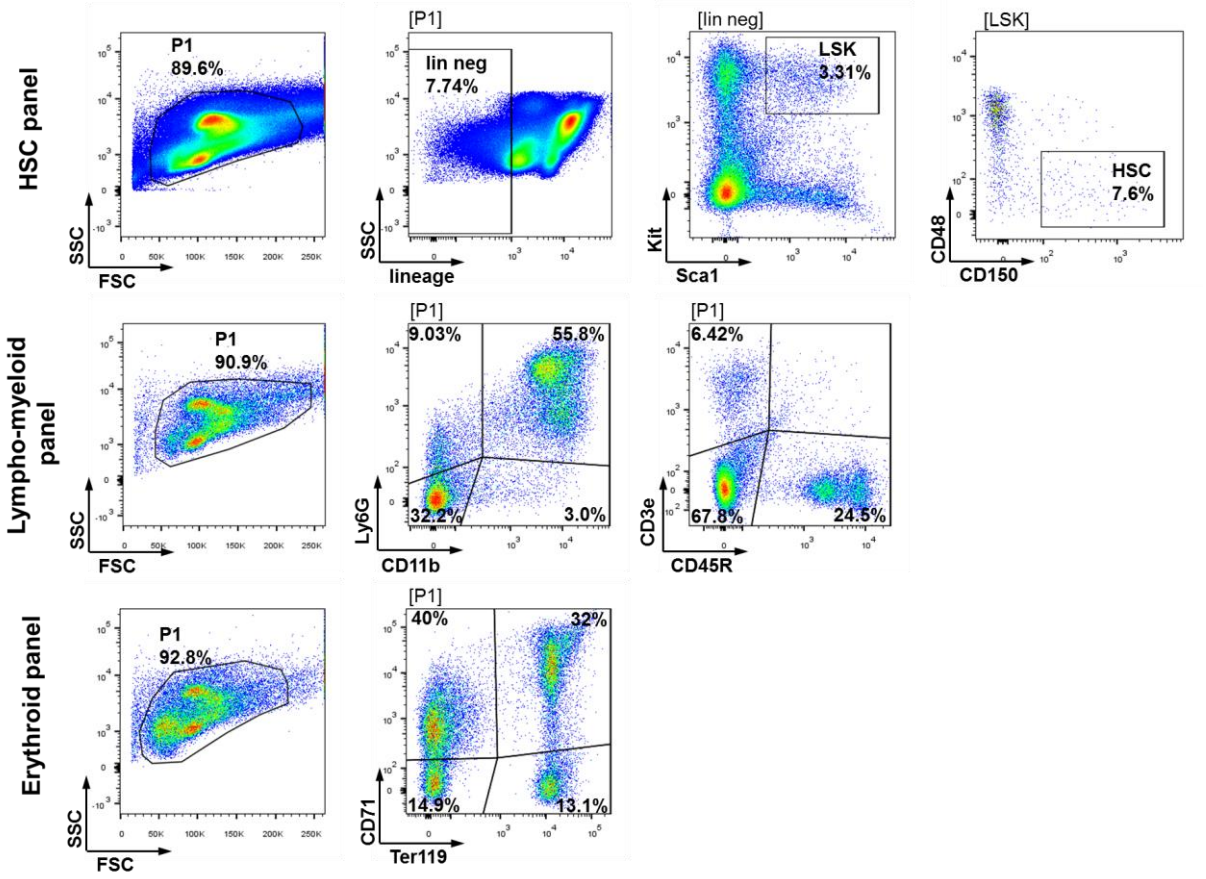

Figure 57: Gating strategies and frequencies of bone marrow subpopulations in a wildtype mouse.
Top: 0.75x10^6 bone marrow cells were stained with an antibody cocktail against lineage markers (CD5, CD11b/Mac1, CD45R/B220, Ly6G/Gr1 and Ter119), Ly6A/Sca1, CD117/Kit, CD48, CD150. Middle: 0.03x10^6 bone marrow cells were stained with CD11b/Mac1, Ly6G/Gr1, CD45R/B220, CD3e. This staining was also performed on splenocytes and peripheral blood cells. Bottom: 60 µl of non-erythrocyte lysed bone marrow was stained with CD71 and Ter119. This staining was also performed on non-erythrocyte lysed splenocytes.

6.2.6.2 Fluorescence activated cell sorting (FACS) of cell populations and single cells

Cell sorting was performed with BD FACS Aria I and III instruments using a 130 µm or 100 µm nozzle, respectively. The drop delay of the instruments was calibrated using fluorochrome-conjugated calibration beads (BD FACS Accudrop Beads, BD). Up to four different cell populations were sorted into respective collection tubes containing cell culture medium. To ensure for high purity of the sorted cell population, a re-analysis of every sorted tube was performed right after sorting. To exclude dead cells, cellular debris, and doublets from the sorted population, a pre-gating strategy of the scattered light (FSC and SSC) was always performed as a pre-requisite to every sort.

For molecular analysis the desired amount of cells was spun down (300 g, 6 min) and the cell pellet was either resuspended in TRIzol reagent for RNA extraction or frozen at -80 °C for subsequent protein extraction. For cell culture experiments, spun down cells were cultivated in cell culture medium containing antibiotics.

6.2.6.3 Cell cycle analysis with propidium iodide staining

Propidium iodide (PI) is a DNA intercalating molecule and its fluorescence intensity is proportional to the amount of PI-bound nucleic acid. As cells duplicate their DNA in the S phase of the cell cycle, a cell in the G2 phase contains double the amount of DNA compared to a cell in G1 phase. Thus, the measurement of the propidium iodide fluorescence intensity allows the generation of a cell cycle profile of cell populations. The PI staining solution was freshly prepared prior to each cell cycle analysis. $0.3x10^6$ cells were resuspended in 500 µl staining solution and incubated for at least 45 min in the dark at room temperature. Flow cytometric analysis was performed on a Beckman Coulter Cytoflex Analyzer.

6.2.7 Protein biochemistry

6.2.7.1 Protein extraction

To extract proteins from cell pellets for western blotting analysis a denaturing SDS-lysis buffer with 1x protease inhibitors (Roche) was used. The cell pellets containing $2–5x10^6$ cells were resuspended in 80-180 µl ice-cold lysis buffer and sonicated 15-20 sec at 50 W using a microtip probe. The samples were heated at 95 °C for 2 min.

6.2.7.2 Determination of protein concentration

To determine the total protein content in the cell extracts the bicinchoninic acid assay (BCA Assay) was used (Smith et al., 1985). The BCA assay depends on the formation of a Cu^{2+}-protein complex in alkaline conditions, followed by the reduction of Cu^{2+} to Cu^{+}. The Cu^{+}-ions chelate with bicinchoninic acid molecules, forming a purple-blue complex that absorbs light at 562 nm. The absorption can be quantified and compared to the absorption of a BSA standard serial dilution in order to calculate the protein content. The concentration of each sample was measured in tripclicates. Briefly, 1-3 µl of sample were added to 15-17 µl water per well in a 96-well microtiterplate and mixed thoroughly with 180 µl working reagent (Thermo Scientific Pierce Protein BCA Assay, according to the manufacturer's protocol). After 30 min incubation at 37 C, the absorption of light at 560 nm was measured with a spectrophotometer.

6.2.7.3 SDS-Polyacrylamide Gel Electrophoresis (SDS-PAGE)

Discontinuous SDS polyacrylamide electrophoresis (SDS-PAGE; Laemmli, 1970) was used to separate proteins by their electrophoretic mobility. SDS, an anionic detergent that dissolves non-covalent bonds of proteins and binds to them in an even ratio of 1.4 g SDS/1 g protein, creates negatively charged linearized proteins that migrate to the positive electrode

when an electrical field is applied. As the proteins are loaded into a polyacrylamide gel matrix, smaller proteins can move faster through the pores than larger proteins, resulting in a separation roughly corresponding to size and therefore molecular weight. A 7% separating gel (8 ml) was made by mixing 1.87 ml acrylamide solution 30%, 2 ml 4x separating gel buffer, 4.13 ml ddH_2O, 15 µl Tetramethylethylenediamine (TEMED) and 50 µl ammonium persulfate (APS) 10%. A stacking gel (3 ml) was made by mixing 0.4 ml acrylamide solution 30%, 0.75 ml 4x stacking gel buffer, 1.85 ml ddH_2O, 4 µl TEMED and 16 µl APS. For western blotting analysis, 6x SDS sample buffer was added to 20-50 µg protein and the samples were subsequently heated at 95 °C for 3 min. The samples and a molecular weight marker (PageRuler Plus Prestained Protein Ladder, Thermo Scientific) were loaded to the gels and run in 1x SDS running buffer at 25-35 mA for approx. 2 hours.

6.2.7.4 Western Blotting

After SDS-PAGE the proteins were transferred to a PVDF membrane (Immobilon-P, Merck Millipore) for the detection of Ctnna1 with antibodies (Renart et al., 1979; Towbin et al., 1979; Burnette, 1981). Using a primary, specific antibody and a secondary, horseradish peroxidase (HRP)-conjugated antibody directed against the primary one, the protein bands can be visualized with chemiluminescence. A tank blot system (wet transfer) was used in these experiments. The SDS-PAGE gel was equilibrated in 1x TGM transfer buffer and placed in the transfer stack: a sponge, three sheets of blotting paper, the gel, the PVDF membrane briefly activated in methanol, three sheets of blotting paper and another sponge. The transfer stack was placed in the transfer tank with the membrane located between the gel and the anode, thus proteins were transferred to the PDVF membrane when an electric current was applied. The blot was run at 65 V for 75 min. After blotting, the membrane was incubated in TBS-T containing 5% non-fat dry milk powder for 30 min at room temperature on a horizontal shaker to block remaining unspecific protein binding sites on the membrane. The primary antibody was diluted in milk-TBS-T and incubated with the membrane at 4 °C overnight on a horizontal shaker. The membrane was washed three times in TBS-T for 10 min to remove excess and unbound antibody. The secondary HRP-conjugated antibody was diluted 1:5,000 in milk-TBS-T and incubated with the membrane for 45 min at room temperature on a horizontal shaker. After three 10 min washing steps with TBS-T, 3 ml of enhanced chemiluminescent HRP substrate (SuperSignal West Pico Chemiluminescent Substrate, Thermo Scientific) were added to the membrane and incubated for 1 min. The chemiluminescence was then immediately measured with a Fusion System.

7 References

Aaltomaa, S., V. Karja, P. Lipponen, T. Isotalo, J. P. Kankkunen, M. Talja and R. Mokka (2005). "Reduced alpha- and beta-catenin expression predicts shortened survival in local prostate cancer." Anticancer Res 25(6C): 4707-4712.

Aaronson, S. A. and G. J. Todaro (1968). "Development of 3T3-like lines from Balb-c mouse embryo cultures: transformation susceptibility to SV40." J Cell Physiol 72(2): 141-148.

Alagia, A. and R. Eritja (2016). "siRNA and RNAi optimization." Wiley Interdiscip Rev RNA.

Alexander, C. M., J. Puchalski, K. S. Klos, N. Badders, L. Ailles, C. F. Kim, et al. (2009). "Separating stem cells by flow cytometry: reducing variability for solid tissues." Cell Stem Cell 5(6): 579-583.

Alimonti, A. (2010). "PTEN breast cancer susceptibility: a matter of dose." Ecancermedicalscience 4: 192.

Alimonti, A., A. Carracedo, J. G. Clohessy, L. C. Trotman, C. Nardella, A. Egia, et al. (2010). "Subtle variations in Pten dose determine cancer susceptibility." Nat Genet 42(5): 454-458.

Amos-Landgraf, J. M., A. A. Irving, C. Hartman, A. Hunter, B. Laube, X. Chen, et al. (2012). "Monoallelic silencing and haploinsufficiency in early murine intestinal neoplasms." Proc Natl Acad Sci U S A 109(6): 2060-2065.

Appelt, J. U., F. A. Giordano, M. Ecker, I. Roeder, N. Grund, A. Hotz-Wagenblatt, et al. (2009). "QuickMap: a public tool for large-scale gene therapy vector insertion site mapping and analysis." Gene Ther 16(7): 885-893.

Bartholomae, C. C., H. Glimm, C. von Kalle and M. Schmidt (2012). "Insertion site pattern: global approach by linear amplification-mediated PCR and mass sequencing." Methods Mol Biol 859: 255-265.

Bejar, R., R. Levine and B. L. Ebert (2011). "Unraveling the molecular pathophysiology of myelodysplastic syndromes." J Clin Oncol 29(5): 504-515.

Bellacosa, A., A. K. Godwin, S. Peri, K. Devarajan, E. Caretti, L. Vanderveer, et al. (2010). "Altered gene expression in morphologically normal epithelial cells from heterozygous carriers of BRCA1 or BRCA2 mutations." Cancer Prev Res (Phila) 3(1): 48-61.

Benjamin, J. M. and W. J. Nelson (2008). "Bench to bedside and back again: molecular mechanisms of alpha-catenin function and roles in tumorigenesis." Semin Cancer Biol 18(1): 53-64.

Berger, A. H., A. G. Knudson and P. P. Pandolfi (2011). "A continuum model for tumour suppression." Nature 476(7359): 163-169.

Borrell-Pages, M., J. C. Romero and L. Badimon (2014). "LRP5 negatively regulates differentiation of monocytes through abrogation of Wnt signalling." J Cell Mol Med 18(2): 314-325.

Boss, M. A., D. Delia, J. B. Robinson and M. F. Greaves (1980). "Differentiation-linked expression of cell surface markers on HL-60 leukemic cells." Blood 56(5): 910-916.

Boultwood, J. (2002). "Narrowing and genomic annotation of the commonly deleted region of the 5q- syndrome." Blood 99(12): 4638-4641.

Boultwood, J., C. Fidler, S. Lewis, S. Kelly, H. Sheridan, T. J. Littlewood, et al. (1994). "Molecular mapping of uncharacteristically small 5q deletions in two patients with the 5q- syndrome: delineation of the critical region on 5q and identification of a 5q-breakpoint." Genomics 19(3): 425-432.

Bric, A., C. Miething, C. U. Bialucha, C. Scuoppo, L. Zender, A. Krasnitz, et al. (2009). "Functional identification of tumor-suppressor genes through an in vivo RNA interference screen in a mouse lymphoma model." Cancer Cell 16(4): 324-335.

Burnette, W. N. (1981). ""Western blotting": electrophoretic transfer of proteins from sodium dodecyl sulfate--polyacrylamide gels to unmodified nitrocellulose and radiographic detection with antibody and radioiodinated protein A." Anal Biochem 112(2): 195-203.

Caplen, N. J., S. Parrish, F. Imani, A. Fire and R. A. Morgan (2001). "Specific inhibition of gene expression by small double-stranded RNAs in invertebrate and vertebrate systems." Proc Natl Acad Sci U S A 98(17): 9742-9747.

Chen, Z., L. C. Trotman, D. Shaffer, H. K. Lin, Z. A. Dotan, M. Niki, et al. (2005). "Crucial role of p53-dependent cellular senescence in suppression of Pten-deficient tumorigenesis." Nature 436(7051): 725-730.

Cheng, H., P. H. Liang and T. Cheng (2013). "Mouse hematopoietic stem cell transplantation." Methods Mol Biol 976: 25-35.

Choi, S. H., C. Estaras, J. J. Moresco, J. R. Yates, 3rd and K. A. Jones (2013). "alpha-Catenin interacts with APC to regulate beta-catenin proteolysis and transcriptional repression of Wnt target genes." Genes Dev 27(22): 2473-2488.

Chomczynski, P. (1993). "A reagent for the single-step simultaneous isolation of RNA, DNA and proteins from cell and tissue samples." BioTechniques 15(3): 532-534, 536-537.

Chomczynski, P. and N. Sacchi (1987). "Single-step method of RNA isolation by acid guanidinium thiocyanate-phenol-chloroform extraction." Anal Biochem 162(1): 156-159.

Cogle, C. R., B. M. Craig, D. E. Rollison and A. F. List (2011). "Incidence of the myelodysplastic syndromes using a novel claims-based algorithm: high number of uncaptured cases by cancer registries." Blood 117(26): 7121-7125.

Corey, S. J., M. D. Minden, D. L. Barber, H. Kantarjian, J. C. Wang and A. D. Schimmer (2007). "Myelodysplastic syndromes: the complexity of stem-cell diseases." Nat Rev Cancer 7(2): 118-129.

Craig, D. W., J. A. O'Shaughnessy, J. A. Kiefer, J. Aldrich, S. Sinari, T. M. Moses, et al. (2013). "Genome and transcriptome sequencing in prospective metastatic triple-negative breast cancer uncovers therapeutic vulnerabilities." Mol Cancer Ther 12(1): 104-116.

Daley, G. Q., R. A. Van Etten and D. Baltimore (1991). "Blast crisis in a murine model of chronic myelogenous leukemia." Proc Natl Acad Sci U S A 88(24): 11335-11338.

Davidson, G. and C. Niehrs (2010). "Emerging links between CDK cell cycle regulators and Wnt signaling." Trends Cell Biol 20(8): 453-460.

Deeg, H. J. and M. de Lima (2013). "Hematopoietic stem cell transplantation for older patients with myelodysplastic syndromes." J Natl Compr Canc Netw 11(10): 1227-1233.

Ding, L., M. J. Ellis, S. Li, D. E. Larson, K. Chen, J. W. Wallis, et al. (2010). "Genome remodelling in a basal-like breast cancer metastasis and xenograft." Nature 464(7291): 999-1005.

Dull, T., R. Zufferey, M. Kelly, R. J. Mandel, M. Nguyen, D. Trono and L. Naldini (1998). "A third-generation lentivirus vector with a conditional packaging system." J Virol 72(11): 8463-8471.

Dutt, S., A. Narla, K. Lin, A. Mullally, N. Abayasekara, C. Megerdichian, et al. (2011). "Haploinsufficiency for ribosomal protein genes causes selective activation of p53 in human erythroid progenitor cells." Blood 117(9): 2567-2576.

Dzierzak, E. and S. Philipsen (2013). "Erythropoiesis: development and differentiation." Cold Spring Harb Perspect Med 3(4): a011601.

Ebert, B. L. (2009). "Deletion 5q in myelodysplastic syndrome: a paradigm for the study of hemizygous deletions in cancer." Leukemia 23(7): 1252-1256.

Ebert, B. L. (2011). "Molecular dissection of the 5q deletion in myelodysplastic syndrome." Semin Oncol 38(5): 621-626.

Ebert, B. L., J. Pretz, J. Bosco, C. Y. Chang, P. Tamayo, N. Galili, et al. (2008). "Identification of RPS14 as a 5q- syndrome gene by RNA interference screen." Nature 451(7176): 335-339.

Elbashir, S. M., J. Harborth, W. Lendeckel, A. Yalcin, K. Weber and T. Tuschl (2001). "Duplexes of 21-nucleotide RNAs mediate RNA interference in cultured mammalian cells." Nature 411(6836): 494-498.

Fire, A., S. Xu, M. K. Montgomery, S. A. Kostas, S. E. Driver and C. C. Mello (1998). "Potent and specific genetic interference by double-stranded RNA in Caenorhabditis elegans." Nature 391(6669): 806-811.

Fisher, E. and P. Scambler (1994). "Human haploinsufficiency--one for sorrow, two for joy." Nat Genet 7(1): 5-7.

Fleming, H. E., V. Janzen, C. Lo Celso, J. Guo, K. M. Leahy, H. M. Kronenberg and D. T. Scadden (2008). "Wnt Signaling in the Niche Enforces Hematopoietic Stem Cell Quiescence and Is Necessary to Preserve Self-Renewal In Vivo." Cell Stem Cell 2(3): 274-283.

Fodde, R. and R. Smits (2002). "Cancer biology. A matter of dosage." Science 298(5594): 761-763.

Foulkes, W. D. (2008). "Inherited susceptibility to common cancers." N Engl J Med 359(20): 2143-2153.

Frasca, D., F. Guidi, M. Arbitrio, C. Pioli, F. Poccia, R. Cicconi and G. Doria (2000). "Hematopoietic reconstitution after lethal irradiation and bone marrow transplantation: effects of different hematopoietic cytokines on the recovery of thymus, spleen and blood cells." Bone Marrow Transplant 25(4): 427-433.

Friend, S. H., R. Bernards, S. Rogelj, R. A. Weinberg, J. M. Rapaport, D. M. Albert and T. P. Dryja (1986). "A human DNA segment with properties of the gene that predisposes to retinoblastoma and osteosarcoma." Nature 323(6089): 643-646.

Fu, C. T., K. Y. Zhu, J. Q. Mi, Y. F. Liu, S. T. Murray, Y. F. Fu, et al. (2010). "An evolutionarily conserved PTEN-C/EBPalpha-CTNNA1 axis controls myeloid development and transformation." Blood 115(23): 4715-4724.

Fu, X. Y. and J. L. Manley (1987). "Factors influencing alternative splice site utilization in vivo." Mol Cell Biol 7(2): 738-748.

Gallagher, R., S. Collins, J. Trujillo, K. McCredie, M. Ahearn, S. Tsai, et al. (1979). "Characterization of the continuous, differentiating myeloid cell line (HL-60) from a patient with acute promyelocytic leukemia." Blood 54(3): 713-733.

Garcia-Manero, G. (2015). "Myelodysplastic syndromes: 2015 Update on diagnosis, risk-stratification and management." Am J Hematol 90(9): 831-841.

Gattinoni, L., X.-S. Zhong, D. C. Palmer, Y. Ji, C. S. Hinrichs, Z. Yu, et al. (2009). "Wnt signaling arrests effector T cell differentiation and generates CD8+ memory stem cells." Nat Med 15(7): 808-813.

Gishizky, M. L., J. Johnson-White and O. N. Witte (1993). "Efficient transplantation of BCR-ABL-induced chronic myelogenous leukemia-like syndrome in mice." Proc Natl Acad Sci U S A 90(8): 3755-3759.

Goldberg, S. L., E. Chen, M. Corral, A. Guo, N. Mody-Patel, A. L. Pecora and M. Laouri (2010). "Incidence and clinical complications of myelodysplastic syndromes among United States Medicare beneficiaries." J Clin Oncol 28(17): 2847-2852.

Gondek, L. P., R. Tiu, C. L. O'Keefe, M. A. Sekeres, K. S. Theil and J. P. Maciejewski (2008). "Chromosomal lesions and uniparental disomy detected by SNP arrays in MDS, MDS/MPD, and MDS-derived AML." Blood 111(3): 1534-1542.

Graham, F. L., J. Smiley, W. C. Russell and R. Nairn (1977). "Characteristics of a human cell line transformed by DNA from human adenovirus type 5." J Gen Virol 36(1): 59-74.

Gratwohl, A., H. Baldomero, M. Gratwohl, M. Aljurf, L. F. Bouzas, M. Horowitz, et al. (2013). "Quantitative and qualitative differences in use and trends of hematopoietic stem cell transplantation: a Global Observational Study." Haematologica 98(8): 1282-1290.

Graubert, T. and M. J. Walter (2011). "Genetics of myelodysplastic syndromes: new insights." Hematology Am Soc Hematol Educ Program 2011: 543-549.

Graubert, T. A., M. A. Payton, J. Shao, R. A. Walgren, R. S. Monahan, J. L. Frater, et al. (2009). "Integrated genomic analysis implicates haploinsufficiency of multiple chromosome 5q31.2 genes in de novo myelodysplastic syndromes pathogenesis." PLoS One 4(2): e4583.

Graubert, T. A., D. Shen, L. Ding, T. Okeyo-Owuor, C. L. Lunn, J. Shao, et al. (2012). "Recurrent mutations in the U2AF1 splicing factor in myelodysplastic syndromes." Nat Genet 44(1): 53-57.

Greenberg, P. L., H. Tuechler, J. Schanz, G. Sanz, G. Garcia-Manero, F. Sole, et al. (2012). "Revised international prognostic scoring system for myelodysplastic syndromes." Blood 120(12): 2454-2465.

Guenet, J. L., D. Simon-Chazottes, M. Ringwald and R. Kemler (1995). "The genes coding for alpha and beta catenin (Catna1 and Catnb) and plakoglobin (Jup) map to mouse chromosomes 18, 9, and 11, respectively." Mamm Genome 6(5): 363-366.

Haase, D., U. Germing, J. Schanz, M. Pfeilstocker, T. Nosslinger, B. Hildebrandt, et al. (2007). "New insights into the prognostic impact of the karyotype in MDS and correlation with subtypes: evidence from a core dataset of 2124 patients." Blood 110(13): 4385-4395.

Haferlach, T., Y. Nagata, V. Grossmann, Y. Okuno, U. Bacher, G. Nagae, et al. (2014). "Landscape of genetic lesions in 944 patients with myelodysplastic syndromes." Leukemia 28(2): 241-247.

Han, S. P. and A. S. Yap (2013). "An alpha-catenin deja vu." Nat Cell Biol 15(3): 238-239.

Harris, T. J. and U. Tepass (2010). "Adherens junctions: from molecules to morphogenesis." Nat Rev Mol Cell Biol 11(7): 502-514.

Harvey, K. F., X. Zhang and D. M. Thomas (2013). "The Hippo pathway and human cancer." Nat Rev Cancer 13(4): 246-257.

Heaney, M. L. and D. W. Golde (1999). "Myelodysplasia." N Engl J Med 340(21): 1649-1660.

Heinrichs, S., L. F. Conover, C. E. Bueso-Ramos, O. Kilpivaara, K. Stevenson, D. Neuberg, et al. (2013). "MYBL2 is a sub-haploinsufficient tumor suppressor gene in myeloid malignancy." Elife 2: e00825.

Heinrichs, S., R. V. Kulkarni, C. E. Bueso-Ramos, R. L. Levine, M. L. Loh, C. Li, et al. (2009). "Accurate detection of uniparental disomy and microdeletions by SNP array analysis in myelodysplastic syndromes with normal cytogenetics." Leukemia 23(9): 1605-1613.

Henry, J. B., R. A. McPherson and M. R. Pincus (2011). Henry's clinical diagnosis and management by laboratory methods. Philadelphia, PA, Elsevier/Saunders,**:** 1 online resource (xxi, 1543 p.

Herrenknecht, K., M. Ozawa, C. Eckerskorn, F. Lottspeich, M. Lenter and R. Kemler (1991). "The uvomorulin-anchorage protein alpha catenin is a vinculin homologue." Proc Natl Acad Sci U S A 88(20): 9156-9160.

Hirano, S., N. Kimoto, Y. Shimoyama, S. Hirohashi and M. Takeichi (1992). "Identification of a neural alpha-catenin as a key regulator of cadherin function and multicellular organization." Cell 70(2): 293-301.

Hochedlinger, K., Y. Yamada, C. Beard and R. Jaenisch (2005). "Ectopic expression of Oct-4 blocks progenitor-cell differentiation and causes dysplasia in epithelial tissues." Cell 121(3): 465-477.

Hollestelle, A., F. Elstrodt, M. Timmermans, A. M. Sieuwerts, J. G. Klijn, J. A. Foekens, et al. (2010). "Four human breast cancer cell lines with biallelic inactivating alpha-catenin gene mutations." Breast Cancer Res Treat 122(1): 125-133.

Horrigan, S. K., Z. H. Arbieva, H. Y. Xie, J. Kravarusic, N. C. Fulton, H. Naik, et al. (2000). "Delineation of a minimal interval and identification of 9 candidates for a tumor suppressor gene in malignant myeloid disorders on 5q31." Blood 95(7): 2372-2377.

Humphries, R. K., A. C. Eaves and C. J. Eaves (1981). "Self-renewal of hemopoietic stem cells during mixed colony formation in vitro." Proc Natl Acad Sci U S A 78(6): 3629-3633.

Ibrahim, S. F. and G. van den Engh (2007). "Flow cytometry and cell sorting." Adv Biochem Eng Biotechnol 106: 19-39.

Jacks, T., L. Remington, B. O. Williams, E. M. Schmitt, S. Halachmi, R. T. Bronson and R. A. Weinberg (1994). "Tumor spectrum analysis in p53-mutant mice." Curr Biol 4(1): 1-7.

Jackson, A. L., S. R. Bartz, J. Schelter, S. V. Kobayashi, J. Burchard, M. Mao, et al. (2003). "Expression profiling reveals off-target gene regulation by RNAi." Nat Biotechnol 21(6): 635-637.

Jacobs, P. A., P. A. Hunt, M. Mayer and R. D. Bart (1981). "Duchenne muscular dystrophy (DMD) in a female with an X/autosome translocation: further evidence that the DMD locus is at Xp21." Am J Hum Genet 33(4): 513-518.

Jadersten, M., L. Saft, A. Smith, A. Kulasekararaj, S. Pomplun, G. Gohring, et al. (2011). "TP53 mutations in low-risk myelodysplastic syndromes with del(5q) predict disease progression." J Clin Oncol 29(15): 1971-1979.

Jaju, R. J., J. Boultwood, F. J. Oliver, M. Kostrzewa, C. Fidler, N. Parker, et al. (1998). "Molecular cytogenetic delineation of the critical deleted region in the 5q- syndrome." Genes Chromosomes Cancer 22(3): 251-256.

Jordan, C. T. and I. R. Lemischka (1990). "Clonal and systemic analysis of long-term hematopoiesis in the mouse." Genes Dev 4(2): 220-232.

Joslin, J. M., A. A. Fernald, T. R. Tennant, E. M. Davis, S. C. Kogan, J. Anastasi, et al. (2007). "Haploinsufficiency of EGR1, a candidate gene in the del(5q), leads to the development of myeloid disorders." Blood 110(2): 719-726.

Julius, M. H., T. Masuda and L. A. Herzenberg (1972). "Demonstration that antigen-binding cells are precursors of antibody-producing cells after purification with a fluorescence-activated cell sorter." Proc Natl Acad Sci U S A 69(7): 1934-1938.

Kim, J. Y., K. B. Kim, G. H. Eom, N. Choe, H. J. Kee, H. J. Son, et al. (2012). "KDM3B is the H3K9 demethylase involved in transcriptional activation of lmo2 in leukemia." Mol Cell Biol 32(14): 2917-2933.

Klepin, H. D., A. V. Rao and T. S. Pardee (2014). "Acute myeloid leukemia and myelodysplastic syndromes in older adults." J Clin Oncol 32(24): 2541-2552.

Knudson, A. G., Jr. (1971). "Mutation and cancer: statistical study of retinoblastoma." Proc Natl Acad Sci U S A 68(4): 820-823.

Kobielak, A. and E. Fuchs (2004). "Alpha-catenin: at the junction of intercellular adhesion and actin dynamics." Nat Rev Mol Cell Biol 5(8): 614-625.

Kulasekararaj, A. G., A. E. Smith, S. A. Mian, A. M. Mohamedali, P. Krishnamurthy, N. C. Lea, et al. (2013). "TP53 mutations in myelodysplastic syndrome are strongly correlated with aberrations of chromosome 5, and correlate with adverse prognosis." Br J Haematol 160(5): 660-672.

Kumar, M. S., A. Narla, A. Nonami, A. Mullally, N. Dimitrova, B. Ball, et al. (2011). "Coordinate loss of a microRNA and protein-coding gene cooperate in the pathogenesis of 5q- syndrome." Blood 118(17): 4666-4673.

Laemmli, U. K. (1970). "Cleavage of structural proteins during the assembly of the head of bacteriophage T4." Nature 227(5259): 680-685.

Lai, F., L. A. Godley, J. Joslin, A. A. Fernald, J. Liu, R. Espinosa, 3rd, et al. (2001). "Transcript map and comparative analysis of the 1.5-Mb commonly deleted segment of human 5q31 in malignant myeloid diseases with a del(5q)." Genomics 71(2): 235-245.

Lamar, J. M., P. Stern, H. Liu, J. W. Schindler, Z. G. Jiang and R. O. Hynes (2012). "The Hippo pathway target, YAP, promotes metastasis through its TEAD-interaction domain." Proc Natl Acad Sci U S A 109(37): E2441-2450.

Le Beau, M. M., R. Espinosa, 3rd, W. L. Neuman, W. Stock, D. Roulston, R. A. Larson, et al. (1993). "Cytogenetic and molecular delineation of the smallest commonly deleted region of chromosome 5 in malignant myeloid diseases." Proc Natl Acad Sci U S A 90(12): 5484-5488.

Li, J. (2013). "Myelodysplastic syndrome hematopoietic stem cell." Int J Cancer 133(3): 525-533.

Li, J., J. Newhall, N. Ishiyama, C. Gottardi, M. Ikura, D. E. Leckband and E. Tajkhorshid (2015). "Structural Determinants of the Mechanical Stability of alpha-Catenin." J Biol Chem 290(31): 18890-18903.

Lien, W. H., O. Klezovitch, T. E. Fernandez, J. Delrow and V. Vasioukhin (2006). "alphaE-catenin controls cerebral cortical size by regulating the hedgehog signaling pathway." Science 311(5767): 1609-1612.

Lim, L. P., N. C. Lau, P. Garrett-Engele, A. Grimson, J. M. Schelter, J. Castle, et al. (2005). "Microarray analysis shows that some microRNAs downregulate large numbers of target mRNAs." Nature 433(7027): 769-773.

Lin, Y. W., C. Slape, Z. Zhang and P. D. Aplan (2005). "NUP98-HOXD13 transgenic mice develop a highly penetrant, severe myelodysplastic syndrome that progresses to acute leukemia." Blood 106(1): 287-295.

Liu, T. X., M. W. Becker, J. Jelinek, W. S. Wu, M. Deng, N. Mikhalkevich, et al. (2007). "Chromosome 5q deletion and epigenetic suppression of the gene encoding alpha-catenin (CTNNA1) in myeloid cell transformation." Nat Med 13(1): 78-83.

Liu, Y., S. E. Elf, Y. Miyata, G. Sashida, Y. Liu, G. Huang, et al. (2009). "p53 regulates hematopoietic stem cell quiescence." Cell Stem Cell 4(1): 37-48.

Loghavi, S., A. Al-Ibraheemi, Z. Zuo, G. Garcia-Manero, M. Yabe, S. A. Wang, et al. (2015). "TP53 overexpression is an independent adverse prognostic factor in de novo myelodysplastic syndromes with fibrosis." Br J Haematol 171(1): 91-99.

Lozzio, C. B. and B. B. Lozzio (1975). "Human chronic myelogenous leukemia cell-line with positive Philadelphia chromosome." Blood 45(3): 321-334.

Lynch, C. J. and J. Milner (2006). "Loss of one p53 allele results in four-fold reduction of p53 mRNA and protein: a basis for p53 haplo-insufficiency." Oncogene 25(24): 3463-3470.

Makishima, H. and J. P. Maciejewski (2011). "Pathogenesis and consequences of uniparental disomy in cancer." Clin Cancer Res 17(12): 3913-3923.

McGarry, M. P. P., C. A.; Lee, J. J. (2010). Mouse Hematology: A Laboratory Manual. USA, Cold Spring Harbor Laboratory Press, New York.

Min, I. M., G. Pietramaggiori, F. S. Kim, E. Passegue, K. E. Stevenson and A. J. Wagers (2008). "The transcription factor EGR1 controls both the proliferation and localization of hematopoietic stem cells." Cell Stem Cell 2(4): 380-391.

Miyoshi, H., U. Blomer, M. Takahashi, F. H. Gage and I. M. Verma (1998). "Development of a self-inactivating lentivirus vector." J Virol 72(10): 8150-8157.

Morrison, S. J. and I. L. Weissman (1994). "The long-term repopulating subset of hematopoietic stem cells is deterministic and isolatable by phenotype." Immunity 1(8): 661-673.

Mullighan, C. G., S. Goorha, I. Radtke, C. B. Miller, E. Coustan-Smith, J. D. Dalton, et al. (2007). "Genome-wide analysis of genetic alterations in acute lymphoblastic leukaemia." Nature 446(7137): 758-764.

Murray, J. M., K. E. Davies, P. S. Harper, L. Meredith, C. R. Mueller and R. Williamson (1982). "Linkage relationship of a cloned DNA sequence on the short arm of the X chromosome to Duchenne muscular dystrophy." Nature 300(5887): 69-71.

Nakahata, T., A. J. Gross and M. Ogawa (1982). "A stochastic model of self-renewal and commitment to differentiation of the primitive hemopoietic stem cells in culture." J Cell Physiol 113(3): 455-458.

Nakopoulou, L., H. Gakiopoulou-Givalou, A. J. Karayiannakis, I. Giannopoulou, A. Keramopoulos, P. Davaris and M. Pignatelli (2002). "Abnormal alpha-catenin expression in invasive breast cancer correlates with poor patient survival." Histopathology 40(6): 536-546.

Naldini, L., U. Blomer, P. Gallay, D. Ory, R. Mulligan, F. H. Gage, et al. (1996). "In vivo gene delivery and stable transduction of nondividing cells by a lentiviral vector." Science 272(5259): 263-267.

Oda, T., Y. Kanai, Y. Shimoyama, A. Nagafuchi, S. Tsukita and S. Hirohashi (1993). "Cloning of the human alpha-catenin cDNA and its aberrant mRNA in a human cancer cell line." Biochem Biophys Res Commun 193(3): 897-904.

Ok, C. Y., K. P. Patel, G. Garcia-Manero, M. J. Routbort, J. Peng, G. Tang, et al. (2015). "TP53 mutation characteristics in therapy-related myelodysplastic syndromes and acute myeloid leukemia is similar to de novo diseases." J Hematol Oncol 8: 45.

Padilla, P. I., A. Wada, K. Yahiro, M. Kimura, T. Niidome, H. Aoyagi, et al. (2000). "Morphologic differentiation of HL-60 cells is associated with appearance of RPTPbeta and induction of Helicobacter pylori VacA sensitivity." J Biol Chem 275(20): 15200-15206.

Pant, V., A. Quintas-Cardama and G. Lozano (2012). "The p53 pathway in hematopoiesis: lessons from mouse models, implications for humans." Blood 120(26): 5118-5127.

Papaemmanuil, E., M. Gerstung, L. Malcovati, S. Tauro, G. Gundem, P. Van Loo, et al. (2013). "Clinical and biological implications of driver mutations in myelodysplastic syndromes." Blood 122(22): 3616-3627; quiz 3699.

Piao, H. L., Y. Yuan, M. Wang, Y. Sun, H. Liang and L. Ma (2014). "alpha-catenin acts as a tumour suppressor in E-cadherin-negative basal-like breast cancer by inhibiting NF-kappaB signalling." Nat Cell Biol 16(3): 245-254.

Pierzchalski, A., A. Mittag and A. Tarnok (2011). "Introduction A: recent advances in cytometry instrumentation, probes, and methods--review." Methods Cell Biol 102: 1-21.

Plumb, C. L., U. Adamcic, S. Shahrzad, K. Minhas, S. A. Adham and B. L. Coomber (2009). "Modulation of the tumor suppressor protein alpha-catenin by ischemic microenvironment." Am J Pathol 175(4): 1662-1674.

Raftopoulos, I., P. Davaris, G. Karatzas, P. Karayannacos and G. Kouraklis (1998). "Level of alpha-catenin expression in colorectal cancer correlates with invasiveness, metastatic potential, and survival." J Surg Oncol 68(2): 92-99.

Renart, J., J. Reiser and G. R. Stark (1979). "Transfer of proteins from gels to diazobenzyloxymethyl-paper and detection with antisera: a method for studying antibody specificity and antigen structure." Proc Natl Acad Sci U S A 76(7): 3116-3120.

Reya, T., A. W. Duncan, L. Ailles, J. Domen, D. C. Scherer, K. Willert, et al. (2003). "A role for Wnt signalling in self-renewal of haematopoietic stem cells." Nature 423(6938): 409-414.

Rosenbauer, F., K. Wagner, J. L. Kutok, H. Iwasaki, M. M. Le Beau, Y. Okuno, et al. (2004). "Acute myeloid leukemia induced by graded reduction of a lineage-specific transcription factor, PU.1." Nat Genet 36(6): 624-630.

Roy, S., S. Javed, S. K. Jain, S. S. Majumdar and A. Mukhopadhyay (2012). "Donor hematopoietic stem cells confer long-term marrow reconstitution by self-renewal divisions exceeding to that of host cells." PLoS One 7(12): e50693.

Saft, L., M. Karimi, M. Ghaderi, A. Matolcsy, G. J. Mufti, A. Kulasekararaj, et al. (2014). "p53 protein expression independently predicts outcome in patients with lower-risk myelodysplastic syndromes with del(5q)." Haematologica 99(6): 1041-1049.

Saiki, R. K., D. H. Gelfand, S. Stoffel, S. J. Scharf, R. Higuchi, G. T. Horn, et al. (1988). "Primer-directed enzymatic amplification of DNA with a thermostable DNA polymerase." Science 239(4839): 487-491.

Sanger, F., S. Nicklen and A. R. Coulson (1977). "DNA sequencing with chain-terminating inhibitors." Proc Natl Acad Sci U S A 74(12): 5463-5467.

Schlegelmilch, K., M. Mohseni, O. Kirak, J. Pruszak, J. R. Rodriguez, D. Zhou, et al. (2011). "Yap1 acts downstream of alpha-catenin to control epidermal proliferation." Cell 144(5): 782-795.

Schmid, M. T., F. Weinandy, M. Wilsch-Brauninger, W. B. Huttner, S. Cappello and M. Gotz (2014). "The role of alpha-E-catenin in cerebral cortex development: radial glia specific effect on neuronal migration." Front Cell Neurosci 8: 215.

Schmidt, M., K. Schwarzwaelder, C. Bartholomae, K. Zaoui, C. Ball, I. Pilz, et al. (2007). "High-resolution insertion-site analysis by linear amplification-mediated PCR (LAM-PCR)." Nat Methods 4(12): 1051-1057.

Schmidt, M., K. Schwarzwaelder, C. C. Bartholomae, H. Glimm and C. von Kalle (2009). "Detection of retroviral integration sites by linear amplification-mediated PCR and tracking of individual integration clones in different samples." Methods Mol Biol 506: 363-372.

Schmidt, M., P. Zickler, G. Hoffmann, S. Haas, M. Wissler, A. Muessig, et al. (2002). "Polyclonal long-term repopulating stem cell clones in a primate model." Blood 100(8): 2737-2743.

Sedic, M., A. Skibinski, N. Brown, M. Gallardo, P. Mulligan, P. Martinez, et al. (2015). "Haploinsufficiency for BRCA1 leads to cell-type-specific genomic instability and premature senescence." Nat Commun 6: 7505.

Serafini, M., S. J. Dylla, M. Oki, Y. Heremans, J. Tolar, Y. Jiang, et al. (2007). "Hematopoietic reconstitution by multipotent adult progenitor cells: precursors to long-term hematopoietic stem cells." J Exp Med 204(1): 129-139.

Silvis, M. R., B. T. Kreger, W. H. Lien, O. Klezovitch, G. M. Rudakova, F. D. Camargo, et al. (2011). "alpha-catenin is a tumor suppressor that controls cell accumulation by regulating the localization and activity of the transcriptional coactivator Yap1." Sci Signal 4(174): ra33.

Smith, P. K., R. I. Krohn, G. T. Hermanson, A. K. Mallia, F. H. Gartner, M. D. Provenzano, et al. (1985). "Measurement of protein using bicinchoninic acid." Anal Biochem 150(1): 76-85.

Sokoloski, J. A., A. C. Sartorelli, C. A. Rosen and R. Narayanan (1993). "Antisense oligonucleotides to the p65 subunit of NF-kappa B block CD11b expression and alter adhesion properties of differentiated HL-60 granulocytes." Blood 82(2): 625-632.

Song, W. J., M. G. Sullivan, R. D. Legare, S. Hutchings, X. Tan, D. Kufrin, et al. (1999). "Haploinsufficiency of CBFA2 causes familial thrombocytopenia with propensity to develop acute myelogenous leukaemia." Nat Genet 23(2): 166-175.

Sprussel, A., J. H. Schulte, S. Weber, M. Necke, K. Handschke, T. Thor, et al. (2012). "Lysine-specific demethylase 1 restricts hematopoietic progenitor proliferation and is essential for terminal differentiation." Leukemia 26(9): 2039-2051.

Staal, F. J. T., T. C. Luis and M. M. Tiemessen (2008). "WNT signalling in the immune system: WNT is spreading its wings." Nat Rev Immunol 8(8): 581-593.

Stewart, S. A., D. M. Dykxhoorn, D. Palliser, H. Mizuno, E. Y. Yu, D. S. An, et al. (2003). "Lentivirus-delivered stable gene silencing by RNAi in primary cells." Rna 9(4): 493-501.

Stoddart, A., A. A. Fernald, J. Wang, E. M. Davis, T. Karrison, J. Anastasi and M. M. Le Beau (2014a). "Haploinsufficiency of del(5q) genes, Egr1 and Apc, cooperate with Tp53 loss to induce acute myeloid leukemia in mice." Blood 123(7): 1069-1078.

Stoddart, A., J. Wang, A. A. Fernald, T. Karrison, J. Anastasi and M. M. Le Beau (2014b). "Cell intrinsic and extrinsic factors synergize in mice with haploinsufficiency for Tp53, and two human del(5q) genes, Egr1 and Apc." Blood 123(2): 228-238.

Thiel, A., M. Beier, D. Ingenhag, K. Servan, M. Hein, V. Moeller, et al. (2011). "Comprehensive array CGH of normal karyotype myelodysplastic syndromes reveals hidden recurrent and individual genomic copy number alterations with prognostic relevance." Leukemia 25(3): 387-399.

Torres, M., A. Stoykova, O. Huber, K. Chowdhury, P. Bonaldo, A. Mansouri, et al. (1997). "An alpha-E-catenin gene trap mutation defines its function in preimplantation development." Proc Natl Acad Sci U S A 94(3): 901-906.

Towbin, H., T. Staehelin and J. Gordon (1979). "Electrophoretic transfer of proteins from polyacrylamide gels to nitrocellulose sheets: procedure and some applications." Proc Natl Acad Sci U S A 76(9): 4350-4354.

Traganos, F. (1984). "Flow cytometry: principles and applications. II." Cancer Invest 2(3): 239-258.

Ulger, C., G. A. Toruner, M. Alkan, M. Mohammed, S. Damani, J. Kang, et al. (2003). "Comprehensive genome-wide comparison of DNA and RNA level scan using microarray technology for identification of candidate cancer-related genes in the HL-60 cell line." Cancer Genet Cytogenet 147(1): 28-35.

Vasioukhin, V., C. Bauer, L. Degenstein, B. Wise and E. Fuchs (2001). "Hyperproliferation and defects in epithelial polarity upon conditional ablation of alpha-catenin in skin." Cell 104(4): 605-617.

Visser, O., A. Trama, M. Maynadie, C. Stiller, R. Marcos-Gragera, R. De Angelis, et al. (2012). "Incidence, survival and prevalence of myeloid malignancies in Europe." Eur J Cancer 48(17): 3257-3266.

Volkert, S., A. Kohlmann, S. Schnittger, W. Kern, T. Haferlach and C. Haferlach (2014). "Association of the type of 5q loss with complex karyotype, clonal evolution, TP53 mutation status, and prognosis in acute myeloid leukemia and myelodysplastic syndrome." Genes Chromosomes Cancer 53(5): 402-410.

White, S. L., L. Belov, N. Barber, P. D. Hodgkin and R. I. Christopherson (2005). "Immunophenotypic changes induced on human HL60 leukaemia cells by 1alpha,25-

dihydroxyvitamin D3 and 12-O-tetradecanoyl phorbol-13-acetate." Leuk Res 29(10): 1141-1151.

Wolf, D. and V. Rotter (1985). "Major deletions in the gene encoding the p53 tumor antigen cause lack of p53 expression in HL-60 cells." Proc Natl Acad Sci U S A 82(3): 790-794.

Xie, H., Z. Hu, B. Chyna, S. K. Horrigan and C. A. Westbrook (2000). "Human mortalin (HSPA9): a candidate for the myeloid leukemia tumor suppressor gene on 5q31." Leukemia 14(12): 2128-2134.

Xu, H., S. Menendez, B. Schlegelberger, N. Bae, P. D. Aplan, G. Gohring, et al. (2012). "Loss of p53 accelerates the complications of myelodysplastic syndrome in a NUP98-HOXD13-driven mouse model." Blood 120(15): 3089-3097.

Ye, Y., M. A. McDevitt, M. Guo, W. Zhang, O. Galm, S. D. Gore, et al. (2009). "Progressive chromatin repression and promoter methylation of CTNNA1 associated with advanced myeloid malignancies." Cancer Res 69(21): 8482-8490.

Yoshimi, A., T. Toya, M. Kawazu, T. Ueno, A. Tsukamoto, H. Iizuka, et al. (2014). "Recurrent CDC25C mutations drive malignant transformation in FPD/AML." Nat Commun 5: 4770.

Zennou, V., C. Petit, D. Guetard, U. Nerhbass, L. Montagnier and P. Charneau (2000). "HIV-1 genome nuclear import is mediated by a central DNA flap." Cell 101(2): 173-185.

Zhao, N., A. Stoffel, P. W. Wang, J. D. Eisenbart, R. Espinosa, 3rd, R. A. Larson and M. M. Le Beau (1997). "Molecular delineation of the smallest commonly deleted region of chromosome 5 in malignant myeloid diseases to 1-1.5 Mb and preparation of a PAC-based physical map." Proc Natl Acad Sci U S A 94(13): 6948-6953.

Zhao, Z., J. Zuber, E. Diaz-Flores, L. Lintault, S. C. Kogan, K. Shannon and S. W. Lowe (2010). "p53 loss promotes acute myeloid leukemia by enabling aberrant self-renewal." Genes Dev 24(13): 1389-1402.

Zufferey, R., J. E. Donello, D. Trono and T. J. Hope (1999). "Woodchuck hepatitis virus posttranscriptional regulatory element enhances expression of transgenes delivered by retroviral vectors." J Virol 73(4): 2886-2892.

Zufferey, R., T. Dull, R. J. Mandel, A. Bukovsky, D. Quiroz, L. Naldini and D. Trono (1998). "Self-inactivating lentivirus vector for safe and efficient in vivo gene delivery." J Virol 72(12): 9873-9880.

Zufferey, R., D. Nagy, R. J. Mandel, L. Naldini and D. Trono (1997). "Multiply attenuated lentiviral vector achieves efficient gene delivery in vivo." Nat Biotechnol 15(9): 871-875.

8 List of Figures

Figure 1: Genes located within the delineated proximal CDR on chromosome 5q31 in MDS. 6
Figure 2: Concepts of tumor suppressor gene inactivation. 8
Figure 3: α-Catenin is a negative regulator of Hippo, Wnt and NFκB signaling pathways. ... 10
Figure 4: Eight shRNA encoding vectors mediated an expression level of Ctnna1 below 50% gene dosage. 13
Figure 5: Schematic experimental design of competitive reconstitution experiment *in vivo*. . 14
Figure 6: Time course of the frequencies of GFP^+ peripheral blood cells in transplanted mice. 15
Figure 7: Regular monitoring of successful reconstitution by evaluation of complete blood counts (CBCs) over six months. 16
Figure 8: Frequency of GFP^+ cells in peripheral blood, bone marrow and spleen of recipient mice. 17
Figure 10: Cells with reduced Ctnna1 expression expanded within the myeloid compartment of the bone marrow of mouse M12. 18
Figure 9: Successful knockdown of Ctnna1 expression by RNAi in GFP^+ bone marrow cells of mouse M12. 18
Figure 11: Mice transplanted with HSPCs with reduced Ctnna1 expression showed signs of impaired erythropoiesis in the bone marrow. 20
Figure 12: The LSK and HSC populations showed increased frequencies of GFP^+ cells in the bone marrow of mouse M12. 20
Figure 13: GFP^+ bone marrow cells from mice M12 and M15 were originating from a mixture of transplanted single-vector transduced HSPCs. 21
Figure 14: Detection of integration sites in gDNA from bone marrow cells of mice M12 and M15. 22
Figure 15: Schematic experimental design of second competitive reconstitution experiment *in vivo*. 23
Figure 16: Time course of the frequencies of GFP^+ peripheral blood cells in transplanted mice. 24
Figure 17: Regular monitoring of successful reconstitution by evaluation of complete blood counts (CBCs) over six months. 25
Figure 18: Frequency of GFP^+ cells in peripheral blood, bone marrow and spleen of recipient mice. 26
Figure 19: RNAi by expression of shRNAs 405 and 409 in murine bone marrow cells mediated reduced levels of Ctnna1 expression *in vivo*. 26
Figure 20: Transplanted mice of group 405 with increased GFP^+ cell population show evidence of a myeloid differentiation bias according to the cellular composition of the bone marrow. 27

Figure 21: Expansion of GFP$^+$ bone marrow cells expressing shRNA 405 led to reduced bone marrow erythropoiesis. 28
Figure 22: HSPCs with reduced Ctnna1 expression expand within the LSK and HSC compartments of transplanted mice. 29
Figure 23: Design of secondary transplantation experiment. 30
Figure 24: Exclusively bone marrow cells expressing shRNA 405 from the primary donor mouse M26 were able to give rise to GFP$^+$ cells in the peripheral blood of secondary transplanted mice. 31
Figure 25: Mice transplanted with bone marrow cells from the primary donor mouse M26 (group 405) showed signs of leukopenia and anemia. 32
Figure 26: Primary GFP$^+$ bone marrow cells of mouse M26 (shRNA 405) expanded upon secondary transplantation. 33
Figure 27: GFP$^+$ bone marrow cells of mouse M26 showed a clonal dominance phenotype upon secondary transplantation 34
Figure 28: Mice transplanted with bone marrow cells from mouse M26 showed a differentiation bias towards the myeloid lineage in the GFP$^+$ cells of peripheral blood, bone marrow and spleen. 35
Figure 29: Secondary recipient mice transplanted with bone marrow from mouse M26 showed reduced bone marrow erythropoiesis. 36
Figure 30: GFP$^+$ cells expressing shRNA 405 expanded within the LSK cell and HSC compartments of secondary recipient mice. 37
Figure 31: Schematic experimental design of the competitive reconstitution experiment *in vivo* implementing a functional inactivation of Tp53. 38
Figure 32: Frequency of Tp53$^{-/-}$ and WT GFP$^+$ cells in peripheral blood, bone marrow and spleen of recipient mice. 39
Figure 33: RNAi by expression of shRNAs 405 and 409 in murine bone marrow cells mediated reduced levels of Ctnna1 expression *in vivo*. 40
Figure 34: Mice transplanted with HSPCs encoding shRNA 405, 409 or control shRNAs did not show signs of hematological disease irrespective of the genetic background of the transplanted HSPCs. 40
Figure 35: Transplanted bone marrow cells with reduced Ctnna1 expression were mostly differentiated within the myeloid lineage. 41
Figure 36: Reduced bone marrow erythropoiesis caused by expansion of cells encoding shRNA 405 in transplanted mice was not further diminished by additional inactivation of Tp53. 43
Figure 37: Inactivation of Tp53 reinforces the clonal dominance of GFP$^+$ cells within the LSK and HSC compartments of transplanted mice. 44
Figure 38: Design of the secondary transplantation experiment of Tp53$^{-/-}$ bone marrow cells from primary recipients. 45

Figure 39: Tp53 inactivation in secondary transplanted bone marrow cells mediated successful engraftment of GFP^+ cells encoding shRNA 405 or 409. 46
Figure 40: Frequencies of GFP^+ cells in peripheral blood, bone marrow and spleen of secondary recipient mice transplanted with $Tp53^{-/-}$ bone marrow cells from primary recipients. 46
Figure 41: Secondary recipient mice transplanted with $Tp53^{-/-}$ bone marrow cells from primary donors did not show overt signs of hematological disease at 12 weeks post transplantation. 47
Figure 42: Bone marrow cells of secondary recipients encoding shRNA 405 or shRNA 409 were mostly differentiated within the myeloid lineage. 49
Figure 43: Reduced bone marrow erythropoiesis caused by the expansion of bone marrow cells expressing shRNA 405 was maintained in secondary recipient mice. 50
Figure 44: The clonal dominance of bone marrow cells with reduced Ctnna1 expression is maintained and reinforced upon secondary transplantation of $Tp53^{-/-}$ bone marrow cells. 51
Figure 45: Genetic inactivation of Tp53 and reduced Ctnna1 gene dosage in the bone marrow of transplanted mice reduced the overall survival of the animals. 52
Figure 46: Reduced Ctnna1 expression in the bone marrow of transplanted mice led to peripheral blood cell dysplasia. 54
Figure 47: GFP^+ bone marrow cells expressing shRNA 405 were primarily composed of granulocytic progenitor cells and myeloblasts. 55
Figure 48: Expression of shRNA 405 immortalizes primary murine bone marrow cells *in vitro*. 56
Figure 49: Lineage negative bone marrow cells are maintained upon immortalization by shRNA 405 and give rise to myeloid cells *in vitro*. 58
Figure 50: Increasing levels of ectopically expressed Ctnna1 gradually impaired the growth of shRNA 405-expressing immortalized bone marrow cells. 59
Figure 51: The growth of HL60 cells was impaired upon induced re-expression of CTNNA1, but not $CTNNA1\Delta N_{267}$. 61
Figure 52: Expression of CTNNA1 mediated a minor block of G1-S transition in HL60 cells. 62
Figure 53: CTNNA1 expression in HL60 cells triggered cell differentiation towards the myeloid lineage. 64
Figure 54: Lentiviral vector designs used for Ctnna1 knockdown in vitro and *in vivo*. 87
Figure 55: Lentiviral vector designs for constitutive ectopic Ctnna1 re-expression in murine bone marrow cells. 88
Figure 56: Lentiviral vector design for doxycycline-inducible CTNNA1 re-expression in the human HL60 cell line. 88

Figure 57: Gating strategies and frequencies of bone marrow subpopulations in a wildtype mouse. 92

9 List of Tables

Table 1: List of cloning primers 75
Table 2: List of primers for shRNA sequence identification by QPCR 75
Table 3: List of primers for expression analysis by QRT-PCR 76
Table 4: List of primers for LAM-PCR. 76
Table 5: Linker oligonucleotides for LAM-PCR 77
Table 6: shRNA sequences 77
Table 7: Antibodies for Western Blot 78
Table 8: Antibodies for flow cytometry 78

10 List of Abbreviations

ACK	Ammonium-Chloride-Potassium
AML	Acute Myeloid Leukemia
APC	Allophycocyanin
approx.	approximately
APS	Ammonium Persulfate
Array-CGH	Array Comparative Genomic Hybridization
ATP	Adenosine-Triphosphate
ATRA	all-trans Retinoic Acid
BCA	Bicinchoninic Acid
BFP	Blue Fluorescent Protein
Blast	Blasticidin
BM	Bone Marrow
BSA	Bovine Serum Albumin
CBCs	Complete Blood Counts
CD	Cluster of Differentiation
cDNA	complementary DNA
CDR	Commonly Deleted Region
CDS	Coding Sequence
CMV	Cytomegalovirus
CN-LOH	Copy Neutral Loss of Heterozygosity
CRISPR	Clustered Regularly Interspaced Short Palindromic Repeats
CTNNA1	alpha-1 Catenin
del	deletion
DMEM	Dulbecco’s Modified Eagle Medium

DMSO	Dimethylsulfoxide
DNA	Desoxyribonucleic Acid
dNTPs	deoxynucleotide trisphosphates
Dox	Doxycycline
DPBS	Dulbecco's PBS
dsDNA	double stranded DNA
DTT	Dithiothreitol
EDTA	Ethylenediaminetetraacetic Acid
e.g.	*exempli gratia*
et al.	*et alia*
etc	*et cetera*
FACS	Fluorescence Activated Cell Sorting
FBS	Fetal Bovine Serum
FSC	Forward Scatter
FW	Forward (Primer)
gDNA	genomic DNA
GFP	Green Fluorescent Protein
GRCm38	Genome Reference Consortium Mouse Build 38
GRCh38	Genome Reference Consortium Human Reference 38
gt	goat
h.i.	heat inactivated
HCT	Hematocrit
HEK	Human Embryonic Kidney
HEPES	4-(2-hydroxyethyl)-1-piperazineethanesulfonic acid
hg38	UCSC genome browser Assembly human 38
HGB	Hemoglobin
HIV-1	Human Immunodeficiency Virus-1
hPGK	human Phosphoglycerate Kinase (promoter)
HRP	Horseraddish Peroxidase
HSC	Hematopoietic Stem Cell
HSPCs	Hematopoietic Stem and Progenitor Cells
hu	human
hU6	human U6 (Polymerase III promoter)
i.e.	*id est*
IgG1κ	Immunglobulin G1, κ light chain
IMDM	Iscove's modified Dulbecco's Medium
IPSS	International Prognostic Scoring System
IRES	Internal Ribosomal Entry Site
LAM-PCR	Linear Amplification-Mediated PCR
LB	Lysogeny Broth
L-ICs	Leukemia-initating Cells
Lin−	Lineage negative
LSK	Lineage negative, $Sca1^+$, Kit^+
LTR	Long Terminal Repeat

MACS	Magnetic Cell Separation
MCV	Mean Corpuscular Volume
MDS	Myelodysplastic Syndromes
mESC	mouse embryonic stem cell
mFlt3L	murine Fms-like tyrosine kinase 3 Ligand
mm10	mus musculus assembly 10
mScf	murine Stem cell factor
mTpo	murine Thrombopoietin
NFκB	Nuclear Factor 'kappa-light-chain-enhancer' of activated B-cells
nt	nucleotide
P2A	Porcine teschovirus-1 derived 2A-peptide
p53-KO	p53 Knockout
PB	Peripheral Blood
PBS	Phosphate-Buffered Saline
PCR	Polymerase Chain Reaction
PE	R-Phycoerythrin
PE-Cy7	PE-Cyanine 7
PerCP-Cy5.5	PE-Cyanine 5.5
PI	Propidium Iodide
PLT	Platelets
PMA	Phorbol 12-myristate 13-acetate
PMT	Photomultiplier Tube
Puro	Puromycin
PVDF	Polyvinylidene difluoride
QPCR	Quantitative PCR
QRT-PCR	Quantitative Reverse Transcritption PCR
R26-M2rtTA	ROSA26 reverse tetracycline-controlled transactivator M2 knockin
rb	rabbit
RBC	Red Blood Cell
RNA	Ribonucleic Acid
RNAi	RNA interference
RPMI	Roswell Park Memorial Institute (medium)
RRE	Rev responsive element
RT	Room Temperature
RV	Reverse (primer)
SDS	Sodium Dodecyl Sulfate
SDS-PAGE	SDS-Poly Acrylamide Gel Electrophersis
SFFV	Spleen Focus-forming Virus
shRNA	short hairpin RNA
SIN	Self inactivating
siRNA	small interfering RNA
SLAM	Signaling Lymphocyte Activation Molecule
SNP	Single Nucleotide Polymorphism
SP	Spleen

SSC	Side Scatter
ssDNA	single stranded DNA
TAE	Tris-Acetate-EDTA
TBS-T	Tris-Buffered Saline-Tween 20
TEMED	Tetramethylethylenediamine
Tet	Tetracycline
TetO7	7x Tet Operon
TGM	Tris-Gylcine-Methanol
TPA	12-O-tetradecanoyl phorbol-13-acetate
TP53	Tumor Protein p53
Tris	Tris(hydroxymethyl)aminomethane
UCSC	University of California, Santa Cruz
UV	Ultra violet
v/v	volume/volume
VSV	Vesicular Stomatitis Virus
w/v	weight/volume
WBC	Whitle Blood Cell
Wnt	*Wg* (*Wingless*) + *Int1*
WPRE	Woodchuck Hepatitis Virus (WHP) Posttranscriptional Regulatory Element
WT	wildtype
1,25-D_3	1α,25-dihydroxyvitamin D3
α-ms	anti-mouse
ψ	Psi (lentiviral packaging signal sequence)

11 Acknowledgements

First of all, I thank Dr. Stefan Heinrichs for his constant support during the past four years I worked on this project. I very much appreciated his patience, his relentless willingness to teach me what he knows and his uncompromising way of pushing me to work harder and become a better scientist. He is one of the best and most dedicated teachers I know.

I owe great thanks to Prof. Dr. Peter Horn for giving me the opportunity to work on my thesis in his institute. I valued his continuous interest in my work as well as the support and feedback he gave me throughout the past years.

To Prof. Dr. Perihan Nalbant I am very thankful for her constant interest in my project during my time at the BIOME graduate school and for agreeing on being the second supervisor of my thesis.

I thank Dr. Joachim Göthert and Dr. Cyrus Khandanpour and their groups (Institute for Hematology, University Hospital Essen) for their support in methodology, their help in data analysis and their positive feedback to my work.

I thank Dr. Michael Rothe and Dr. Reinhard Hämmerle from the Institute of Experimental Hematology, MHH Hannover, for their constructive help to establish the LAM-PCR method in our lab.

Furthermore, I want to thank the entire staff of the Animal Facility, especially Jessica, Esra and Andrea, for their help and support with the mice.

I thank all current and former members of the Heinrichs Lab, especially Julia, Diana, Christina, and Renata, for their companionship, support and encouragement.

I owe a big “Thank you!” to all the current and former colleagues at the Institute of Transfusion Medicine at the University Hospital Essen. You made my day, every day, by supplying me with plenty of chocolate, cake, waffles, chats and laughter and an encouraging smile whenever I needed one.

I want to thank my friends I made in Essen during the last four years for their companionship and their never-ending will to hang around, getting our heads off work and drink a beer. Tina, Nina, Simon, Jenny, Nico, Ivo, Josephine, Anna, Stefan, Sören and Liska, I valued every minute with you, in laughter or tears.

I cannot express how thankful I am to have you in my life, André. Your love and support encourages me every day. You are the best that ever happened to me. I love you.

Last, but most certainly not least, I thank my entire family for everything you did for me. You do not only provide me with constant financial support, but give me a loving and caring home I always want to come back to. If it was not for you, I would have never made it this far. I love you.

Lebenslauf

Der Lebenslauf ist in der Online-Version aus Gründen des Datenschutzes nicht enthalten.

Liste der wissenschaftlichen Publikationen

Zickler AM, Hampp S, Messiaen L, Bengesser K, Mussotter T, Roehl AC, Wimmer K, Mautner VF, Kluwe L, Upadhyaya M, Pasmant E, Chuzhanova N, Kestler HA, Högel J, Legius E, Claes K, Cooper DN, Kehrer-Sawatzki H.
Characterization of the nonallelic homologous recombination hotspot PRS3 associated with type-3 *NF1* deletions.
Hum Mutat. 2012 Feb; 33(2):372-83

Roehl AC, Vogt J, Mussotter T, **Zickler AM**, Spöri H, Högel J, Chuzhanova NA, Wimmer K, Kluwe L, Mautner VF, Cooper DN, Kehrer-Sawatzki H.
Intrachromosomal mitotic nonallelic homologous recombination is the major molecular mechanism underlying type-2 *NF1* deletions.
Hum Mutat. 2010 Oct; 31(10):1163-73

Eidesstattliche Erklärung

Erklärung:
Hiermit erkläre ich, gem. § 6 Abs. 2, g der Promotionsordnung der Fakultät für Biologie zur Erlangung des Dr. rer. nat., dass ich das Arbeitsgebiet, dem das Thema „α-Catenin is a dosage-dependent tumor suppressor gene in MDS“ zuzuordnen ist, in Forschung und Lehre vertrete und den Antrag von Antje Maria Zickler befürworte.

Essen, den _____ _____ _____

Name des wissenschaftl. Betreuers/Mitglieds der Universität Duisburg-Essen	Unterschrift d. wissenschaftl. Betreuers/ Mitglieds der Universität Duisburg-Essen

Erklärung:
Hiermit erkläre ich, gem. § 7 Abs. 2, d und f der Promotionsordnung der Fakultät für Biologie zur Erlangung des Dr. rer. nat., dass ich die vorliegende Dissertation selbständig verfasst und mich keiner anderen als der angegebenen Hilfsmittel bedient habe und alle wörtlich oder inhaltlich übernommenen Stellen als solche gekennzeichnet habe.

Essen, den _____ _____

Unterschrift der Doktorandin

Erklärung:
Hiermit erkläre ich, gem. § 7 Abs. 2, e und g der Promotionsordnung der Fakultät für Biologie zur Erlangung des Dr. rer. nat., dass ich keine anderen Promotionen bzw. Promotionsversuche in der Vergangenheit durchgeführt habe, dass diese Arbeit von keiner anderen Fakultät abgelehnt worden ist, und dass ich die Dissertation nur in diesem Verfahren einreiche.

Essen, den _____ _____

Unterschrift der Doktorandin